PLANT-SCALE MANUFACTURING METHOD FOR COVAXIN, A NOVEL INACTIVATED COVID-19 VACCINE

A Research Paper submitted to the Department of Chemical Engineering
In Partial Fulfillment of the Requirements for the Degree
Bachelor of Science in Chemical Engineering

Paul Imbrogulio, Mucui Lin, Kevin Macera, and Sara Richardson

By

Nana Aba Acquaah

April 16, 2021

On my honor as a University student, I have neither given nor received unauthorized aid on this assignment as defined by the Honor Guidelines for Thesis-Related Assignments.

ADVISOR
Eric W. Anderson, Department of Chemical Engineering

Table of Contents

I. Executive Summary

This project aims to scale up the inactivated COVID-19 vaccine from the Indian company Bharat Biotech, to be produced in Durham, NC, with a global target market. The upstream process consists of a seed train and three 1000 L bioreactors, and it utilizes Vero cells on microcarriers to increase productivity. The downstream process consists of TFF (tangential flow filtration), Benzonase treatment, ultrafiltration/diafiltration, viral inactivation, affinity chromatography, size exclusion chromatography, and sterile filtration. Formulation will occur after downstream to add a preservative, a buffer, and adjuvants. The formulated product will be filled into 10 mL vials and be ready for packaging. This plant aims to produce 570 million doses in the first year and 713 million doses in subsequent years to satisfy the market demand.

The economic feasibility of the project was determined based on the operational financial analysis for the first five years. The cost of operation includes fixed capital investment, and operating costs, which includes labor, raw materials, utilities, legal expenses, and taxes. After five years of operation, the cumulative cash flow is $4,891,160,054 with the Internal Rate of Return (IRR) of 379% with substandard conditions. Since the IRR is above the recommended industry standard, the project is economically feasible.

I. Introduction

The outbreak of Severe Acute Respiratory Syndrome Coronavirus 2, colloquially identified as Sars-CoV-2, has disrupted health care systems, crippled economies, and prompted a profound loss of human life worldwide. The virus results in a respiratory disease named COVID-19, first documented with the name "2019 novel coronavirus". Due to a delayed onset or absence of symptoms and the highly contagious nature of the disease, countries have struggled to control its rate of transmission (Jaimes et al., 2020, p. 3321).

The illness has had a profound impact on the United States. According to Yong (2020), the U.S. constitutes four percent of the world's population but possesses 25 percent of its COVID-19 cases and deaths as of September 2020, when this project was commenced. Dynamic, aggregate forecasts compiled by the Centers for Disease Control and Prevention (CDC) predicts the United States is on track to report between 240,000 to 500,000 cases and 3,500 to 7,600 deaths every four weeks without intervention (Center for Disease Control and Prevention [CDC], 2020b; CDC 2020a). As the disease continues to propagate through the country, the competition to achieve herd immunity through natural infection or vaccination progresses. Epidemiology experts report the minimum percentage of the United States population that must recover from COVID-19 to confer immunity is 70 percent (Kwok et al., 2020, p. e32). While scientists support a vaccination-based approach because of the enormous death toll that would result from allowing the disease to spread with minimal interference, the protocols in place that control the vaccine production process for COVID-19 restrict the plausibility of one high-efficacy vaccine reaching the market (Mayo Clinic 2020; Zimmer 2020). The consequence of this system is the wide availability of moderate efficacy vaccines released on a rolling basis. Even so, Dr. Poland of the

Mayo Clinic asserts these vaccines will be instrumental in reducing the cases of COVID-19 (Zimmer, 2020).

As of Spring 2021, there are 12 vaccine candidates that have been approved across countries, and 58 more candidates seeking approval (Corum, Wee, & Zimmer, 2020). Five of the approved vaccines are inactivated or attenuated vaccines, providing evidence of this methodology as a promising solution to the pandemic (Corum, Wee, & Zimmer, 2020).

A collaboration between the Indian Council of Medical Research, the National Institute of Virology, and the Indian company Bharat Biotech developed an inactivated vaccine called Covaxin that has been successful at protecting against COVID-19 in animal and preliminary human trials (Corum, Wee, & Zimmer, 2020). Bharat Biotech has shown promising efforts in creating an efficient and effective vaccine, with plans to distribute their product across the globe. This vaccine project will achieve an industrial scale manufacturing process for an inactivated COVID-19 vaccine, based on the research and published data from Bharat Biotech's Covaxin technology.

II. Previous Work

The global effort to rapidly develop and manufacture a SARS-CoV-2 vaccine led to several insights around vaccinology. Most prominently, the emergence of mRNA vaccines from Moderna and Pfizer/BioNTech as the dominant vaccine modality marks an important milestone in the field. While this capstone project features an inactivated virus product, a comparison with the more recent mRNA vaccines is warranted in assessing a global response to the pandemic.

Conventionally, vaccines provide immunity to pathogens/antigens by providing a weakened or fragmented segment of the foreign body; this exposure allows B cells to recognize and develop antibodies in response to the specific invader (Roghanian and Newman, 2021). Alternatively, mRNA vaccines, "carry only the directions for producing these invaders' proteins. The aim is that they can slip into a person's cells and get them to produce the antigens," (Dolgin, 2021).

As a response to a global pandemic, the spread of infection is not limited solely by a highly effective vaccine, but the proportion of the world population which has been vaccinated. In the developing world, the cold supply chain (-70 ^{o}C) required for mRNA vaccines is not feasible. This limitation leaves a large portion of the global population open to infection. In these areas, a vaccine that is easily stored and transported, such as the product presented in this capstone, is necessary.

As of March 2021, WHO has authorized emergency use listing status for four vaccines for SARS-CoV-2 (Status of COVID-19 Vaccines, 2021), with 13 others awaiting clearance. The vaccines developed by companies in developing nations heavily rely upon adenovirus or inactivated virus platforms, such as Sinovac from China and Covaxin from India.

Ng et al. (2003) demonstrated the utility of virus production and replication in Vero cells. The study tracks the proliferation of virus replication chronologically post-infection. Major findings include the presence of extracellular virus in 5% of cells to 30% of cells between the 5 and 6 hour mark, post infection. Experiments showed the common presence of extracellular virus crystalline arrays by 24-30 hours post infection.

Jureka et al. (2020) developed inactivation procedures for SARS-CoV-2 viruses. The protocols used in the study demonstrated inactivation by TRIzol, 10% neutral buffered formalin, beta-propiolactone, and heat. The inactivation measures were tested against virus infectivity by plaque assay to show the effectiveness of virus inactivation.

Ganneru et al. (2020) described a manufacturing process to produce an inactivated SARS-CoV-2 vaccine by infection of Vero cells. While vaccine production with Vero cells in itself is not novel, the study's elaborate experimentation into the efficacy of different adjuvants as candidates during formulation is insightful in producing an effective product. Further, the inactivation procedures detail a robust operation to ensure the virus in the final product is safe for human use. This project will utilize and build upon these groundbreaking findings to recommend a feasible process design.

III. Design Basis

4.1 Target Market Analysis

Product Demand

People are racing to acquire immunity from COVID-19 through vaccination as the pandemic celebrates its 1st birthday in March 2021. The demand for this vaccine is of global concern, therefore the global population will be used to analyze this vaccine's market. The following visualization shows the expected demand for our product and is explained below.

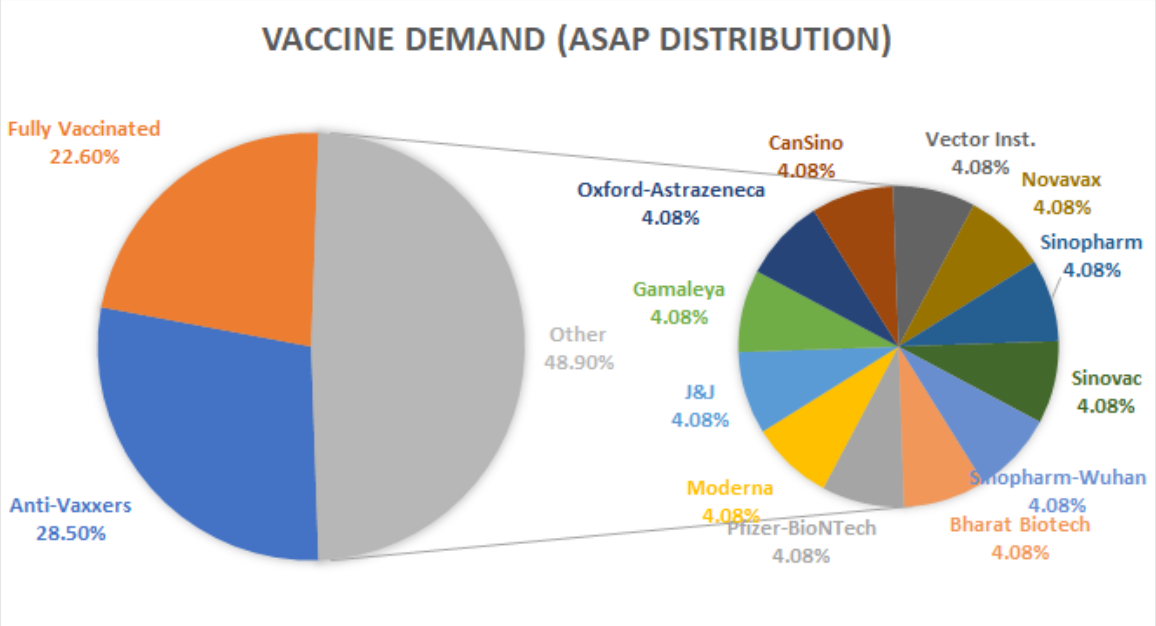

Figure 4.1a: Vaccine demand for global distribution, based on the current global vaccine necessity in April 2021.

In a study conducted by researchers of Carnegie Mellon University, it was found that approximately 28.5% of people globally do not have the intention of getting vaccinated against COVID-19 due to various concerns and/or religious objections. (Kish, 2021) This figure is labeled "Anti-Vaxxers" in Figure 4.1a. As of April 2021, 22.6% of the world's population is fully vaccinated (Our World in Data, 2021). This leaves 57.4% of the world's population still seeking

vaccination; this group is labeled “Other”. Currently, there are 12 vaccines that have been approved in different countries and are seeking approval globally, including Covaxin by Bharat Biotech (Zimmer, Corum & Wee, 2021). By dividing the “Other” group equally amongst all 12 companies, it was found that each company has the responsibility to vaccinate 4.8% of the world's population. Given that there are approximately 5.7 billion people in the world over the age of 16, and therefore, eligible for vaccination, each company will need to produce 273 million vaccines as soon as possible (Szmigiera, 2021). The Covaxin vaccine requires 2 doses, consequently necessitating the production of 545 million doses this year. The process outlined in this paper will be capable of producing 570 million doses in the first year of operation; the dosages exceeding global demand are expected to be lost in transit or expired before injection, etc.

In an endemic situation, people will need yearly boosters of this vaccine. This demand scenario is shown below.

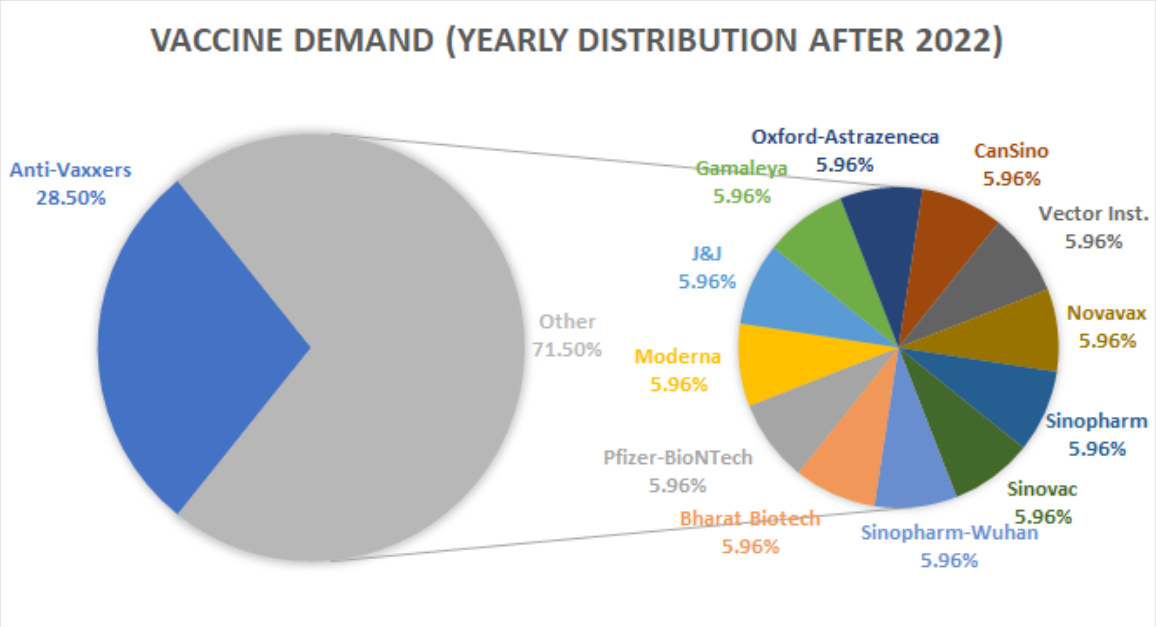

Figure 4.1b: Vaccine demand for global distribution, based on the yearly necessity in years following 2021.

Removing the “Fully Vaccinated” category from the pie chart, each company receives a greater vaccination responsibility in subsequent years. The number of vaccines needed per company per year based on the growing global population will be approximately 338 million. After the first year, the plant will be capable of operating at full scale and will produce 713 million doses per year (vaccinating 356.5 million people per year). Once again, the excess doses are made to mitigate any inevitable losses.

Product Pricing

Many countries have promised their residents that the COVID-19 vaccine will cost them nothing. The vaccines will be paid for by the government in trade agreements with private companies. These trade deals vary by company and by country, making it hard to predict the selling price of this product. Bharat Biotech released a statement stating they would sell their vaccine to the Indian government for $4 USD per dose, but no information is given for other countries (Ghosh, 2021). We will assume that Covaxin can be sold to other countries for an average price of $15 per dose, given information about prices of the other vaccines already in global distribution. (Hooker & Palumbo, 2020). These price scenarios are further analyzed in section 8.4: Financial Analysis.

4.2 Product Description

The final COVID-19 vaccine consists of two 0.5 mL doses, each containing 3 μg of whole-virion inactivated SARS-Cov-2 antigen with 250 μg of aluminum hydroxide, 15 μg of imidazoquinoline TLR 7/8 agonist, 2.5 mg of 2-phenoxyethanol, and up to 0.5 mL of phosphate buffer saline (Bharat Biotech, n.d.). After the purification process in the downstream, the product will contain 1.5 ng of host cell proteins- well below the acceptable concentration (Toinon et al., 2018). The final product will be sealed in multi-dose 10 mL vials, which provide twenty 0.5 mL doses in each vial. The complete composition of the vaccine is summarized in Table 4.2.

To guarantee the safety and the quality of the vaccine, the plant will be designed in accordance with current good manufacturing practices (cGMP) and other regulations, and the production will occur under an aseptic environment per CDC and OSHA guidelines.

Table 4.2: Final Product Composition

Component	Concentration (g/mL)
Inactivated SARS-Cov-2 antigen	1.20×10^{-5}
$Al(OH)_3$	5.00×10^{-4}
TLR 7/8	3.00×10^{-5}
2-phenoxyethanol	5.00×10^{-3}
Host Cell Proteins	3.24×10^{-6}

IV. Design Specifications

5.1 Upstream Processing

Upstream processing comprises of progressive cell growth via seed train and the production of SARS-CoV-2 virions by infection of mammalian host cells, Vero cells. Automation within the seed train minimizes the risk of contamination and increases conformity to optimal operating conditions. The purpose of the seed train is to generate a sufficient cell density to inoculate the bioreactors. A sufficient cell density is necessary to ensure a feasible fermentation timeline in the bioreactor and also mitigates the lag phase experienced by the mammalian cells when they are initially inoculated. The purpose of the bioreactor is to continue replicating the Vero cells then infect them to generate enough antigen to reach the target number of doses regardless of losses during downstream processing, where the contents of the bioreactor are refined.

5.1.1 Seed Train

The process of propagating frozen Vero cells from seed stock to bioreactor quantity requires 7 days to complete when factoring in intermittent sterilization and maintenance. Vero cells are epithelial, which mandates monolayer culture for both the flasks and subsequent cell factories. Frozen Vero cell stocks are first cultured in stages of shake flasks; culture volumes increase with each stage, and cells are promoted to the next stage when the cells reach 90% confluence. Cell quantity is estimated to double every 24 hours (Ammerman et al., 2008).

Shake Flasks

Frozen cell stocks (American Type Culture Collection, VERO C1008 [Vero 76, clone E6, Vero E6]) are thawed on ice before bench-top centrifugal separation and discarding of its travel

media. The cells are then resuspended in media within a 175 cm^2 culture flask (T175, Thermo-Fisher). Next, the culture is incubated until cell proliferation reaches the requisite 90% confluence. An iterative solution approach was used, given the known cell quantity needed to seed the bioreactor, and the production goal for this step in the process to take approximately one week when all stages are run simultaneously. Shake flask stage information and schedule are detailed in Table 5.1.1a.

Table 5.1.1a: Details and Schedule for Shake Flask Serial Cultures

Stage 1		**Stage 2**		**Stage 3**	
Frozen Stock into T175		**T225 Flasks, qty=2**		**T225 Flasks, qty=10**	
Details:		**Details:**		**Details:**	
Required Cell Density to Seed Next Stage (cells/cm^2)	1.50E+04	Required Cell Density to Seed Next Stage (cells/cm^2)	1.50E+04	Required Cell Density to Seed Next Stage (cells/cm^2)	1.50E+04
Vessel type	T175 Flask	Vessel type	T225 Flask	Vessel type	T225 Flask
Culture area (cm^2)	175	Total culture area (cm^2)	450	Total culture area (cm^2)	2250
Vessel Qty	1	Vessel Qty	2	Vessel Qty	10
Cell Count input (cells)	3.00E+06	Cell Count input (cells)	6.75E+06	Cell Count input (cells)	3.38E+07
Cell Count to seed next step	6.75E+06	Cell Count to seed next step	3.38E+07	Cell Count to seed next step	4.93E+08
Media Volume Required (mL):	50	Media Volume Required (mL):	128.57	Media Volume Required (mL):	642.86
Schedule:		**Schedule:**		**Schedule:**	
Hours since inoculation:	**cell count:**	**Hours since inoculation:**	**cell count:**	**Hours since inoculation:**	**cell count:**
0	3.00E+06	0	6.75E+06	0	3.38E+07
24	6.00E+06	24	1.35E+07	24	6.75E+07
48	1.20E+07	48	27000000	48	1.35E+08
		72	5.40E+07	72	2.70E+08
				96	5.40E+08

High-Density Cell Factory

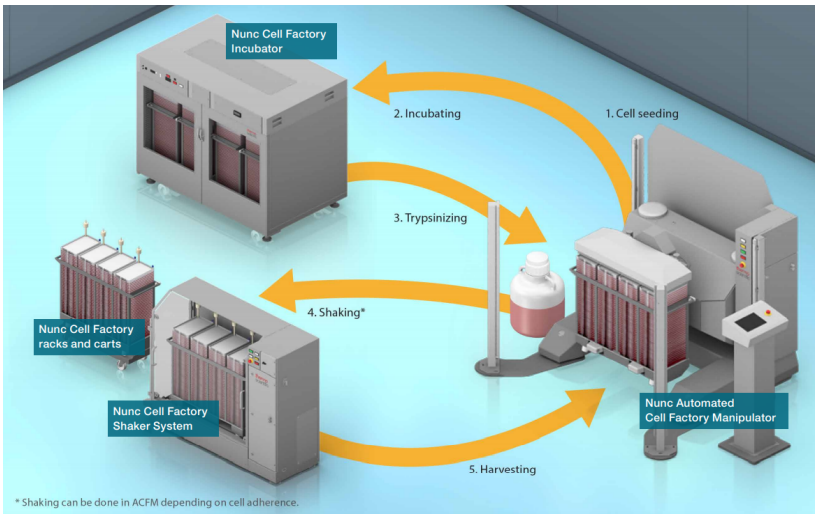

Figure 5.1.1a: Work flow diagram of cell factory seed train (ThermoFisher, 2020)

A programmable pumping and incubation system designed around their 52-tray cell factories is utilized to reach the final culturing volume before loading the cells to the bioreactor. The workflow of this system is shown above in Figure 5.1.1a by an illustration from Thermo-Fisher. The left side of the image shows a rack that contains four cell factories. The system consists of three main operations: an incubator, a programmable filling/draining unit, and a shaker to remove adhered cells from cell factory surfaces. In addition to the media volume of each stage, 0.25% trypsin-EDTA is added to aid dissociation of the culture in the shaker. Trypsin is an enzyme that helps remove the cell culture from the surface of the growth trays. Table 5.1.1b shows the details for the cell factory stages. All five stages are to be run concurrently. The longest stage requires 5 days. As a conservative estimate to include time for sterilization and maintenance, the seed train section of the process is estimated to take seven days to complete.

Table 5.1.1b. Details and Schedule for Cell Factory Stages of Seed Culture Scaling

4		5	
Cell Factory 1		**Final Step Before Bioreactor**	
Details:		**Details:**	
Required Cell Density to Seed Next Stage (cells/cm^2)	1.50E+04	Required Cell Density to Seed Next Stage (cells/cm^2)	2.80E+04
Vessel type	52 layer high density cell factory	Vessel type	52 layer high density cell factory
Culture area (cm^2)	32864	Culture area (cm^2)	525824
Vessel Qty	1	Vessel Qty	16
Cell Count input (cells)	4.93E+08	Cell Count input (cells)	7.89E+09
Cell Count to seed next step	1.47E+10	Cell Count to seed next step	2.00E+11
Media Volume Required (mL):	10,400	Media Volume Required (mL):	166,400
Schedule:		**Schedule:**	
time since inoculation (h):	**cell count:**	**time since inoculation (h):**	**cell count:**
0	4.93E+08	0	1.47E+10
24	9.86E+08	24	2.94E+10
48	1.97E+09	48	5.89E+10
72	3.94E+09	72	1.18E+11
96	7.89E+09	96	2.36E+11
120	1.58E+10	120	**4.71E+11**
		144	**9.42E+11**

5.1.2 Bioreactor

SARS-CoV-2 Growth Kinetics

Chu et al. (2020) investigated similarities in replication kinetics, cell damage, and cellular susceptibility between SARS-CoV and SARS-CoV-2; the authors determined SARS-CoV-2 caused milder cell damage and exhibited equivalent virus production and susceptibility in Vero cells (p. e18). SARS-CoV growth in Vero cells was studied by Ng et al. in 2003.

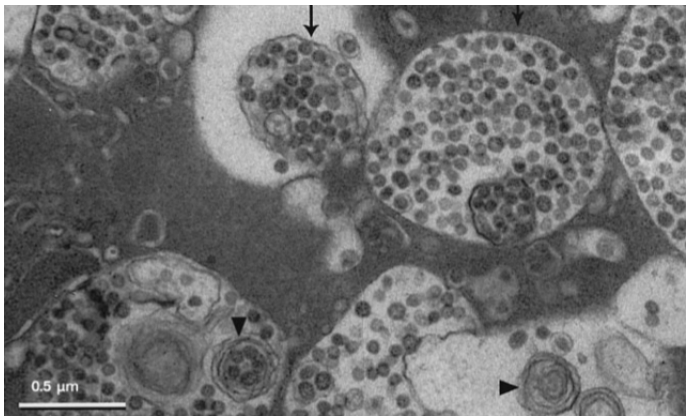

Figure 5.1.2a: Ng, M. L. et al. (2003). Proliferative growth of SARS coronavirus in Vero cells. Journal of General Virology, 84(1), 3291-3303. doi: 10.1099/vir.0.19505-0

They reported a five-hour latent period, and at 12 hours post-infection, the mature virus was expelled into the titer and was also contained in large vacuoles in the cytoplasm of the cells (Ng et al., 2003, p. 3291-3302). Those vacuoles contained virus particles with different maturity levels, virus particles with surface spikes present are the desired antigen in this production process (Ng et al., 2003, p. 3291). It was determined from this paper that at least fifty percent of the Vero cells would be infected 15 hours post-infection and approximately fourteen percent of the Vero cell volume is occupied by mature SARS-CoV virions (Ng et al., 2003, p. 3299). A multiplicity of infection (MOI) of 0.001 was used in this study and will be used in our manufacturing process to ensure comparable virus production (Ng et al., 2003, p. 3293). Jiang et

al. (2019) determined an MOI of 0.0001 resulted in an extended stationary Vero cell growth phase and a higher virus titer than an MOI of 0.01, at the same time of infection (p. 160). Using an MOI smaller than 0.01, and the extended stationary cell growth phase it creates, allows some flexibility in the bioreactor schedule to allow for specialized apoptosis.

Vero Cell Growth Kinetics

Vero cell growth in the bioreactor is modeled using Monod kinetics, the empirical Monod equation is shown below. In equation 5.2.1a, [S] represents the concentration of substrate and μ represents the specific growth constant, the other variables are described in Table 5.1.2a. We assume that Vero cell growth is limited by nutrient availability, cell decay is negligible compared to cell growth and the VPSFM media does not supply additional carbon-based nutrients. L-Glutamine, suggested by ThermoFisher Scientific, will be the substrate in the bioreactor (ThermoFisher Scientific, n.d., p. 1). Time-course data for substrate concentration, Vero cell density, OUR, and GUR are shown below in Figure 5.1.2b and are based on the parameters in Table 5.1.2a.

$$\mu = \mu_{max} * \frac{[S]}{[S] + K_s} \qquad \text{(Eqn. 5.1.2a)}$$

Table 5.1.2a: Monod Model Parameters

Parameter	Symbol	Value
Maximum Specific Growth Rate	μ_{max}	0.026
Substrate Yield Coefficient	$Y_{x/s}$	0.6
Monod Constant	K_s	1

Data specifically about L-glutamine is not available for Vero cell growth. Therefore, the parameters were based on yields and Monod constants for Glutamax and glucose (Petiot et al., 2010).

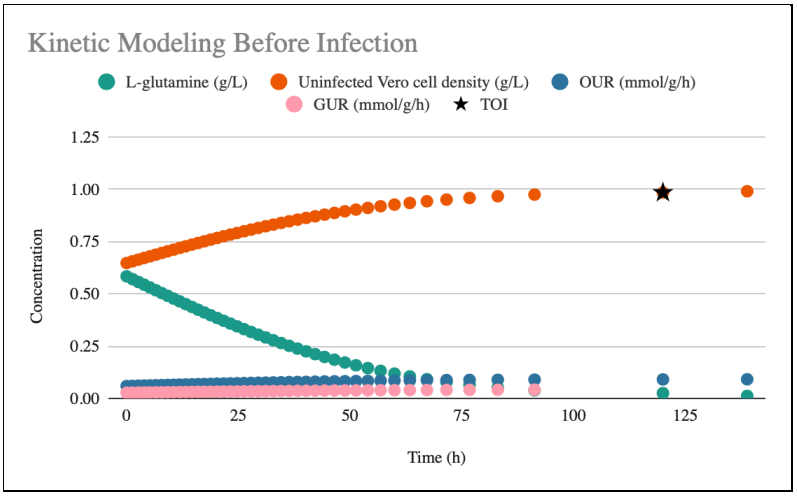

Figure 5.1.2b: Monod Kinetic Model of Vero cell Growth on Cytodex-1 Microcarriers

Based on the model, 120 hours after inoculation, there will be 3.8 x 10^{11} Vero cells present. An additional 72.58 grams of L-Glutamine will be added with the virus stock at the TOI, all of the glutamine in the bioreactor will be depleted after 16 hours, which will induce apoptosis. We assume that 80% of the mature virions will be in the cell lysate through a combination of exocytosis and apoptosis. Based on a total Vero cell lysing rate of 80%, an infection rate of 50%, and mature virions constituting over thirteen percent of the volume inside the Vero cells, 53 grams of the virus will exit each 1000 L bioreactor. The total processing time for the bioreactor is 142 hours excluding necessary maintenance and preparation.

Microcarrier Preparation

According to the instructions given by GE, 146 grams of dry Cytodex-1 microcarriers need to be added to a siliconized glass bottle with 7.3 liters of Ca^{2+}, Mg^{2+} free PBS and allowed to swell for three hours at room temperature with occasional, gentle agitation (GE, 2005, p. 112). The remaining PBS will be decanted and the swollen microcarriers will be washed with 5.8 liters of fresh PBS (GE, 2005, p. 112). The PBS will be replaced again before the bottle is placed into an autoclave for two cycles at 115℃ and 15 psi for 15 minutes each (GE, 2005, p. 112,

Synthecon, n.d., p. 13). The microcarriers will be allowed to settle, the supernatant will be decanted, and the microcarriers will be washed with 5.8 liters of warm VPSFM before use (GE, 2005, p. 112). This process will take approximately four hours.

Bioreactor Design Target

The operating parameters for the bioreactor will be compared to a design target based on Vero cell oxygen uptake rate at the maximum cell concentration, as determined through the kinetic analysis above. Those values are compiled in Table 5.1.2b.

Table 5.1.2b: Design Target Parameters

Parameter	Symbol	Value
Cell Concentration	X	0.975 g/L
Oxygen Uptake Rate	q_{O2}	0.0925 $\frac{mmol\ O^2}{g-h*X}$
Oxygen Transfer Coefficient	kLa	8.47 hr^{-1}

Agitation of the cell slurry is another important design target to be considered for this bioreactor. Grein et al. (2019) concluded that for microcarriers with diameters ranging from 150 to 250 μm, agitation rates should be lower than 79 RPM (Grein et al., 2019, p. 8) to prevent excessive cell damage. Agitation rates lower than 79 RPM, equivalent to shear stress values lower than 0.12$\frac{N}{m^2}$, results in greater energy dissipation through eddies that influence suspension than microcarrier interactions that cause cell damage (Grein et al., 2019, p. 8-9). The axial and radial flow of pitched-blade impellers allow for gentle, efficient mixing and creates higher oxygen transfer rates, making them ideal for shear-sensitive, oxygen-exhaustive Vero cells (Mirro & Voll, 2009, p. 52-53). The agitation speed for minimal shear needs to be balanced with the speed necessary to achieve microcarrier suspension in the bioreactor.

Sufficient microcarrier suspension generates optimal interfacial area between the solid and liquid phases and mitigates accumulation at the bottom of the bioreactor (Tagawa et al., 2006, p. 818). Complete suspension of solid particles occurs when the liquid velocity at the bottom of the tank is significantly greater than the settling velocity of the solid particles. The minimum rotation speed required to achieve complete suspension can be calculated using Zwietering's correlation (Equation 5.1.2a). With the parameters for a pitched-blade impeller listed below in Table 5.1.2b, the minimal rotation speed for complete suspension is 100 RPM.

$$n_c D_i^{0.85} = S v^{0.1} D_p^{0.2} \left(g \frac{\Delta\rho}{\rho}\right)^{0.45} B^{0.13} \qquad \text{(Eqn. 5.1.2b)}$$

Table 5.1.2c: Zwietering's Correlation Parameters

Parameter	Symbol	Value
Impeller Diameter	D_i	0.36 m
Shape Factor	S	4.2
Average Particle Size	D_p	1.9×10^{-4} m
Kinematic Viscosity of the Liquid	v	$6.96 \times 10^{-7} \frac{m^2}{s}$
Gravitational Acceleration Constant	g	$9.81 \frac{m}{s^2}$
Difference Between Particle and Liquid Density	Δρ	$9.64 \frac{kg}{m^3}$
Liquid Density	ρ	$993.36 \frac{kg}{m^3}$
Weight of Solid Particle per Weight of Liquid	B	0.003

Ankur (2016) determined the shape factor of a reactor system with these design specifications. The proximity to this value will gauge the type of suspension achieved in the bioreactor. The mathematical algorithm used to design a bioreactor with the above growth and suspension targets is explained below.

Bioreactor Design Specifications

The bioreactor must be designed to ensure the cell and virus growth kinetics as outlined above. The relevant criteria pertinent to the design include sufficient microcarrier agitation, appropriate oxygen mass transfer within the media, and a low shear environment for the Vero cells. All three of these parameters are interconnected and they each depend on reactor geometry, aeration rate, and impeller characteristics. Therefore, the design of the bioreactor is an iterative process that requires the guess-and-check method to find the optimal operating parameters. The steps to the design algorithm are as follows.

First, the design targets and constraints of the system are specified (Table 5.1.2b). The specific oxygen uptake rate (OUR) of infected Vero cells in serum-free media was found by Oller et al. (1989) to be 2.40×10^{-10} mmol O2/(cell*h). Importantly, this OUR represents a system that is not limited by mass transfer, therefore, it is referred to as OUR_{max}, since bioreactors are typically limited by oxygen mass transfer to cells. The oxygen saturation concentration (C*) in the media at 37℃ was found to be .00663g/L, found from a water/oxygen saturation curve (source?). The critical oxygen concentration ($C_{O2,\ critical}$) of the system was found through the following equation:

$$C_{O2,critical} = C^{*} * \frac{P_{O2}}{P_{atm}} \qquad \text{(Eqn. 5.1.2c)}$$

Where P_{O2} is the partial pressure of oxygen in the atmosphere and P_{atm} is atmospheric pressure. This equation yields $C_{O2,\ critical}$ as 0.00139 g/L. The physical fluid properties of the media (density and viscosity) were assumed to be those of water. The target oxygen transfer coefficient (kLa), which represents the capacity of the bioreactor to transfer oxygen into the cultures, was found using the following equation:

$$kLa_{target} = \frac{OUR_{max}}{C^{*} - C_{O2,crit}} \qquad \text{(Eqn. 5.1.2d)}$$

Where kLa is in unit h^{-1}.

The next step in the design algorithm is to specify the geometry and dimensions of the bioreactor. Standard geometry was selected for the bioreactor, due to the vast amount of research and literature on design correlations for this geometry. Standard geometry is defined as a cylindrical bioreactor that is as wide as it is tall (ie. $D_t=H_t$). Additionally, the impeller diameter will be one-third of the tank diameter ($D_i/D_t=⅓$). It was decided that the bioreactor would have a working volume of 1000 L to produce the viral kinetics needed to achieve the vaccine production goals in a year. With these three equations solved simultaneously, the tank height and diameter were calculated to be 1.083 m. The impeller diameter is therefore 0.361 m. Polyethylene single-use bags will be placed on the inside of each bioreactor, but we assume that they will not interfere with standard geometry.

Next, an iterative loop is used to "guess and check" multiple variables until six "rules of thumb" are satisfied in the design algorithm. These six rules of thumb for bioreactor design were determined for microbial systems, but will serve as a basis for our mammalian system until further testing can be done. The variables that are to be "guessed" are impeller rotation rate (N), volumetric air inflow rate (Q_g), and the number of impellers (N_i). Q_g can be picked first, and must be chosen to satisfy the first rule of thumb:

$$v_s = \frac{Q_g}{\pi D_t^2/4} < 125\text{m/h} \qquad \text{(Eqn. 5.1.2e)}$$

Where v_s represents the superficial gas velocity. The superficial gas velocity must be lower than 125m/h to prevent gas slugging. The chosen value of Q_g must also satisfy the second rule of thumb, intended to prevent gas flooding:

$$Q_g \leq 0.6\left(\frac{D_i^5 N^2}{D_t^{1.5}}\right) \qquad \text{(Eqn. 5.1.2f)}$$

Where N is an impeller rotation rate in revolutions per second.

The number of impellers (N_i), must be chosen to satisfy the third rule of thumb:

$$\frac{H_t - D_i}{D_i} \geq N_i \geq \frac{H_t - 2D_i}{D_i} \quad \text{(Eqn. 5.1.2g)}$$

and

$$3 \geq N_i \quad \text{(Eqn. 5.1.2h)}$$

The fourth rule of thumb requires a certain impeller tip speed (s) to ensure sufficient sheer for good gas dispersion:

$$s = \pi N D_i \geq 2.5\text{m/s} \quad \text{(Eqn. 5.1.2i)}$$

The fifth rule of thumb is based on power consumption, which can be calculated through the following steps. First, the Reynolds Number (Re) can be calculated by the following equation:

$$Re = \frac{\rho D_i^2 N}{\mu} \quad \text{(Eqn. 5.1.2j)}$$

Where ρ is media density in kg/m^3 and μ is media viscosity in Pa*s. Next, the Power Number (N_P) for the pitch blade turbine must be determined from an experimental curve relating the Power Number to the Reynolds Number. This curve can be seen in Figure 5.1.2c below:

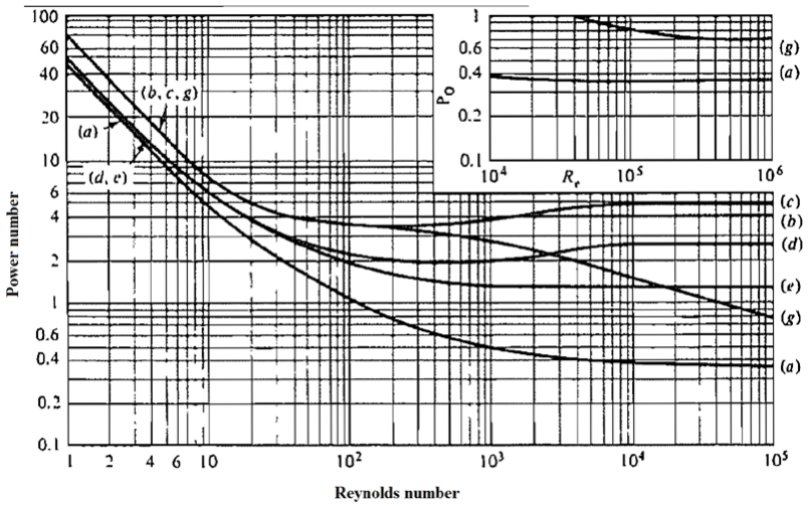

Figure 5.1.2c: Power number for agitation impellers. Line (e) represents pitched blade turbines. (Mayvan et al. 2014)

The power input to an ungassed system can be calculated using the following equation:

$$P_r = N_p * \rho * N^2 * D_i^5 \qquad \text{(Eqn. 5.1.2k)}$$

Where P is power in watts. This system is gassed, therefore, requiring additional calculation. The aeration number (N_a), can be calculated using the following equation:

$$N_a = \frac{Q_g}{N(D_i)^2} \qquad \text{(Eqn. 5.1.2l)}$$

The following curve can be utilized to determine the power requirement of a gassed (ie. aerated) system:

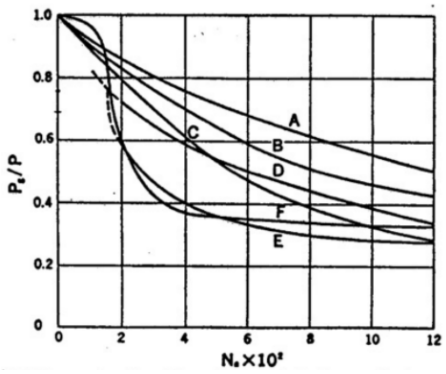

Figure 5.1.2d: Power requirements for agitation in a gassed system with standard geometry. Line F represents a pitch blade impeller. (Prpich, 2021)

The power requirement of a gassed system (P_g), can be determined by multiplying the P_g/P_r value from Figure X with the ungassed power (P_r) from Eqn. X. The fifth rule of thumb refers to the value P_g/P, which significantly impacts both capital and operating costs. Therefore, the following rule should be maintained (Prpich, 2021):

$$P_g/V \leq 15,000 \text{W/m}^3 \qquad \text{(Eqn. 5.1.2m)}$$

Finally, the sixth and final rule of thumb requires that the system's kLa value is within 10% error of the design target as specified at the beginning of this section. The operational kLa can be calculated using a correlation for our system's geometry and impeller, shown below:

$$kLa = 0.002 * \left(\frac{P_g}{V}\right)^{0.5} * \left(v_s\right)^{0.4} \qquad \text{(Eqn. 5.1.2n)}$$

These equations were solved simultaneously to yield the following bioreactor design parameters, which satisfies 5 rules of thumb, shown in Table 5.1.2d. These rules are specified for microbial growth in bioreactors, so a tip speed lower than 2.5 m/s may be acceptable for mammalian cells. This Q_g supplies the cells with enough oxygen to replicate and the rotation speed selected is within 30% of the critical speed needed for complete suspension. According to MilliPoreSigma (2018) this value is sufficient for off-bottom suspension, which is ideal for slurries that need to be pumped out of a reactor (p. 6).

Table 5.1.2d: Bioreactor Design Parameters

Variable	Value	Unit
Q_g	0.001	m^3/min
N	74	RPM
N_i	1	unitless

5.2 Downstream Processing

Downstream processing entails antigen purification steps that isolate and concentrate the target molecule, remove contaminants, and remove trace impurities. All approved drugs in a given nation must go through this purification process to ensure that the product is of sufficient standards and is safe for human consumption. The most significant impurities to be removed from the antigen slurry are DNA and host cell protein (HCP) products from the lysis of the Vero cells in upstream processing. Toinon et al. (2018) cites that HCP concentrations should be in or below the range of 20-30 ng/mL for an injectable vaccine. The following downstream process is capable of reducing the HCP concentration to 3.24 ng/mL, far below this ceiling value.

5.2.1 Microcarrier Separation

Microcarrier separation is a unit operation specifically designed to remove Cytodex microcarriers from media using a semipermeable membrane. The membrane chosen for microcarrier separation is the Harvestainer BioProcess Container which is a single-use bag made by Thermo Scientific. The average pore size of Cytodex-1 is 190 um with a range of 147-248 um for 90% of beads (GE Healthcare, 2009). The Harvestainer bag is rated to retain all microcarriers above 90um in size. The design assumes based on manufacturer-provided studies that 100% of microcarriers are retained in the bag. Due to the pore size distribution, only 85% of detached cells can pass through the membrane (ThermoFisher, 2018). Similarly, most proteins and viruses are significantly smaller than 90um so it is assumed that all pass through the membrane, yielding 100% recovery.

		Cytodex 1	Cytodex 3
Density* (g/ml)		1.03	1.04
Size*	d_{50} (µm)	190	175
	d_{5-95} (µm)	147–248	141–211
Approx. area* (cm^2/g dry weight)		4400	2700
Approx. no of micro-carriers/g dry weight		4.3×10^6	3.0×10^6
Swelling factor* (ml/g dry weight)		20	15

Size is based on diameter at 50% of the volume of a sample of microcarriers (d_{50}), or the range between the diameter at 5% and 95% of the volume of a sample of microcarriers (d_{5-95}). Thus size is calculated from cumulative volume distributions.

* in 0.9% NaCl.

Figure 5.2.1a: Physical Characteristics of Cytodex Microcarriers (GE Healthcare, 2009).

The maximum pressure that can be placed across the membrane is 0.5 psi and flow rates are recommended to be below 6.7 L/min (ThermoFisher, 2017). Based on manufacturer studies, a flow rate higher than 6.5 L/min performs well and similarly has 100% microcarrier separation. Therefore a 6.5 L/min flow rate will be used in this design (ThermoFisher, 2017). At a full capacity of 3000L, it will take 7.7 hours to filter all media.

The final design parameter is the holding capacity of the Harvestainer bag. From Thermo Scientific, the holding bags come in 3, 12, 25, or 50L in bag sizes to hold the microcarriers. Based on the bioreactor design, the expected volume of microcarriers to be used is 10-15 L. The bag chosen for the separation is the 25 L size to ensure all the microcarriers are captured.

5.2.2 Microfiltration with TFF

Microfiltration is a variety of filtration in which size-based separations may be achieved through a semipermeable membrane. Microfiltration is defined by the usage of membranes with pore sizes between 0.1-10 nm (Carta, 2020). Pores of this size are intended to retain contaminants such as whole Vero cells, large proteins, or other cell debris while allowing smaller particles such as virions to pass through the membrane. Tangential flow filtration (TFF) is a

filtration technique in which the starting solution passes tangentially along the surface of the filter membrane. Figure 5.2.2a below illustrates the general scheme of a TFF system.

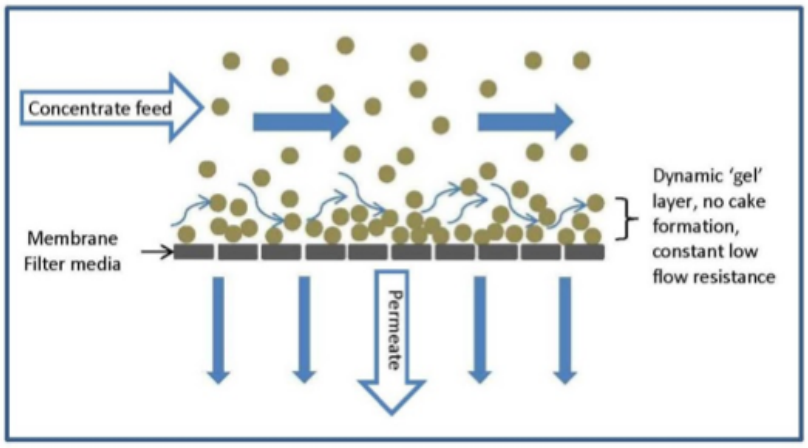

Figure 5.2.2a: (Porex Filtration, 2021)

The retentate is circulated through the system, continuously passing over the membrane until the desired separation is achieved. An important feature of TFF is that the flow of fluid across the membrane sweeps away any buildup of material on the filter surface and prevents filter fouling, a common obstacle in membrane filtration. The key operational parameter in TFF design is permeate flux through the membrane. Flux data is experimentally determined and is dependent on the applied trans-membrane pressure (TMP), in addition to the fluid properties of the feed solution.

Due to the necessity of cleaning and performing quality tests on reusable filters, it was determined that single-use membranes would be the most economically appropriate choice for batch ultrafiltration. Previous literature has highlighted that hollow-fiber tube membranes are optimal for the purification of virions due to their open-channel architecture and low shear stress within the system as compared to flat plate membranes (Mundle and Anderson, 2013). Low shear is very important for this system, as active virus particles are shear sensitive and require

gentle processing (Wolf & Reichl, 2011). Figure 5.2.2b below shows the configuration of a tubular hollow fiber cartridge.

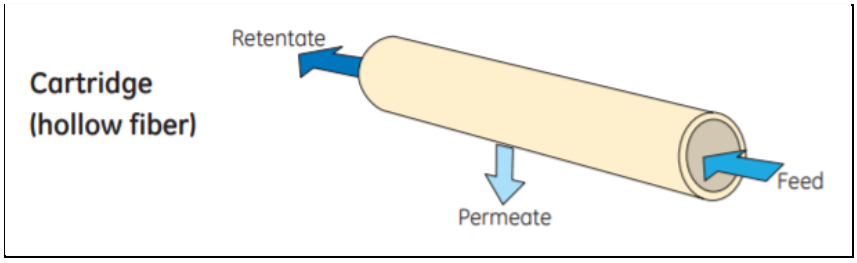

Figure 5.2.2b: Configuration of a tubular hollow fiber cartridge (GE Healthcare, 2014)

The next consideration in membrane selection is pore size. Microfiltration membranes are typically marketed in terms of pore size. The approximate size of a single Sars-CoV-2 particle is 0.1 um, signalling that a relatively large microfiltration membrane should be used to minimize the amount of virus retained by the membrane (Bar-On et al., 2020). Although Microfiltration membranes range from 0.1 - 10um kDa in size, research has found that filters with larger pores have a high tendency to fouling, because particulate material can penetrate and block the pores (GE Healthcare, 2014). For this reason, the largest pore size filters will be avoided. A 0.65 um pore size was selected for this process. The Sterile ReadyToProcess Hollow Fiber Cartridge, 0.65 um (Product Number RTPCFP-6-D-6S), by Cytiva Lifesciences meets all design specifications required. This membrane's operating handbook allows for the following selection of operational conditions.

The feed to microfiltration will be what has just left the microcarrier separation unit. Much published data for Cytiva Lifesciences's filters was conducted with a feed of water so the feed will be assumed to have similar properties.

The feed stream flow rate into microfiltration was chosen to be 6.6 L/min. This flow rate corresponds to a shear rate of ~2000 s^{-1}. This shear rate has been deemed appropriate for shear

sensitive streams, such as active virions. The pressure drop of the system is described as a linear function of feed flow rate. The following linear equation was determined from two data points provided by GE for a similar filter and assumed to be similar to the one chosen for this process.

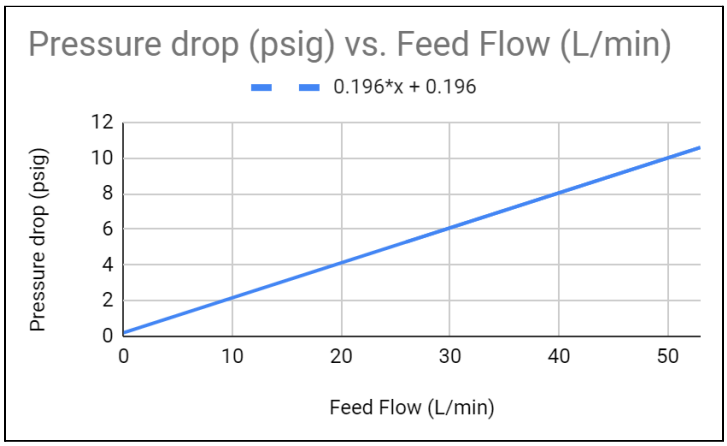

Figure 5.2.2c: Pressure drop across the UF membrane as a linear function of feed flow rate (GE Healthcare, 2005)

From the above plot, pressure drop across the membrane at the specified feed flow rate was determined to be 1.49 psig. GE cites the permeate flow rate as 4.7 L/min with a TMP of 5 psig at 25 ^{o}C. With each membrane's surface area of 4.9 m^2, the flux through each membrane is calculated by the following equation:

$$\Phi = \frac{Q}{A} * \left(\frac{1m^3}{1000L}\right) \qquad \text{(Eqn. 5.2.2a)}$$

Where Φ is flux in unit m/min, Q is permeate flow rate in L/min, and A is membrane area in m^2. Eqn. 5.2.2a is used to calculate the membrane's flux as 0.00096 m/min.

Assuming that no volume loss occurs in the previous downstream processing steps, an incoming volume of 1000-3000L will enter microfiltration. It was chosen that the stream retentate would be concentrated by a factor of 30. The permeate volume will change depending

on the output of the upstream processing for a particular batch. The decrease in batch volume needed achieve this concentration factor can be found using the following equation:

$$V = \frac{V_o}{(\frac{C}{C_o})^{\frac{1}{\sigma}}} \quad \text{(Eqn. 5.2.2b)}$$

Where V is concentrated batch volume in L, Vo is initial volume in L, C/Co is the concentration factor, and σ is the rejection coefficient of the virus. In this system, σ is 0.1, as will be explained in detail in the following mass balance paragraph. Using Eqn 5.2.2b, if a full scale batch is used the concentrated volume was determined to be 100L. Each filter capacity is given as 200 L/m^2. In order to treat all 3000L of bioreactor effluent simultaneously in microfiltration, the following equation was used to find the number of parallel filters needed:

$$\#\ of\ filters = \frac{V_o - V}{\alpha * A} \quad \text{(Eqn. 5.2.2c)}$$

Where α is the filter capacity in L/m^2. This equation reveals that 2.9 filters are needed, which is rounded up to 3 filters. Finally, the process time of the microfiltration unit can be determined using the following equation:

$$t = \frac{V_o - V}{\Phi * A * (\#\ of\ filters) * (1000 L/m^3)} \quad \text{(Eqn. 5.2.2d)}$$

Where t is processing time in minutes. The time requirement at full scale of this microfiltration step is 3.4 hours.

In calculating the filtration efficiency of the microfiltration unit operations, assumptions about host cell proteins size and quantity must be made due to lack of published data about Vero cell lysate. Kornecki et al. (2017) found that mammalian host cell proteins (HCP) range in size from 10-200 kDa. Also, Thermofisher reports that HeLa cells, a well published human cell line, contain about 300 pg of HCP per cell (ThermoFisher, n.d.) . This number will be used as an HCP quantity estimation for Vero cell lysate due to the structural similarities between the cell lines.

With these numbers, it was assumed that 33% of HCP will be “small” (10-50 kDa), 33% will be “medium” (50-100 kDa), and 33% will be “large” (100-200 kDa). The membrane’s rejection of different components by weight can be estimated using the following experimentally determined rejection curve. While this specific curve shown below is a different filter size, the curve is similar for three other filter sizes when comparing percentage rejection and distance from filter size so the curve is also utilized for the microfiltration filter chosen.

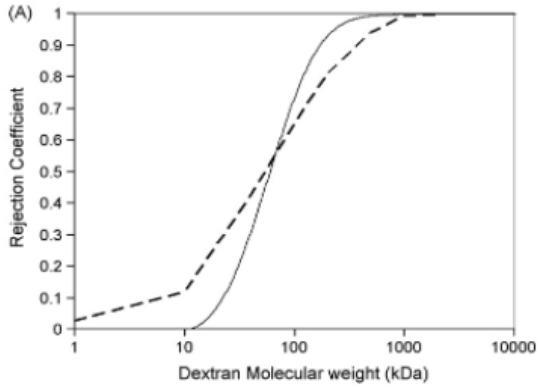

Figure 5.2.2d: 300 kDa filter rejection curve (Wickramasinghe et al., 2009)

From Figure X, it is observed that the rejection coefficient of Sars-CoV-2 is around 0.1. The rejection coefficients of small, medium and large HCP are approximated to be 0.001, 0..02, and 0.05 respectively. The fraction of each size HCP exiting DF and moving on to affinity chromatography can be calculated by the following equation:

$$HCP_i = \left(\left(\frac{V_o}{V}\right)^{\sigma_i - 1}\right) * e^{-\frac{V_w}{V_o}*(1-\sigma_i)} \quad \text{(Eqn. 5.2.2e)}$$

Where HCP_i represents the fraction of HCP of size *i* exiting microfiltration, and σi represents the rejection coefficient of HCP of size *i*. Using the HaLa estimation of total HCP per cell and combining retained HCP fractions, it was determined that microfiltration will remove 99.9% of

total Vero cells that enter microfiltration. Microfiltration will allow 95.32% of virion to pass through as well as 96.37% of HCP.

5.2.3 Benzonase Treatment

Microfiltration removes whole Vero cells from the slurry leaving the bioreactor, but Vero cell DNA and RNA remain. The removal of Vero cell nucleic acids will reduce the viscosity of the slurry and facilitate processing. Nuclease enzymes cleave phosphodiester bonds in nucleic acid chains (Rittié & Perbal, 2008, p. 35). Exonuclease enzymes require free 5' phosphate or 3' hydroxyl ends to initiate a reaction. Endonuclease enzymes cleave bonds internally at specific sequences (Chauhan, 2020, p. 3-5). This specificity results in oligonucleotides with uniform lengths, making them ideal for applications where complete digestion is desirable (Chauhan, 2020, p. 4). Millipore Sigma's Benzonase® Nuclease, derived from Serratia marcescens, degrades nucleic acids without breaking down proteins and retains activity after several months of refrigeration (Millipore Sigma [MS], n.d.a, p. 1, MS, n.d.b, p. 1). For optimal activity, Benzonase® Nuclease requires 1-2 mM of Mg2+ and a pH range between 8.0-9.2 (MS, n.d.a, p. 1, MS, n.d.b, p. 1).

Assuming all of the Vero cell DNA and RNA make it to this unit operation reduces the potential of those nucleic acids being present in the final formulation of the vaccine. With a maximum cell density dictated by the amount of L-Glutamine available in the reactor, the maximum number of Vero cells leaving the reactor would be 3.83×10^{11} (Jiang et al., (2019, p. 159). Assuming 80% of Vero cells undergo lysis, nucleic acids from 3.06×10^{11} cells will be available for treatment. According to Noorafshan et al. (2016), the size of the nucleus of a Vero cell post-inoculation does not vary significantly over time (p. 37). Therefore, its volume is 5×10^{-14} L (Noorafshan et al., 2016, p. 40). According to Cao et al. (2012), Vero cell DNA has a

density of 6.4 x 10^{-2} g/L (p. 413). Therefore, the treatment will need to digest 9.7 x 10^{-4} grams of DNA. This calculation assumes Vero cell DNA occupies the volume of the nucleus.

The unit definition of Benzonase® Nuclease communicates the amount of enzyme that results in ΔA_{260} = 1.0 optical density units in 30 minutes at a pH of 8.0 and 37° C (MS, n.d.a, p. 1). An absorbance reading of 1.0 converts to the digestion of 3.7 x 10^{-5} grams of single-stranded DNA, a smaller amount than double-stranded DNA, and approximately equal to the amount of single-stranded RNA (MS, n.d.c, p. 3). 3.49 x 10^{-4} L of Benzonase® Nuclease would be needed to digest all of the Vero cell DNA and RNA from 3.06 x 10^{11} cells. To ensure DNA is not detectable by Southern blotting, the incubation time for the treatment should be 24 hours (Novagen, 2012, p. 3).

Units of Benzonase® Nuclease need to be diluted in a Tris-HCl buffer solution to ensure optimal enzymatic activity. This solution consists of 50 mM Tris HCl pH 8.0, 1 mM $MgCl_2$, and 0.1 mg/ml BSA, a carrier protein that ensures viability during storage, at 37° C (Novagen, 2012, p. 3). Additional HCl may be required to maintain the pH of the reactor. We assume that the buffer exchange will remove ionic components, and the amino acid chains will leave in the retentate during Ultrafiltration/Diafiltration.

Table 5.2.3: Molecular Weights of Treatment Components in kDa

Component	Molecular Weight
BSA	66.50
Benzonase® Nuclease	30.00
Oligonucleotides	1.54

These molecular weights were compiled from “Bovine serum albumin” (2021), MilliPoreSigma (2020), and ThermoFisher Scientific (n.d.c) respectively.

5.2.4 Ultrafiltration/Diafiltration

Ultrafiltration is a variety of filtration in which size-based separations may be achieved through a semipermeable membrane. Ultrafiltration is defined by the usage of membranes with pore sizes between 2-30nm (Carta, 2020). Pores of this size are intended to retain macromolecules such as virions and/or proteins while allowing smaller particles to pass through the membrane. An important distinction can be made between the two typical unit operations that achieve separations within the ultrafiltration spectrum, “ultrafiltration (UF)” and “diafiltration (DF)”. UF is used to decrease the fluid volume of a batch solution in an effort to concentrate macromolecules. Alternatively, DF is used to exchange the buffer in which the macromolecules reside. These two unit operations are completed in series, typically using the same ultrafiltration membrane.

Tangential flow filtration (TFF) is a filtration technique in which the starting solution passes tangentially along the surface of the filter membrane. Figure 5.2.4a below illustrates the general scheme of a TFF system.

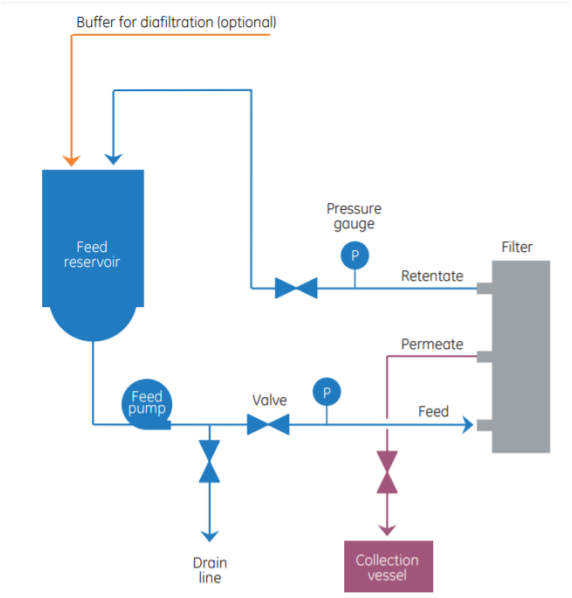

Figure 5.2.4a: Schematic of an ultrafiltration/diafiltration TFF system. (GE Healthcare, 2014, pp. 10)

The retentate is circulated through the system, continuously passing over the membrane until the desired separation is achieved. An important feature of TFF is that the flow of fluid across the membrane sweeps away any buildup of material on the filter surface and prevents filter fouling, a common obstacle in membrane filtration. TFF is beneficial for systems in which it is desired to directly recover material in the retentate (such as large virus particles), since the retentate remains as a solution. (GE Healthcare, 2014, pp. 6-7) The key operational parameter in UF/DF design is permeate flux through the membrane. Flux data is experimentally determined and is dependent on the applied trans-membrane pressure (TMP), in addition to the fluid properties of the feed solution.

Due to the necessity of cleaning and performing quality tests on reusable filters, it was determined that single-use membranes would be the most economically appropriate choice for batch ultrafiltration. Previous literature has highlighted that hollow-fiber tube membranes are

optimal for the purification of virions due to their open-channel architecture and low shear stress within the system as compared to flat plate membranes (Mundle and Anderson, 2013). Low shear is very important for this system, as active virus particles are shear sensitive and require gentle processing (Wolf & Reichl, 2011). Figure 5.2.5b below shows the configuration of a tubular hollow fiber cartridge.

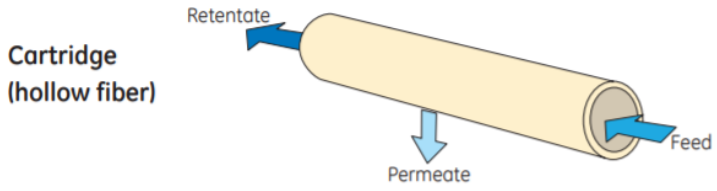

Figure 5.2.4b: Configuration of a tubular hollow fiber cartridge (GE Healthcare, 2014).

The next consideration in membrane selection is pore size. Ultrafiltration membranes are typically marketed in terms of molecular weight cut off (MWCO), representing the size designation, in Daltons, of globular proteins that are 90% retained by the membrane (Cytiva, 2021). The approximate size of a single Sars-CoV-2 particle is 10^6 kDa, signalling that a relatively large UF membrane should be used to maximize impurity filtration (Bar-On et al., 2020). Although UF membranes range from 10-500 kDa in size, research has found that filters with larger pores have a high tendency to fouling, because particulate material can penetrate and block the pores (GE Healthcare, 2014). For this reason, the largest pore size filters will be avoided. A 300 kDa MWCO offers the best balance between minimizing fouling and maximizing filtration efficiency, and therefore will be selected for this process. The Sterile ReadyToProcess Hollow Fiber Cartridge, 300 kDa (Product Number RTPUFP-30-C-55), by GE Healthcare meets all design specifications as described above. This membrane's operating handbook allows for the following selection of operational conditions.

Much published data for GE Healthcare's filters was conducted with a feed of water. The feed to UF will have just left the benzonase endonuclease treatment reactor as described in the previous section, allowing the assumption that all cellular DNA and RNA will be broken up into nucleic acids. In designing the operational parameters for UF, it is assumed that the cell lysate after depth filtration and benzonase treatment will have the fluid properties of water, therefore facilitating the use of GE's published data. Also, the main UF foulant from mammalian cell cultures has been found to be cell debris. After depth filtration, we can make the assumption that cell debris are approximately completely removed from solution, allowing the assumption that fouling will not be an issue in our single-use membranes. (GE Healthcare, 2005)

The feed stream flow rate into UF was chosen to be 6.6 L/min. This flow rate corresponds to a shear rate of ~2000 s^{-1}. This shear rate has been deemed appropriate for shear sensitive streams, such as active virions. The pressure drop of the system is described as a linear function of feed flow rate. The following linear equation was determined from two data points provided by GE.

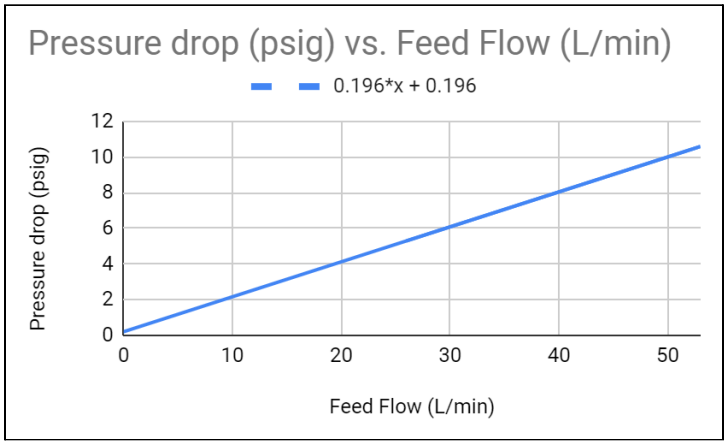

Figure 5.4.2c: Pressure drop across the UF membrane as a linear function of feed flow rate (GE Healthcare, 2005)

From the above plot, pressure drop across the membrane at the specified feed flow rate was determined to be 1.48 psig. GE cites the permeate flow rate as 4.7 L/min with a TMP of 5 psig at 25 ^{o}C. With each membrane's surface area of 3.25 m^2, the flux through each membrane is calculated by the following equation:

$$\Phi = \frac{Q}{A} * \left(\frac{1m^3}{1000L}\right) \quad \text{(Eqn. 5.4.2a)}$$

Where Φ is flux in unit m/min, Q is permeate flow rate in L/min, and A is membrane area in m^2. Eqn. 5.4.2a is used to calculate the membrane's flux as 0.00145 m/min.

Assuming that no volume loss occurs in the previous downstream processing steps, an incoming volume of 3000L will enter UF. The concentrated volume of this stream will remain constant at 150 L, no matter the incoming volume. The concentration factor needed achieve this change in volume can be found using the following equation:

$$\frac{C}{C_o} = \left(\frac{V_o}{V}\right)^{\sigma} \quad \text{(Eqn. 5.4.2b)}$$

Where V is concentrated batch volume in L, V_o is initial volume in L, C/C_o is the concentration factor, and σ is the rejection coefficient of the virus. In this system, σ is 1, as will be explained in detail in the following mass balance paragraph. Using Eqn. 5.4.2b, the concentration factor at full scale was determined to be 20. Each filter capacity is given as 120 L/m^2. In order to treat all 3000L of bioreactor effluent simultaneously in UF, the following equation was used to find number of parallel filters needed:

$$\#\ of\ filters = \frac{V_o - V}{\alpha * A} \quad \text{(Eqn. 5.2.4c)}$$

Where α is the filter capacity in L/m^2. This equation reveals that 7.3 filters are needed at full scale, which is rounded up to 8 filters. Finally, the process time of the UF unit can be determined using the following equation:

$$t = \frac{V_o - V}{\Phi * A * (\#\ of\ filters) * (1000L/m^3)} \quad \text{(Eqn. 5.2.4d)}$$

Where t is process time in minutes. The time requirement of this UF step, to treat 3000L, is 75.8 minutes.

Diafiltration will be used to exchange the solution buffer used in benzonase treatment to the buffer needed in affinity chromatography. Under the assumption that 96% of the solute must be removed and exchanged to the new buffer, the following plot was used to estimate that the DF unit must be flushed with about 3.5 times the liquid volume.

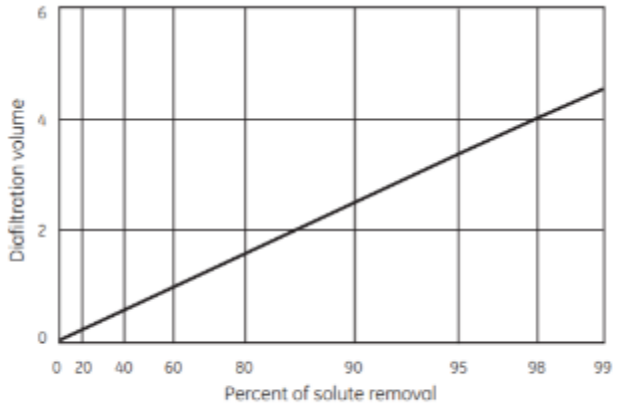

Figure 5.2.4d: Diafiltration volume requirement as a function of solute removal (Cytvia, 2021)

Figure 5.2.4d, above, is a model of the following equation:

$$\frac{V_w}{V_o} = -\ ln([\frac{C}{C_o}]_{salt}) \quad \text{(Eqn. 5.2.4e)}$$

Where V_w/V_O represents the factor by which the tank must be flushed, and $[C/C_o]_{salt}$ represents the concentration of the old buffer to remain in the retintate. This equation reveals that the exact diafiltration volume needed is 3.22 times the liquid volume. The new buffer introduced in DF is 10mM sodium phosphate. Therefore, 482.8L of 10mM sodium phosphate is needed to exchange 96% of the solution. Utilizing Eqn. 5.2.4c again, 2 filters will run in parallel to treat this volume. This DF step will take 51.4 minutes.

In calculating the filtration efficiency of the UF/DF unit operations, assumptions about host cell proteins size and quantity must be made due to lack of published data about Vero cell lysate. Kornecki et al. (2017) found that mammalian host cell proteins (HCP) range in size from 10-200 kDa. Also, Thermofisher reports that HeLa cells, a well published human cell line, contain about 300 pg of HCP per cell. This number will be used as an HCP quantity estimation for Vero cell lysate due to the structural similarities between the cell lines. (ThermoFisher, n.d.) With these numbers, it was assumed that 33% of HCP will be "small" (10-50 kDa), 33% will be "medium" (50-100 kDa), and 33% will be "large" (100-200 kDa). The membrane's rejection of different components by weight can be estimated using the following experimentally determined rejection curve.

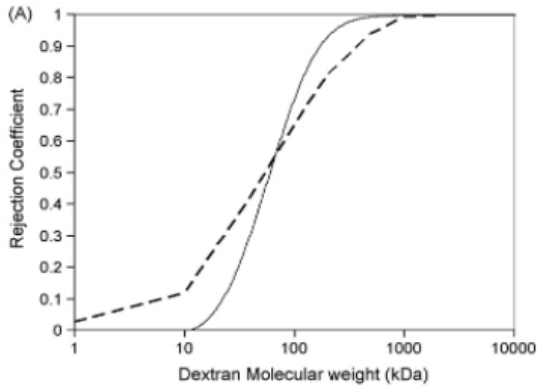

Figure 5.2.4e: 300 kDa Membrane Rejection Curve (Wickramasinghe et al., 2009)

From Figure 5.2.4e, it is observed that the rejection coefficient of Sars-CoV-2 (MW~ 10^6 kDa) is no less than 1. The rejection coefficients of small, medium and large HCP are approximated to be 0.2, 0.75, and 0.9, respectively. The fraction of each size HCP exiting DF and moving on to affinity chromatography can be calculated by the following equation:

$$HCP_i = \left(\left(\frac{V_o}{V}\right)^{\sigma_i - 1}\right) * e^{-\frac{V_w}{V_o}*(1-\sigma_i)} \qquad \text{(Eqn. 5.2.4f)}$$

Where HCP_i represents the fraction of HCP of size *i* exiting DF, and σ_i represents the rejection coefficient of HCP of size *i*. Using the HaLa estimation of total HCP per cell and combining retained HCP fractions, it was determined that the UF and DF unit operations in series will remove 72% of total HCP that enters UF. No virion is lost and it can be assumed that any remaining cells not removed in-depth filtration are completely removed in UF.

5.2.5 Viral Inactivation

After the virus has been concentrated via ultrafiltration, the virus will be inactivated. Viral inactivation will eliminate the infectivity of the antigen product. There are several methods of inactivation: heat, pH change, radiation, chemical modification, or chemical solvent. Recent studies have demonstrated the effectiveness of using β-propiolactone (BPL) to inactivate the SARS-CoV-2 virus. BPL is an organic compound that is widely used for the inactivation of virus DNA and RNA. With it's four-membered ring, it is highly reactive with nucleophilic reagents, including proteins, and nucleic acids. Studies have found that it is mainly purine residues, especially guanine, that are modified by BPL. The BPL-modified guanine can induce cross-linking of the helix, compacting the DNA and interfering with its replication (Perrin & Morgeaux, 1995).

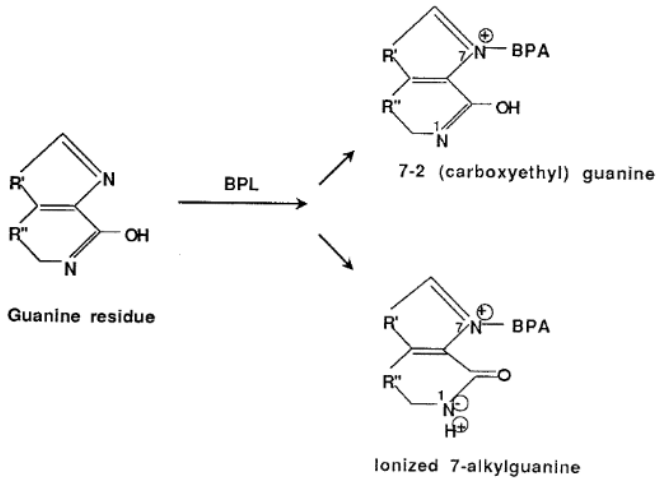

Figure 5.2.5a: Chemical reaction of BPL with Guanine residue (Perrin & Morgeaux, 1995)

The product leaving diafiltration will be pumped into the Sartorius 200L single-use bioreactor, and BPL will be added at a volume ratio of 1:4000. The mixer will be maintained at 4℃ for 16 hours and operate at 750 RPM stirring speed to ensure homogeneity. To prevent cytotoxicity, the product solution is incubated for an additional 2 hours at 37℃, ensuring complete hydrolysis of BPL (Jureka et al., 2020).

5.2.6 Affinity Chromatography

Affinity chromatography will be used as a method of separation that focuses on the interaction between a target and the column-defined matrix. Specifically, for this column, it will be the SARS-CoV-2 virus particle interacting with a ceramic hydroxyapatite ligand. The focus of the affinity matrix is to ensure limited adsorption from non-virus particles while having specific binding to virus particles. By the time affinity chromatography occurs, DNA will be broken down and removed and virus particles will have been inactivated.

Bio-Rad's ceramic hydroxyapatite (CHT) Type 2 resin was chosen for this process due to previous data indicating efficient separation of a mouse coronavirus in the same genus as

SARS-CoV which is assumed to be similar in structure and properties as SARS-CoV-2 (Kurosawa, 2014). CHT Type 2 resin has a nominal mean particle size of 40 +-4 um. The resin allows for large capacity for high titer upstream feeds and exceptional selectivity at high flow rates ensuring high process efficiency and yield compared to other purification media (Bio-Rad, n.d). CHT type 2 was chosen over Type 1 because it was better suited for capturing virus particles than proteins.

The rough size of the column was determined using the dynamic binding capacity and expected weight of virus particles entering the column. Based on manufacturers' data and published studies, the dynamic binding capacity of CHT is 20 g/L which would mean that based on an assumed 150g of virus particles at this step a total chromatic volume of at least 7.5L is needed (Bio-Rad, 2020). Extra volume may need to be added depending on how much non-virus particles are expected to bind. Manufacturing common practice for chromatography scale-up is to keep bed height and linear flow velocity constant as volume increases to ensure consistent residence times in the column for separation (Erickson, 2018). Previous studies of CoV particles on CHT resins have illustrated efficiency separation at 13cm bed height at 350 cm/hr flow rate which will both be used for this process (Bio-Rad, 2020). To accommodate the total volume, the bed diameter will be adjusted to fit the required total volume as virus weight to the chromatography step is finalized. Currently, at a maximum of 150g of virus, the diameter is 28 cm for the column. The maximum operating pressure is 1500 psid but the column pressure estimated at a linear flow rate of 350 cm/hr is 40 psid so there is no risk of exceeding the maximum pressure.

Based on the study mentioned above, separation efficiencies are assumed to be the same after scaling up indicating that the virus will be retained in captured elution steps at a ~92% yield

while only ~1% of HCP will remain. The separation will be conducted using a sodium phosphate buffer that will increase in concentration until the virus particles are eluted. Using a volumetric flow rate based on the defined area of the column and flow rate, the affinity column will require 3.3 hours to run.

5.2.7 Size Exclusion Chromatography

Residual viral and host cell proteins are removed via chromatography over a multimodal resin. Figure 5.2.7a, lists abundant proteins found in the virus, their size, and isoelectric points, and is given as a guide for chromatographic protocol .

Virus	Protein	UniProt-ID	MW [kDa]	p*I*	GRAVY
SARS-CoV-1	Replicase polyprotein 1a	P0C6U8 · R1A_CVHSA	486.373	5.91	–0.020
	Replicase polyprotein 1ab	P0C6 × 7 · R1AB_CVHSA	790.248	6.19	–0.071
	Spike glycoprotein	P59594 · SPIKE_CVHSA	139.125	5.56	–0.045
	Nucleoprotein	P59595 · NCAP_CVHSA	46.025	10.11	–1.027
	Protein 3a	P59632 · AP3A_CVHSA	30.903	5.75	0.239
	Protein 7a	P59635 · NS7A_CVHSA	13.941	8.24	0.218
	Envelope small membrane protein	P59637 · VEMP_CVHSA	8.361	6.01	1.141
	Membrane protein	P59596 · VME1_CVHSA	25.061	9.63	0.417
	Nonstructural protein 3b	P59633 · NS3B_CVHSA	17.750	10.82	0.099
	Nonstructural protein 6	P59634 · NS6_CVHSA	7.527	4.64	0.297
	Protein 9b	P59636 · ORF9B_CVHSA	10.802	4.90	–0.122
	Protein nonstructural 7b	Q7TFA1 · NS7B_CVHSA	5.302	3.77	1.414
	Nonstructural protein 8b	Q80H93 · NS8B_CVHSA	9.560	9.45	–0.029
	Nonstructural protein 8a	Q7TFA0 · NS8A_CVHSA	4.327	8.30	0.644
	Uncharacterized protein 14	Q7TLC7 · Y14_CVHSA	7.852	6.25	0.310
SARS-CoV-2	Replicase polyprotein 1a	P0DTC1 · R1A_SARS2	489.989	6.04	–0.023
	Spike glycoprotein	P0DTC2 · SPIKE_SARS2	141.178	6.24	–0.079
	Replicase polyprotein 1ab	P0DTD1 · R1AB_SARS2	794.058	6.32	–0.070
	Protein 3a	P0DTC3 · AP3A_SARS2	31.123	5.55	0.275
	Membrane protein	P0DTC5 · VME1_SARS2	25.147	9.51	0.446
	Protein 7a	P0DTC7 · NS7A_SARS2	13.744	8.23	0.318
	Nucleoprotein	P0DTC9 · NCAP_SARS2	45.626	10.07	–0.971
	Envelope small membrane protein	P0DTC4 · VEMP_SARS2	8.365	8.57	1.128
	Nonstructural protein 6	P0DTC6 · NS6_SARS2	7.273	4.60	0.233
	Protein 9b	P0DTD2 · ORF9B_SARS2	10.797	6.56	–0.085
	Nonstructural protein 8	P0DTC8 · NS8_SARS2	13.831	5.42	0.219
	Uncharacterized protein 14	P0DTD3 · Y14_SARS2	8.050	5.79	0.603
	Protein nonstructural 7b	P0DTD8 · NS7B_SARS2	5.180	4.17	1.449
	A0A663DJA2 · A0A663DJA2_SARS2		4.449	7.93	0.637

Figure 5.2.7a: Physical property data for virus proteins (Scheller, et al., 2020).

The 15.7 L (500 mm height, 200 mm inner diameter) column is first equilibrated to a pH of 10.5 with Tris-NaCl buffer. The virus-containing solution is then loaded into the column packed with a multi-modal column resin (Capto Core 700). The resin functions through size

exclusion (molecular weight cut off = 700 kDa) as well as binding selectivity in the particle ligands (pKa = 10.4).

The virus-containing fraction is the first collected, as depicted in the sample chromatogram in Figure 5.2.7b. Following product collection, the column is eluted with a gradually decreasing pH buffer, followed by an ethanol wash cycle. With a flow velocity of 300 cm/h, the time to process one batch is 56.5 minutes.

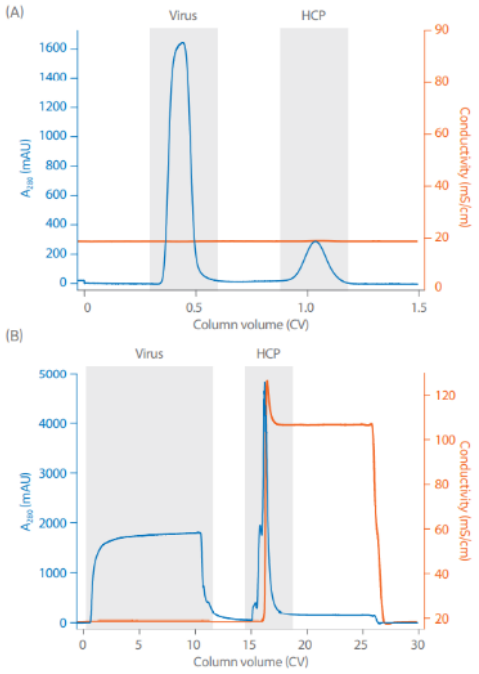

Figure 5.2.7b: Chromatograph illustrating virus collection in initial band with Capto Core 700. (Cytiva, 2015).

5.2.8 Sterile Filtration

Sterile filtration is added as a final precaution for vaccine manufacturing processes to reduce bioburden by removing any bacterial or large particle that may have passed through the process before formulation and filling (FDA, 2004). A high-performance polyethersulfone (PES) membrane was chosen for its high filtration efficiency and stability at high flow rates. A pore diameter of 0.2 um is the standard for a final filtration step. Therefore, the filter chosen for this

unit is a 10-inch cartridge with 0.2um pores produced by Missner filtration. According to manufacturer data in Figure 5.2.8a, the pressure drop at a 15L/min flow rate is about 100 mbar (Meissner, 2020). At this flow rate, the time required to process 200L of the product would be 13 min.

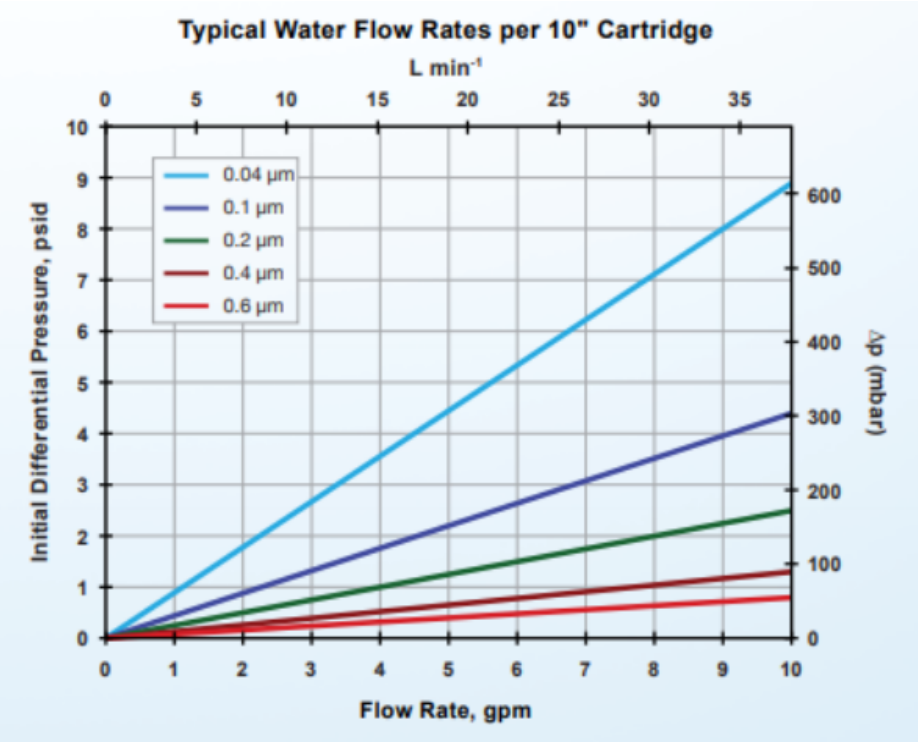

Figure 5.2.8a: Differential pressure of water flow rates per 10" cartridges (Meissner, 2020)

5.2.9 Formulation & Filling

Formulation

At full scale, 392.5 L (per batch) of inactivated virus solution is available for formulation from sterile filtration. Preservatives and adjuvants are commonly added to vaccines to prevent contamination and to help boost immune system response, respectively (CDC, 2019). A common vaccine preservative is 2-phenoxyethanol; it is an organic compound that is approved by FDA for vaccine use (FDA, 2018). Two different adjuvants are added to the vaccine: aluminum

hydroxide gel and Toll-like Receptors (TLR) 7/8. The aluminum hydroxide gel will increase the attraction and the uptake of the antigen by antigen-presenting cells, and TLR 7/8 agonist will enhance Th1 response for intracellular pathogens (InvivoGen, n.d.; Tomai & Vasilakos, 2017, 149-162). Additionally, phosphate buffer saline (PBS) is added to adjust the pH level of the vaccine (Blades, 1980). For every 6 μL of the inactivated virus, 2.5 mg of 2-phenoxyethanol, 250 μg of aluminum hydroxide gel, 15 μg of Imidazoquinolinone TLR 7/8 agonist, and 0.5 mL of phosphate buffer saline will be added (Bharat Biotech, n.d.).

Filling

Due to the high demands and immediate needs, the vaccine will be filled into multidose vials with 20 doses in each 10 mL vial. To limit the growth of bacteria, an antimicrobial preservative is often added to multidose vials; phenoxyethanol is the most frequently used preservative in vaccines (CDC, n.d.; Meyer et al., 2007, 3155-67). As the demand decreases, the vaccine can be filled in single-dose vials to prevent contamination.

At maximum capacity, 1189 g of antigen will be produced in a quarter year but 10% of it is expected to be lost during the filling process. Consequently, 178,350,000 doses of the COVID-19 vaccines will be filled into 8,917,500 glass vials. With one filling line at a filling speed of 36,000 bpm/hr, vaccines will be filled 3 times a month, 2.82 days at a time. The downtime can serve as a buffer for any delays or maintenance. The machine can also fill other products during this downtime to increase the plant's efficiency.

In an aseptic production environment, glass vials will be loaded onto the vial feeder where the vials will be sent into the washer to be washed, sterilized, and depyrogenated. The heat tunnel used for vial sterilization will feed the vials to the Bausch FFV 12024 filling machine for vaccine filling and capping. The filled vials will then be transferred to a cold room for storage.

All the equipment that enters the production area will be autoclaved and all personnel will be gowned to prevent contamination of the cleanrooms.

5.3 Ancillary Equipment

5.3.1 Pumps

Within each process, fluids are transferred between unit operations and tanks using pumps. Each pump had its required flow rate and power requirement determined so that the estimated purchase cost and utilities cost can be estimated using CAPCOST. Within the process, peristaltic pumps were chosen to be used due to our low flow rate requirements and the ability to keep the product isolated from the atmosphere and machinery. To determine the power requirements needed for a CAPCOST estimation, each pump had the required pressure difference between the feed and receiving units calculated. In addition to the calculated pressure difference, an allowance of 1 atm of losses due to friction in the pipe or losses for a control valve was added. Significant elevation changes were not expected so the gravity head was assumed to be negligible. The power requirement of the pump was calculated by multiplying the volumetric flow rate with the pressure difference. The efficiency of the pump was assumed to be 70%. Using these basis of calculations, each pump in the process was determined to have a smaller size and power requirements than the minimum allotted pump in CAPCOST so the minimum pump was used as the basis for price and utilities in the design report.

5.3.2 Heating Jackets

There will be seven heating jackets of note in this process. The first three jackets will be found surrounding the three 1000L Sartorius Bioreactors in upstream processing. The second

three jackets will surround the three 1000L reactors in the benzonase treatment step of downstream processing. The third jacket will surround the reactor in the inactivation step of downstream processing. These jackets will initially heat incoming materials and maintain system temperatures at 37ºC. The jackets will surround the cylindrical reactors in the manner shown in Figure 5.3.2 below. The energy balances on these jackets are to follow.

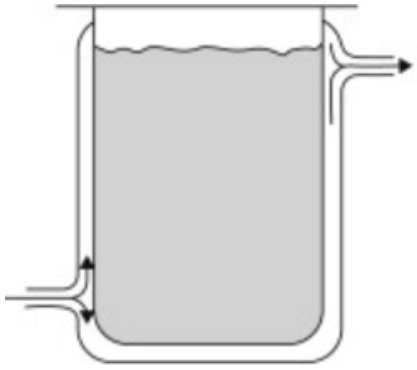

Figure 5.3.2: Heating jacket illustration (Doran, 2013)

At the start of the bioreactor process, the steel bioreactor and polyethylene single-use bag will be at room temperature. The incoming media will be 4ºC. The heating jacket will utilize 50ºC water to achieve the necessary heat transfer to bring these three components to the required 37ºC. The time required to heat up each reactor was calculated using the following equation:

$$t = \frac{MC_p}{UA} ln(\frac{T_{HW} - T_i}{T_{HW} - T_f}) \qquad \text{(Eqn. 5.3.2a)}$$

Where t is time in seconds, M is the mass being heated in kg, C_p is the specific heat capacity in J/kg-K, U is the overall heat transfer coefficient in W/m^2-K, A is the heat transfer surface area in m^2, T_{HW} is the temperature of heating water in ºC, T_i is the initial temperature in ºC, and T_f is the final temperature in ºC.

Equation 5.3.2a was used to calculate the time required to heat the steel bioreactor, single-use bag, and the media. For all three calculations, the overall heat transfer coefficient is

approximated to be 400 W/m^2-K (Carpenter, 2011). The heat transfer surface area was calculated to be 3.69 m^2 through the following equation:

$$A = 2\pi r_{SU} L_{SU} \quad \text{(Eqn. 5.3.2b)}$$

where r_{SU} is the single use bag radius and L_{SU} is the single use bag height in m. The dimensions of the bioreactor and single-use bag are $r = 0.54m$and $L = 1.08m$. The steel of the bioreactor has a total mass of 1000kg and the material's heat capacity is 502 J/kg-K. With the assumption that the media has the properties of water, the mass of media is 800 kg and the heat capacity is 4185 J/kg-K. The single use polyethylene bag has a total mass of 60 kg and has a heat capacity of 2101 J/kg-K (Chang & Bestul, 1973).

The heat duty and power requirement for the heating jacket during bioreactor startup can be calculated using the following equations:

$$q = MC_p(T_f - T_i) \quad \text{(Eqn. 5.3.2c)}$$

$$P_w = \frac{q}{t} \quad \text{(Eqn. 5.3.2d)}$$

where q is heat duty in J, and P_w is power in W. The total heat duty during startup is 129,000 kJ and the total power needed is 40.6 kW. Table 5.2.3a, below, summarizes the heating time and heat duty for the 3 materials in the bioreactor system.

Table 5.2.3a: Summary of Time and Heat Duty Requirements at Startup

	Time (s)	**Heat Duty (kJ)**
Media	2866	110484
Stainless Steel	249	16566
Polyethylene Bag	62	1765
Total	3177	129000

After the initial heating during bioreactor startup, the heating jacket will be utilized to maintain the process at 37°C for the duration of the 144 hour fermentation and infection cycle. The amount of heat lost through the steel and into the atmosphere was calculated using the following equation:

$$Q_{steel} = \frac{2\pi L_{SU} k_t (T_{in} - T_{out})}{ln(\frac{r_{SU}+r_{steel}}{r_{SU}})} \quad \text{(Eqn. 5.3.2e)}$$

where Q_{steel} is the heat loss through steel in J/s, k_t is the thermal conductivity of steel in W/m-K, T_{in} is the inner temperature of steel in °C, T_{out} is the outer temperature of steel in °C, and r_{steel} is the steel thickness in m. The thermal conductivity of steel is 14.4 W/m-K and the outer temperature of steel is estimated to be 23°C at room temperature. The thickness was approximated to be 0.025m. Through the use of Eqn. 5.3.2e, it was determined that 31,000 J/s of heat is lost and will need to be replenished.

In order to keep the bioreactor at 37°C, a closed loop of heating water will continually circulate. The water will exit the heating jacket at 37°C and flow to an electric water heater where it will be heated to 40.1°C. The additional 0.1°C accounts for the cooling that occurs during transportation. This heated water will then flow back to the heating jacket continuing the cycle. The flow rate of 40°C water needed to keep the bioreactor temperature constant can be found through the following equation:

$$\dot{m} = \frac{P_W}{\Delta T C_p} \quad \text{(Eqn. 5.3.2f)}$$

where $\dot{m}$ is the mass flow rate in kg/s and ΔT is the difference in temperature between the heating water and the system. During startup, the mass flow rate of water needed is 0.968 kg/s. During operation, the mass flow rate needed is 2.507 kg/s. The benzonase reactors will also need to keep the media at 37°C. The exact same process as above was followed to find that the mass flow rate

of water needed in the benzonase reactor heat jacket is 0.03 kg/s. The heat jacket surrounding the inactivation reactor will need less heating water because it is a much smaller size tank compared to the bioreactor and benzonase reactor. The mass flow rate of water needed to heat the inactivation reactor is 2.7 g/s.

An industrial immersion heater was selected to achieve the necessary heating of the water as it passes through the loop. A 5,000L holding tank with an immersion heater, estimated using the CAPCOST 2017 program, is capable of heating 5000 kg of water in 10 minutes. The heat duty of the heater at maximum capacity can be found by using Eqn. 5.3.2c. The mass of water will be taken as 5,000 kg. It is approximated that the heating water will lose 0.1ºC while travelling though piping from reactor to heater. Therefore, the initial temperature of water is 36.9ºC and the final temperature is 40.1ºC. The heat duty was calculated to be 15500 kJ. In 10 minutes time, the power requirement is 25.83 kW.

5.3.3 Cooling Jacket

A cooling jacket is needed to surround the 200 L stainless steel Sartorius Bioreactor to cool and maintain the BPL-contained virus slurry at 4℃. The cooled ethylene glycol will flow through the annular space created by the second shell over the mixer and cool the mixer along with the media. The time required to cool to the mixer is calculated using:

$$t = ln(\frac{T_i - T_c}{T_f - T_c}) \frac{MC_p}{UA} \qquad \text{(Equation 5.3.3a)}$$

Where t is the time in s, T_i is the initial temperature of the liquid in the mixer in ℃, T_f is the final temperature of the liquid in the mixer in ℃, T_c is the temperature of the coolant in ℃, M is

the mass of the media heated in kg, C_p is the specific heat capacity of the batch in J/kg-K, U is the heat transfer coefficient in W/m^2-K, and A is the heat transfer area in m^2 (Pietranski, n.d.).

For the inactivation cooling step, the initial temperature is 20℃, the final temperature is 4℃, and the temperature of the coolant is 0℃. The property of the virus slurry is assumed to be similar to that of water; mass of the media will be 200L with a specific heat capacity of 4182 J/kg-℃ ("Specific heat", n.d.). The overall heat transfer coefficient is approximately 340 W/m2-K ("Fluid heat", n.d.). The shape of the mixer is assumed to be a right cylinder, with a heat transfer area of approximately 2 m^2.

The reactor has a weight of 327 kg and has a specific heat capacity of 502.4 J/kg-K ("200 L", n.d.; Engineers Edge, 2015). The total cool down time is approximately 39 minutes, with details displayed in Table 5.3.3-i. The heat removed from the system and the power requirement are calculated using Equation 5.3.2c and Equation 5.3.2d, respectively. The total heat absorbed by the coolant during the inactivation startup is 16011 kJ and the total power requirement is 6.92 kW.

Table 5.3.3-i. Summary of time and heat removed during inactivation startup.

	Time (s)	**Heat Duty (kJ)**
Media	1936	13382
Stainless Steel	380	2629
Total	2317	16011

After the startup, the coolant will continue to circle through the cooling jacket to maintain the mixer temperature at 4℃ for the duration of 16 hours of the inactivation step. The amount of heat absorbed from the environment through the steel can be calculated using Equation 5.3.2d, with approximately 0.025m thickness of stainless steel. With thermal conductivity of 16 W/m-K, inner steel temperature of 0℃, outer steel temperature of approximately 5℃ and a cooling jacket

thickness of approximately 0.05m, the coolant will absorb 1417 J/s of heat from the atmosphere and will need to be removed.

The coolant runs through a closed loop system, entering the cooling jacket at 0℃ and exiting at 8℃. Exiting ethylene glycol will undergo refrigeration to remove the heat absorbed from the mixer. The chilled ethylene glycol will then flow back to the cooling jacket to continue the process. The flow rate of the ethylene glycol can be determined using Equation 5.3.2e. During the initial cool down, the mass flow rate of ethylene glycol is 0.275kg/s and it will decrease to 0.056 kg/s to maintain the temperature. The formulation process would also require the mixer to maintain at a low temperature of 6°C and the same process will be used to find the mass flow of ethylene glycol running through the cooling jacket. For the formulation process, ethylene glycol will flow through the system at a mass flow rate of 0.22kg/s.

V. Recommended Operation

The following section describes the process operation and plant schedule that will achieve the desired design basis. It also includes illustrations of the components of each unit operation.

6.1 Overall Process Flow Diagram

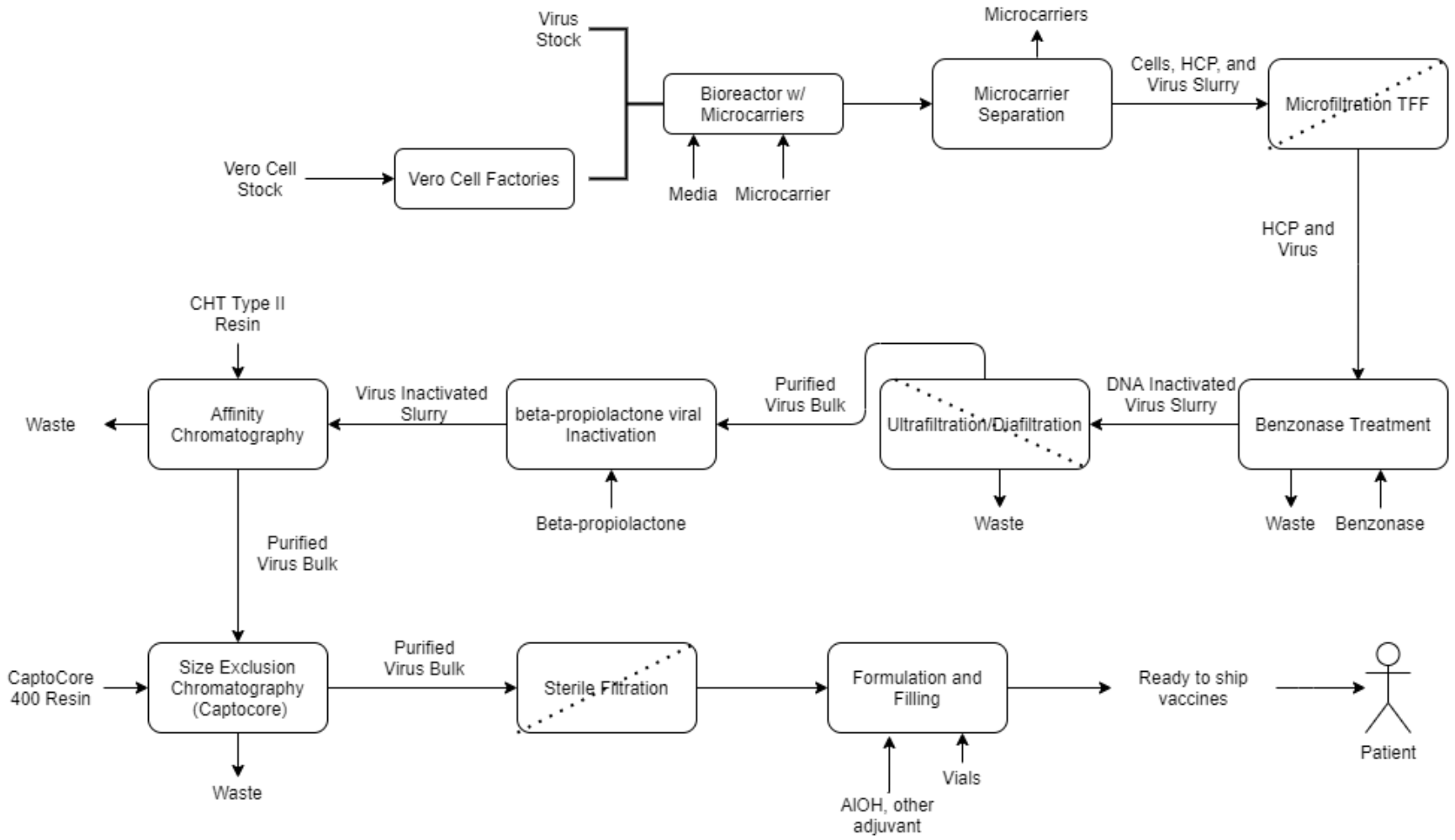

6.2 Scheduling

The Gantt charts, Figures 6.2a, 6.2d, and 6.2c, show the overall process schedule for the first year of operation, while Figures 6.2d, 6.2e, and 6.2f provide a detailed catalog of daily plant operations. The plant will operate for 48 weeks in the first year. The remaining four weeks, in addition to the blank squares in Figures 6.2a, 6.2b, and 6.2c, will be used for maintenance and cleaning. The use of single-use bags in the bioreactors, Benzonase treatment, and BPL inactivation mitigate some downtime due to CIP, SIP, and cleaning validation. Upstream processing time exceeds downstream processing time, taking 262 to 310 hours compared to 91 to 135 hours. Disparities in processing times for unit operations are due to fixed operational flow rates and, for the seed train, differences in desired cell density. Ultrafiltration/diafiltration serves as a purification and concentration step. This stipulation allows for the reactor volumes for subsequent unit operations to remain the same throughout manufacturing.

Figures 6.2a, 6.2b, and 6.2c show blocks on the days specific unit operations take place. Breaks in the schedule like "Week 0", "last week in Q1", and last week in Q2" depict changes in the day of T175 flask inoculation. This step is the first one involved in the seed train. Increasing the duration of the seed train generates higher cell densities, which are used to inoculate more bioreactors. Each quarter comprises an even week and odd week following a break in the schedule. Within quarters 1 and 2, the transition from the even week back to the odd week occurs five times, and the last week in the quarter includes the change to the seed train and the remaining downstream processing steps. The dashes in the figures indicate the unit operations, seed train or bioreactors, the restart on the same day. Accordingly, a new T175 flask is inoculated on the same day the contents of the cell factory is transported to the bioreactors, or the bioreactors are emptied and inoculated on the same day.

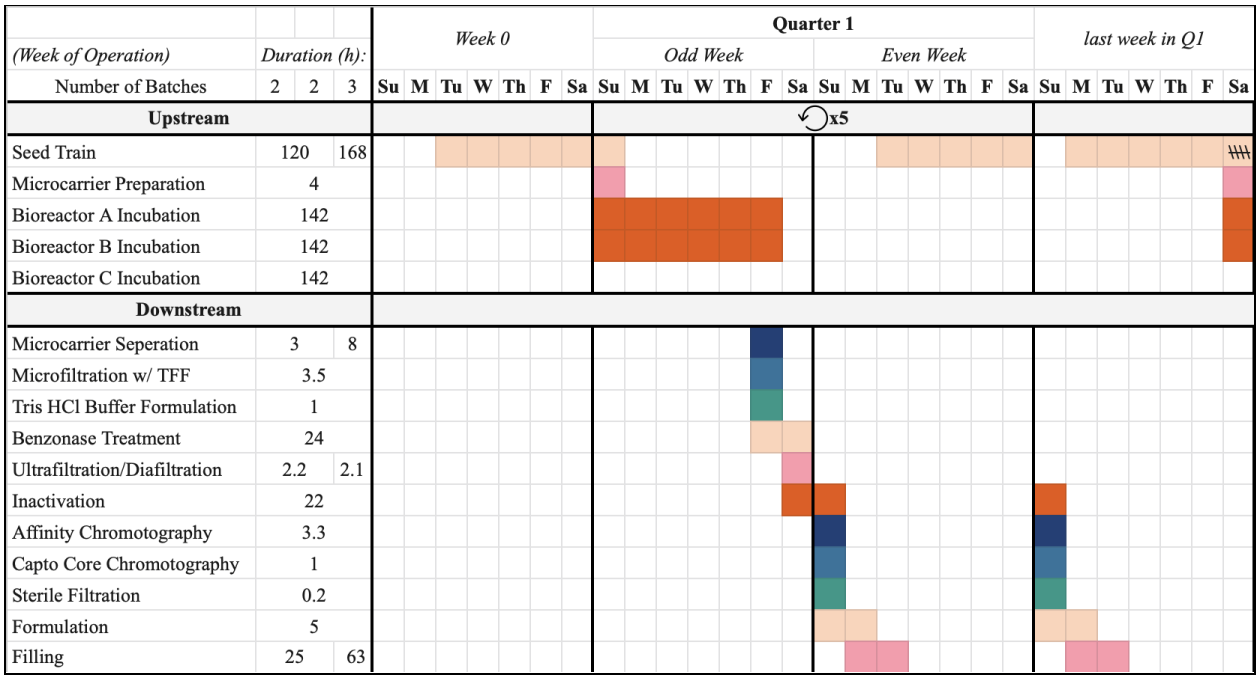

(Week of Operation)	Duration (h):		
Number of Batches	2	2	3
Upstream			
Seed Train	120		168
Microcarrier Preparation	4		
Bioreactor A Incubation	142		
Bioreactor B Incubation	142		
Bioreactor C Incubation	142		
Downstream			
Microcarrier Seperation	3		8
Microfiltration w/ TFF	3.5		
Tris HCl Buffer Formulation	1		
Benzonase Treatment	24		
Ultrafiltration/Diafiltration	2.2		2.1
Inactivation	22		
Affinity Chromotography	3.3		
Capto Core Chromotography	1		
Sterile Filtration	0.2		
Formulation	5		
Filling	25		63

Figure 6.2a: Gantt Batch Schedule for Q1 where dashes indicate duplicate unit operations

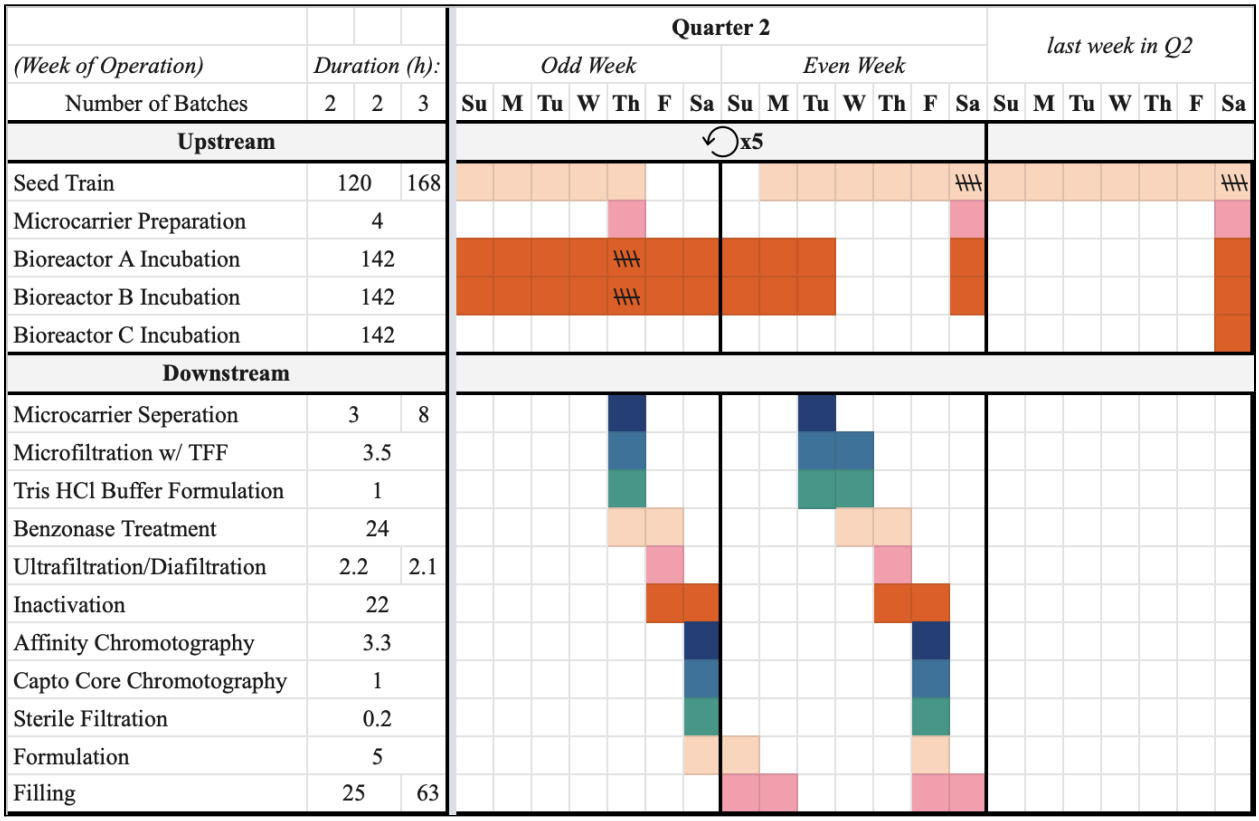

(Week of Operation)	Duration (h):		
Number of Batches	2	2	3
Upstream			
Seed Train	120		168
Microcarrier Preparation	4		
Bioreactor A Incubation	142		
Bioreactor B Incubation	142		
Bioreactor C Incubation	142		
Downstream			
Microcarrier Seperation	3		8
Microfiltration w/ TFF	3.5		
Tris HCl Buffer Formulation	1		
Benzonase Treatment	24		
Ultrafiltration/Diafiltration	2.2		2.1
Inactivation	22		
Affinity Chromotography	3.3		
Capto Core Chromotography	1		
Sterile Filtration	0.2		
Formulation	5		
Filling	25		63

Figure 6.2b: Gantt Batch Schedule for Q2 where dashes indicate duplicate unit operations

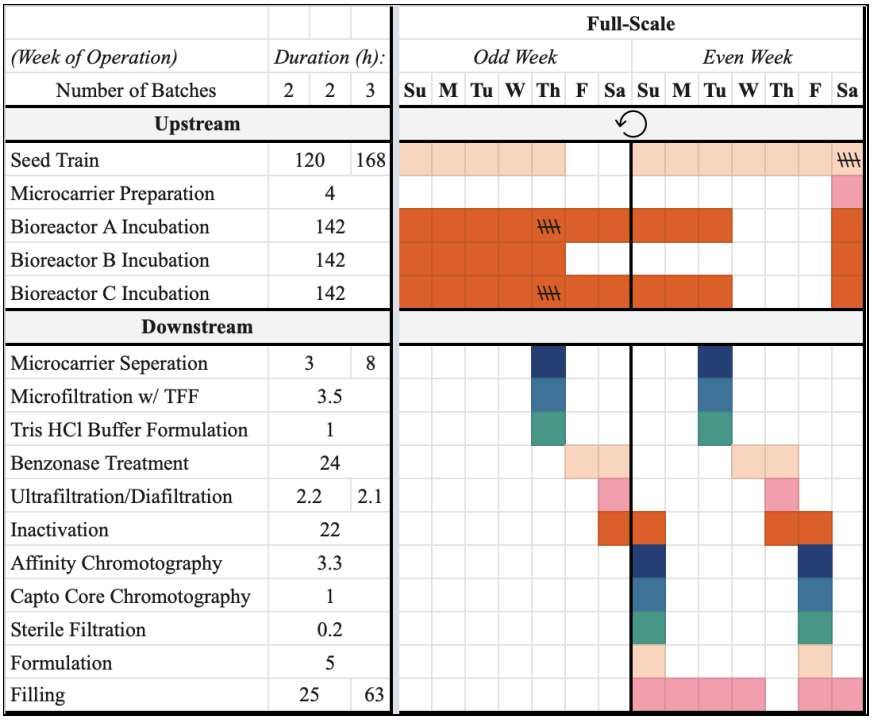

Figure 6.2c: Gantt Batch Schedule for Q2 where dashes indicate duplicate unit operations

Q1		
Seed Train		Begins Tu at 10 AM, Ends Su at 10 AM
M Prep		Begins Su at 9 AM, Ends Su at 1 PM
Bioreactors		Begins Su at 2 PM, Ends F at 10 AM
M Sep.		Begins F at 11 AM, Ends F at 2 PM
TFF		Begins F at 3 PM, Ends F at 6:30 PM
Buffer Form.		Begins F at 5 PM, Ends F at 6 PM
BT		Begins F at 7 PM, Ends Sa at 7 PM
UF/DF		Begins Sa at 8 PM, Ends Sa at 10:30 PM
Inactiviation		Begins Sa at 11 PM, Ends Su at 9 AM
AC		Begins Su at 10 AM, Ends Su at 1:30 PM
CCC		Begins Su at 2:30 PM, Ends Su at 3:30 PM
Sterile Filt.		Begins Su at 4:30 PM, Ends Su at 6 PM
Formulation		Begins Su at 7 PM, Ends M at 12 AM
Filling		Begins M at 1 AM, Ends Tu at 2 AM

Figure 6.2d: Detailed Biweekly Schedule for Q1

Q2		
Seed Train (1)		Begins M at 10 AM, Ends Sa at 10 AM
M Prep (1)		Begins Sa at 9 AM, Ends Sa at 1 PM
Bioreactors (1)		Begins Sa at 2 PM, Ends Th at 10 AM
Seed Train (2)		Begins Sa at 4 PM, Ends Th at 4 PM
M Prep (2)		Begins Th at 3 PM, Ends Th at 7 PM
Bioreactors (2)		Begins Th at 8 PM, Ends Tu at 4 PM
M Sep. (1)		Begins Th at 11 AM, Ends Th at 2 PM
TFF (1)		Begins Th at 3 PM, Ends Th at 6:30 PM
Bffr Form. (1)		Begins Th at 5 PM, Ends Th at 6 PM
BT (1)		Begins Th at 7 PM, Ends F at 7 PM
UF/DF (1)		Begins F at 8 PM, Ends F at 10:30 PM
Inactivatn (1)		Begins F at 11 PM, Ends Sa at 9 AM
AC (1)		Begins Sa at 10 AM, Ends Sa at 1:30 PM
CCC (1)		Begins Sa at 2:30 PM, Ends Sa at 3:30 PM
Sterile Filt. (1)		Begins Sa at 4:30 PM, Ends Sa at 6 PM
Formu. (1)		Begins Sa at 7 PM, Ends Su at 12 AM
Filling (1)		Begins Su at 1 AM, Ends M at 2 AM
M Sep. (2)		Begins Tu at 5 PM, Ends Tu at 8 PM
TFF (2)		Begins Tu at 9 PM, Ends W at 12:30 AM
Bffr Form. (2)		Begins Tu at 11 PM, Ends W at 12 AM
BT (2)		Begins W at 1 AM, Ends Th at 1 AM
UF/DF (2)		Begins Th at 2 AM, Ends Th at 4:30 AM
Inactivatn (2)		Begins Th at 5 AM, Ends F at 3 AM
AC (2)		Begins F at 4 AM, Ends F at 7:30 AM
CCC (2)		Begins F at 8:30 AM, Ends F at 9:30 AM
Sterile Filt. (2)		Begins F at 10:30 AM, Ends F at 12 PM
Formu. (2)		Begins F at 1 PM, Ends F at 6 PM
Filling (2)		Begins F at 7 PM, Ends Sa at 8 PM

Figure 6.2e: Detailed Biweekly Schedule for Q2

Full Scale		
Seed Train (1)		Begins Su at 10 AM, Ends Sa at 10 AM
M Prep (1)		Begins Sa at 9 AM, Ends Sa at 1 PM
Bioreactors (1)		Begins Sa at 2 PM, Ends Th at 10 AM
Seed Train (2)		Begins Sa at 4 PM, Ends Th at 4 PM
M Prep (2)		Begins Th at 3 PM, Ends Th at 7 PM
Bioreactors (2)		Begins Th at 6 PM, Ends Tu at 2 PM
M Sep. (1)		Begins Th at 11 AM, Ends Th at 7 PM
TFF (1)		Begins Th at 8 PM, Ends Th at 11:30 PM
Bffr Form. (1)		Begins Th at 10 PM, Ends Th at 11 PM
BT (1)		Begins F at 12 AM, Ends Sa at 12 AM
UF/DF (1)		Begins Sa at 1 AM, Ends Sa at 3:30 AM
Inactivatn (1)		Begins Sa at 4:30 AM, Ends Su at 2:30 AM
AC (1)		Begins Su at 3:30 AM, Ends Su at 7 AM
CCC (1)		Begins Su at 8 AM, Ends Su at 9 AM
Sterile Filt. (1)		Begins Su at 10 AM, Ends Su at 2 PM
Formu. (1)		Begins Su at 3 PM, Ends Su at 8 PM
Filling (1)		Begins Su at 9 PM, Ends W at 12 PM
M Sep. (2)		Begins Tu at 3 PM, Ends Tu at 6 PM
TFF (2)		Begins Tu at 7 PM, Ends Tu at 10:30 PM
Bffr Form. (2)		Begins Tu at 9 PM, Ends Tu at 10 PM
BT (2)		Begins Tu at 11 PM, Ends W at 11 PM
UF/DF (2)		Begins Th at 12 AM, Ends Th at 2:30 AM
Inactivatn (2)		Begins Th at 3 AM, Ends F at 1 AM
AC (2)		Begins F at 2 AM, Ends F at 5:30 AM
CCC (2)		Begins F at 6:30 AM, Ends F at 7:30 AM
Sterile Filt. (2)		Begins F at 8:30 AM, Ends F at 10 AM
Formu. (2)		Begins F at 11 AM, Ends F at 4 PM
Filling (2)		Begins F at 5 PM, Ends Sa at 6 PM

Figure 6.2f: Detailed Biweekly Schedule for Full Scale Manufacturing

Figures 6.2d, 6.2e, and 6.2f leave an hour between each unit operation for draining/filling and preparation. As shown in Figures 6.2a, 6.2c, and 6.2c, manufacturing in Quarter 1 entails processing the contents of two 1000 L bioreactors, while Quarter 3 involves five 1000 L bioreactors biweekly. The contents of the bioreactors can be treated as collective batches throughout manufacturing since the bioreactors will be drained at the same time. Therefore, downstream processing either handles 2000 L or 3000 L of inlet volume.

The figures below, in sections 6.3 and 6.4, illustrate individual unit operation process flow diagrams. The accompanying descriptions detail the anticipated procedure to process the contents of two 1000 L bioreactors. The numbering of specific equipment and streams is based on an AICHE instrumentation diagram guide (Cook, 2010). Each piece of equipment or stream is labeled using the guide X-Y-ZZ where X is the unit operation number, Y is the equipment type code in Figure 6.3a and streams assume the Y value to be 0. And ZZ is the equipment number.

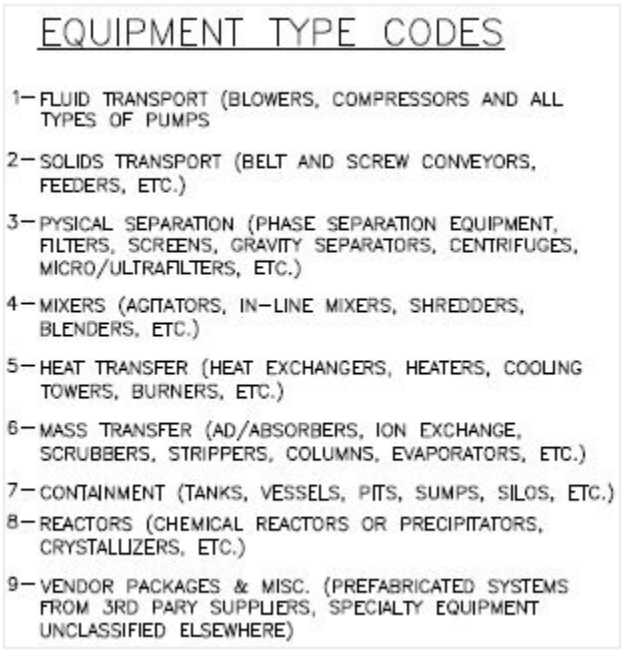

Figure 6.3a: Equipment Type Codes (Cook, 2010)

6.3 Upstream Processing Diagrams

6.3.1 Seed Train

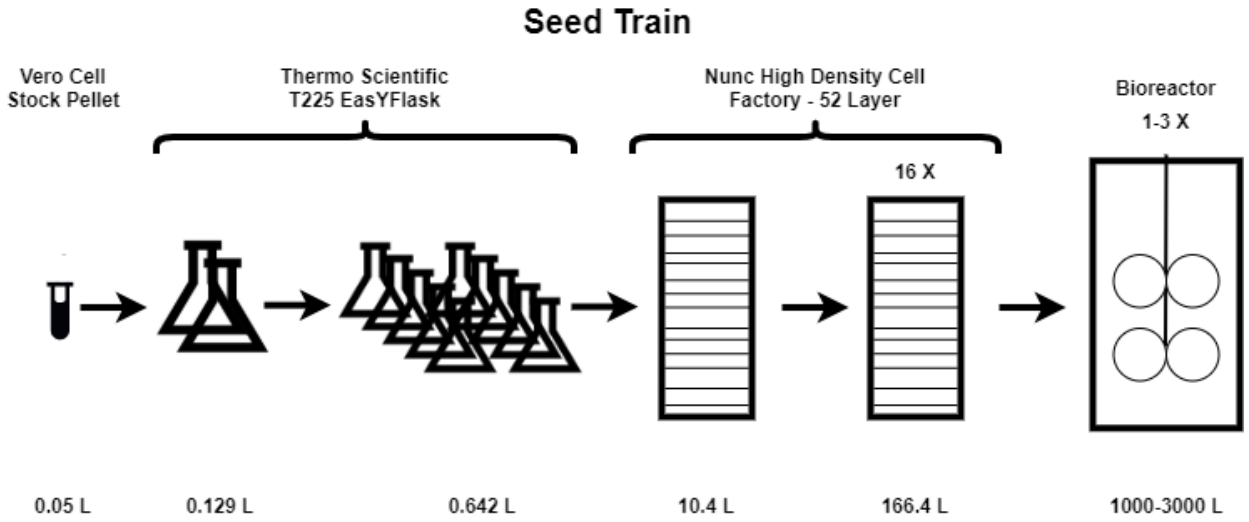

Figure 6.3.1: Seed Train Processing Diagram

To initialize the process, a frozen stock will be used to inoculate the first T225 flask. Following the required incubation time and cell density requirements outlined in Section 5.1.1, the cells will be manually washed, collected, and inoculated on the next part of the seed train by operators while in the flasks. The initial three steps are conducted in Thermo Scientific EasYFlasks until they are transferred into 52 Layer Nunc High Density Cell Factory. Machinery provided by Thermo Scientific are able to incubate and wash the High Density Cell Factories so operators are not needed for that step. All operating conditions will be at 37 ^{0}C and a CO_2 percentage of 5%.

6.3.2 Bioreactor

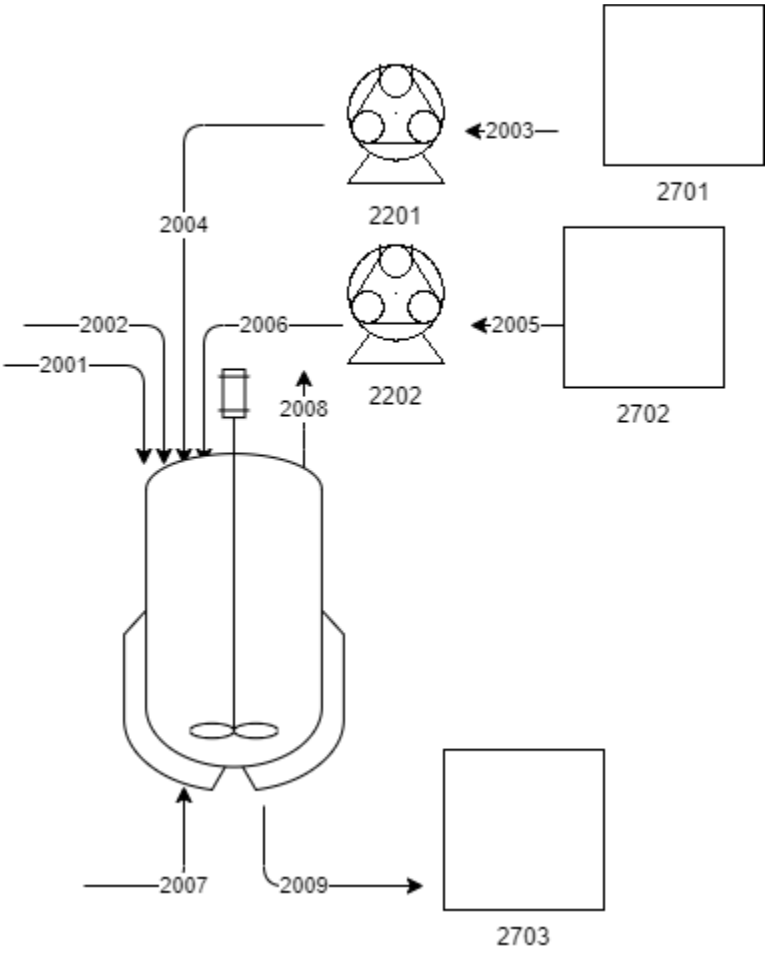

Figure 6.3.2: Bioreactor Processing Diagram

Table 6.3.2: Bioreactor PFD Label Descriptions

Equipment or Stream Label	Equipment or Stream Description
2001	Vero Cell input
2002	SARS-CoV-2 input
2701	Prepared microcarrier holding tank
2003, 2004	Microcarrier stream
2201	Microcarrier pump
2702	Media holding tank
2005, 2006	Media stream
2202	Media pump
2801	1000 L Bioreactor
2007	Sterile air stream
2008	Exhaust air stream
2009	Bioreactor output stream
2703	Bioreactor output holding tank

Prior to fermentation, pump 2202 will pump 800 L of VPSFM media, from holding tank 2702, at 5℃ into tank 2801 and will be stirred at a rate of 74 RPM. After 45 minutes of heating, when the media reaches 37℃, pump 2201 will pump 3,000 grams of Cytodex-1 microcarriers into tank 2801 from holding tank 2701. 467.65 grams of L-Glutamine powder will be added to tank 2801 and allowed to dissolve and sterile air flow will commence through stream 2007 at 1 L/min. Unused air will be vented through exhaust stream 2008. 200 L of solution containing 2.52 x 10^{11} Vero cells and VPSFM media will be pumped into tank 2801. After 120 hours, stock solution containing 2.52 x 10^{8} SARS-CoV-2 virions will be added to the tank through stream 2001 with 72.58 grams of L-Glutamine powder. After 16 hours, the contents of tank 2801 will be transported to holding tank 2703. The whole process will take approximately 145 hours.

6.4 Downstream Processing Diagrams

6.4.1 Microcarrier Separation

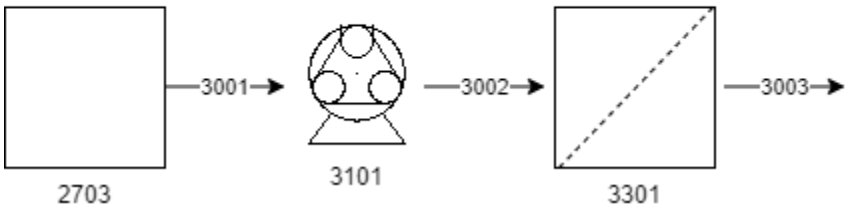

Figure 6.4.1: Microcarrier Separation Processing Diagram

Table 6.4.1: Microcarrier Separation PFD Label Descriptions

Equipment or Stream Label	Equipment or Stream Description
2703	Feed holding tank
3001, 3002	Feed stream
3101	Feed pump
3301	Thermo Scientific Harvestainer BioProcess Container 12L
3003	Microcarrier separation output stream

Media from the bioreactor containing microcarriers, cells, virus particles, and other salts in holding tank 2703 are pumped to the Harvestainier BioProcess Container 3301 by pump 3101. The pump 3101 will flow the media at a rate of 6.5L/min to the filter 3301. The media that passes through the filter continues to the microfiltration TFF unit through stream 3003.

6.4.2 Microfiltration with TFF

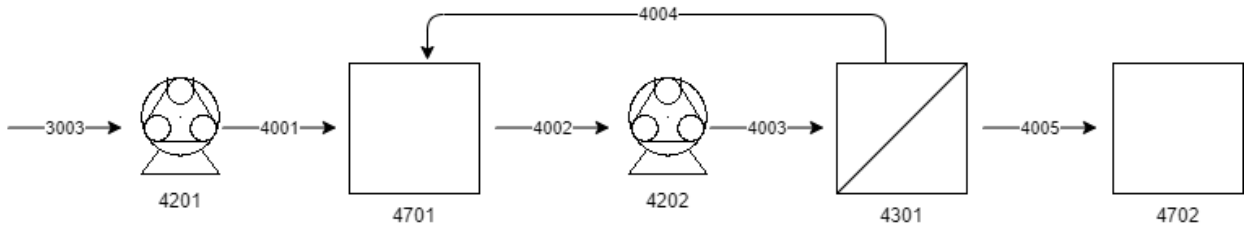

Figure 6.4.2: Microfiltration with TFF Processing Diagram

Table 6.4.2: Microfiltration with TFF PFD Label Descriptions

Equipment or Stream Label	Equipment or Stream Description
3003, 4001	Feed stream
4201	Feed pump
4701	Feed reservoir tank
4002, 4003	Filter feed stream
4301	Microfiltration TFF filter
4202	Filter feed pump
4004	Retentate recycle stream
4005	Permeate stream
4702	Permeate collection tank

Media from the microcarrier separation unit is pumped to the reservoir tank 4701 by pump 4201. The contents of tank 4701 are pumped by pump 4202 to the filter 4301 at a rate of 6.6 L/min. The permeate will flow at a rate of 4.7 L/min and will be collected in tank 4702. The retentate stream will recycle back to tank 4701 by stream 4004. Once the volume in tank 4701 has reached a thirtieth of its original volume, the process will stop and the remaining volume in tank 4701 will be considered waste.

6.4.3 Benzonase Treatment

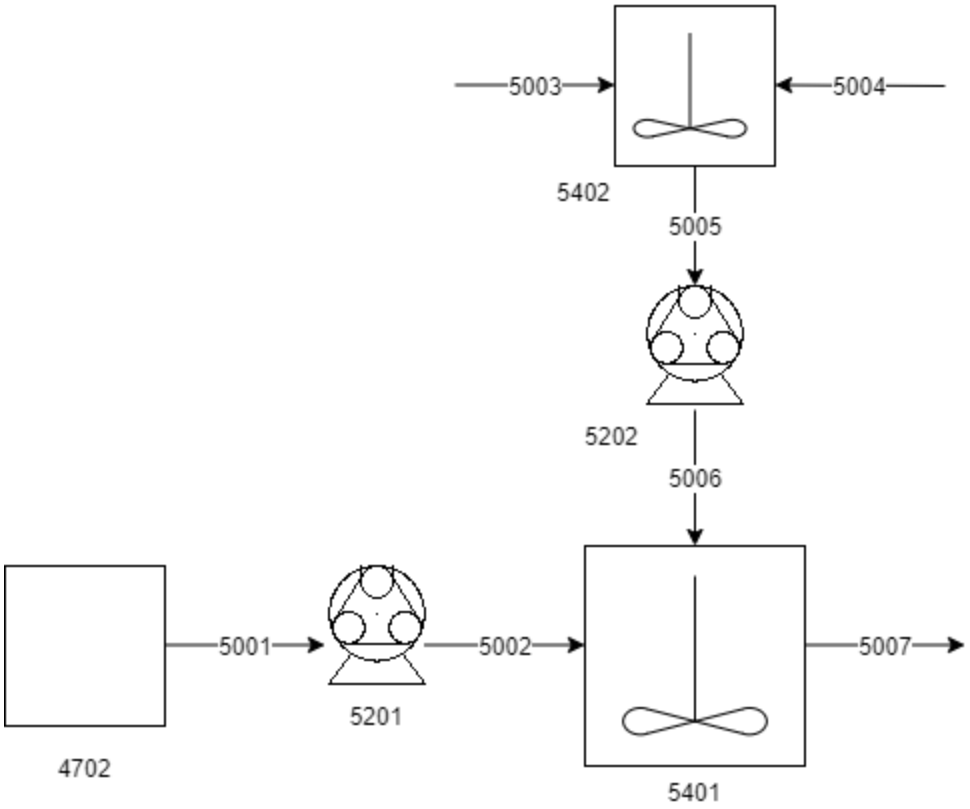

Figure 6.4.3: Benzonase Treatment Processing Diagram

Table 6.4.3: Benzonase Treatment PFD Label Descriptions

Equipment or Stream Label	Equipment or Stream Description
4702	Permeate collection tank
5001, 5002	Feed stream
5201	Feed pump
5003	WFI stream
5004	Benzonase and other solid salts
5401	Media mixing tank
5005, 5006	Media stream
5202	Media pump
5401	Benzonase treatment tank
5007, 5008	Output stream
5203	Output pump
5701	Output collection tank

Tris buffer preparation will begin an hour and a half before microfiltration concludes. 33.34 L of WFI will be added to mixing tank 5402, through stream 5003, with 95.21 g of $MgCl_2$, 100 g of BSA, 7880 g of trizma hydrochloride, and 0.349 mL of Benzonase treatment. 1000 L of permeate in tank 4702 will be transported to mixing tank 5401 by pump 5201. The contents of mixing tank 5402 will be pumped into mixing tank 5401 by pump 5202. After mixing for 24 hours, the contents of mixing tank 5401 will be transported to output collection tank 5701. The whole process will take approximately 26 hours.

6.4.4 Ultrafiltration/Diafiltration

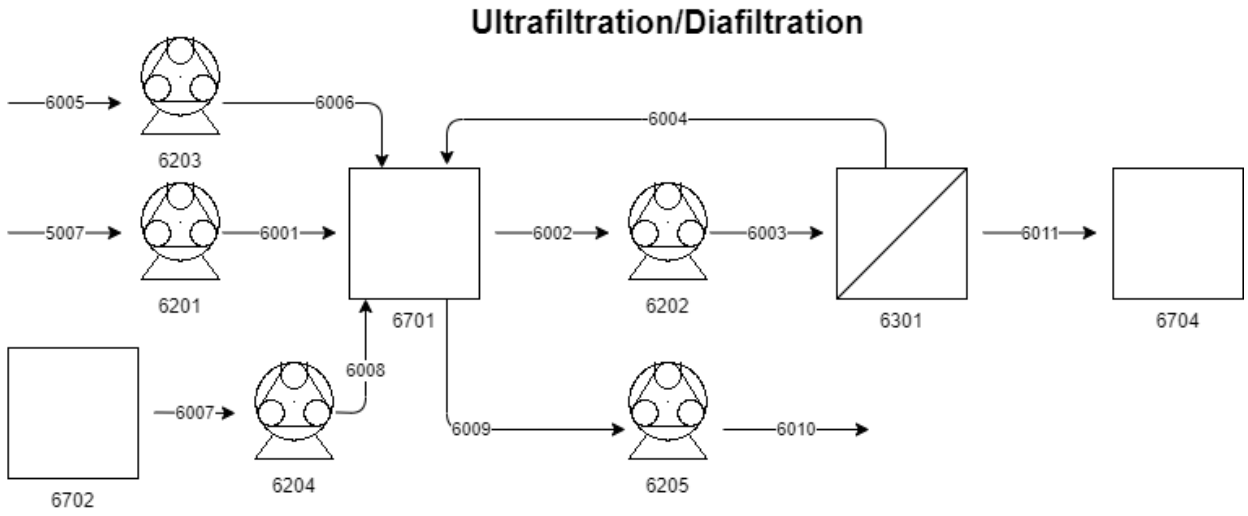

Figure 6.4.4: Ultrafiltration/Diafiltration Processing Diagram

Table 6.4.4: Ultrafiltration/Diafiltration TFF PFD Label Descriptions

Equipment or Stream Label	Equipment or Stream Description
5007, 6001	Feed stream
6201	Feed pump
6701	Feed reservoir tank
6702	Diafiltration buffer holding tank
6007, 6008	Diafiltration buffer stream
6204	Diafiltration buffer pump
6005, 6006	WFI stream
6203	WFI pump
6002, 6003	Filter feed stream
6202	Filter feed pump
6301	TFF filters
6004	Retentate recycle stream
6704	Permeate waste tank
6011	Permeate waste stream
7701	Retintate collection tank
6009, 6010	Output stream
6205	Output pump

Prior to the input of batch material into the TFF unit, WFI from stream 6005 will be used to rinse the filter membranes in filter module 6301 by pump 6203 at a flow rate of 5 L/min. The media input from benzonase treatment will flow through pipe 5007, through pump 6201 at a flow rate of 5 L/min into the TFF feed reservoir holding tank, 6701. Once the entirety of the media is in tank 6701, UF will begin with pump 6202 operating at a flow rate of 6.6 L/min. The TFF system will operate in a loop as the media passes through pipe 6002 to 6003, through filter module 6301, then the retintate will go back to feed tank 6701 by way of pipe 6004. The permeate will flow through pipe 6011 to tank 6704. After UF concentration is complete, the sodium phosphate buffer will be introduced to tank 6701. The buffer will come from tank 6702 and will be pumped to tank 6701 by pump 6204 at a flow rate of 4.7 L/min. After the completion of buffer exchange in DF, the retintate will be collected through output stream 6009 and pumped by pump 6205 to the retintate holding tank 7701. This tank will feed the following inactivation step.

6.4.5 Viral Inactivation

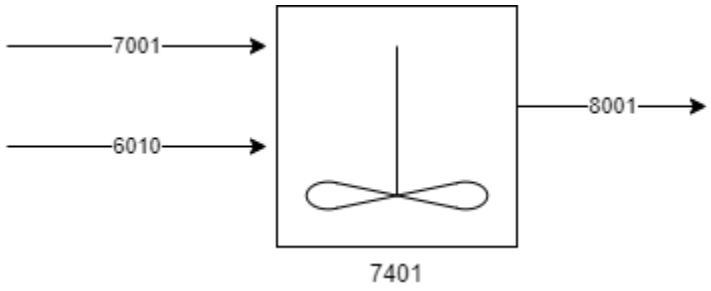

Figure 6.4.5: Viral Inactivation Processing Diagram

Table 6.4.5: Inactivation PFD Label Descriptions

Equipment or Stream Label	Equipment or Stream Description
6010	Feed stream
7001	BPL input stream
7401	Inactivation mixing tank
8001	Inactivation output stream

The concentrated viral product, stream 6010, from UF/DF will be pumped into the 7401 inactivation mixing tank. BPL will be measured and added manually at a volume ratio of 1:4000 (BPL:solution). The tank will be mixing at a rate of 750 RPM for 16 hours at 4℃ to ensure complete inactivation of the virus. The solution in the 7401 tank will then be incubated at 37 ℃ for additional 2 hours to eliminate any excess BPL before exiting the process through stream 8001.

6.4.6 Affinity Chromatography

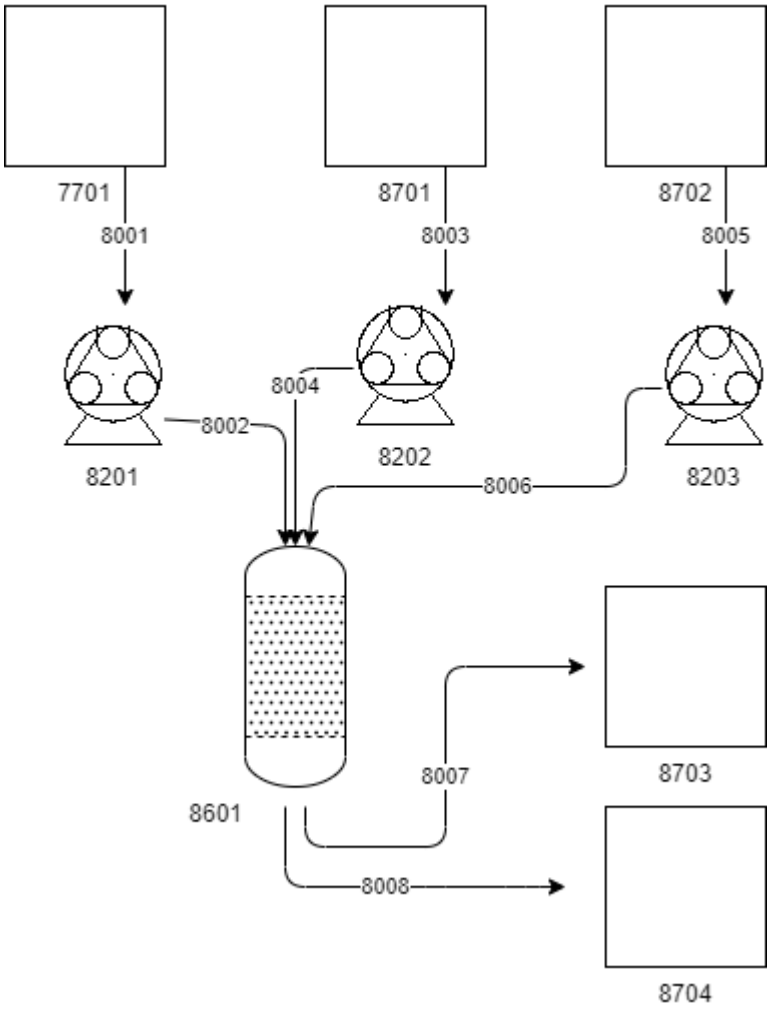

Figure 6.4.6: Affinity Chromatography Processing Diagram

Table 6.4.6: Affinity Chromatography PFD Label Descriptions

Equipment or Stream Label	Equipment or Stream Description
7701	Feed tank
8001, 8002	Feed stream
8201	Feed pump
8701, 8702	Wash/Elution buffer tank
8003, 8004, 8005, 8006	Wash/Elution buffer stream
8202, 8203	Wash/Elution buffer pump
8601	CHT Type II Affinity Chromatography Column
8007	Waste stream
8703	Waste collection tank
8008	Output stream
8704	Output collection tank

Chromatography column 8601 with a column volume of 8L loaded with CHT type II beads is initially washed using the wash buffer from tank 8701 containing 600 mM sodium phosphate pH 7.2. The wash buffer flows at 3.6 L/min for eight column volumes by pump 8202. The column is then equilibrated by pumping an equilibration buffer from tank 8701 containing 10 mM sodium phosphate pH 7.2. The equilibration buffer is dlows at 3.6 L/min for 16 column volumes by pump 8203. The column is then loaded with the sample from tank 7701 and the entire volume is pumped to the column by pump 8201. The column is then washed using 16 column volumes of 10mM sodium phosphate from tank 8702. All liquid passing through the column up to this point is collected in a waste tank 8703. The product will then be eluted by pumping a linearly increasing gradient of 10 mM to 600mM sodium phosphate for 24 column volumes from tank 8701 using pump 8202 and tank 8702 using pump 9203. The elution will be collected in tank 8704 after 12 CV exits the column. After the elutions are collected, a final wash of 8 column volumes of 600 mM sodium phosphate are pumped to the column from tank 8701 and should exit to waste tank 8703. These steps take a total of 3.3 hours.

6.4.7 Size Exclusion Chromatography

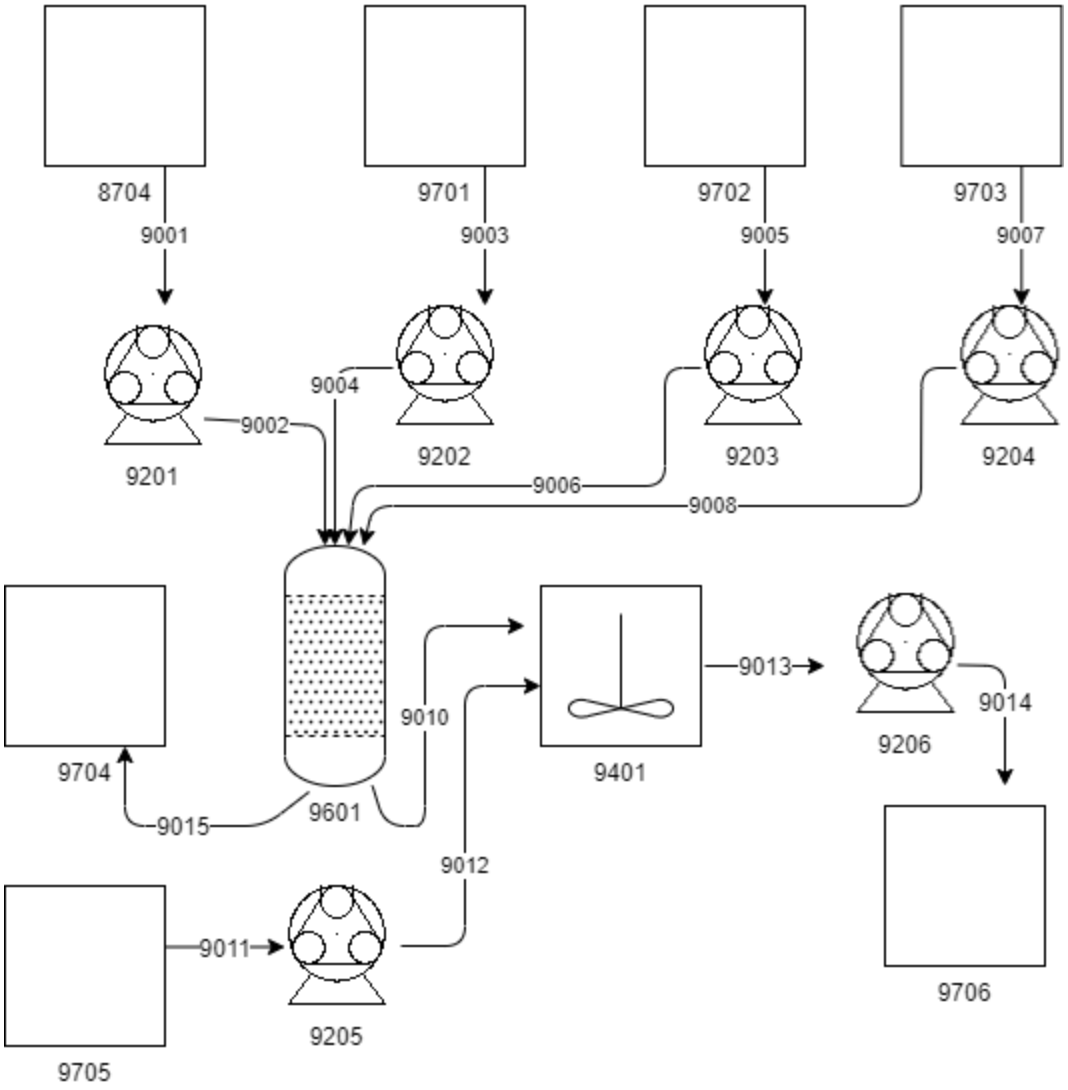

Figure 6.4.7: Size Exclusion Chromatography Processing Diagram

Table 6.4.7: Size Exclusion Chromatography PFD Label Descriptions

Equipment or Stream Label	Equipment or Stream Description
8704	Feed tank
9001, 9002	Feed stream
9201	Feed pump
9701, 9702	Elution buffer tank
9003, 9004, 9005, 9006	Elution buffer stream
9202, 9203	Elution buffer pump
9703	Wash buffer tank
9007, 9008	Wash buffer stream
9204	Wash buffer pump
9601	Size Exclusion Chromatography Column
9015	Waste stream
9704	Waste collection tank
9010	Eulution collection stream
9401	Elution media exchange mixing tank
9705	Media exchange holding tank
9011, 9012	Media exchange stream
9205	Media exchange pump
9013, 9014	Output stream
9206	Output pump
9706	Output holding tank

Size exclusion chromatography in column 9706 will follow a stepwise process of equilibration, solution loading, elution along a linearly decreasing pH gradient, and finally a wash cycle. The column is equilibrated with 1 CV of 0.4 mM NaOH Tris-NaCl buffer, contained in tank 9701. The viral solution is then loaded into the 15.7 L column from tank 8704. Throughout the elution phase, the buffer flow rate remains at 300 cm/h, from both the alkaline (tank 9701) and acidic (tank 9702); initially, the elution buffer is fed from 9701, and the ratio of volume contribution from each elution tank is graded such that the buffer added at the end of this stage is from 9702. In total, 6 CV of buffer is fed in this stage of the process. The molecular

weight cut off of the CaptoCore-700 resin allows the virus to be eluted in the first band (stream 9010), and is collected in tank 9401 to prepare a buffer exchange prior to sterile filtration. The isoelectric points of contaminants to be removed are below equilibration pH, allowing them to bind to the column resin. This residual HCP is stripped from the column resin by the buffer gradient during column elution, and discarded to waste tank 9704. After the elution phase, the column is washed with 1 CV of 1 M NaOH in 30% isopropanol. Cleaning-in-place (CIP) is achieved by allowing 30 minutes of contact time with the wash solution, stored in tank 9703 and fed from pump 9204 to prevent salt and/or contamination to maintain the integrity of the flow and binding properties of the resin. Wash solution is discarded to tank 9704. The column is then prepared for equilibration for the next batch.

The virus solution buffer is exchanged in tank 9704 with PBS before being transferred to tank 9706 prior to sterile filtration. The volume of the virus-containing PBS solution going to sterile filtration is 200 L.

6.4.8 Sterile Filtration

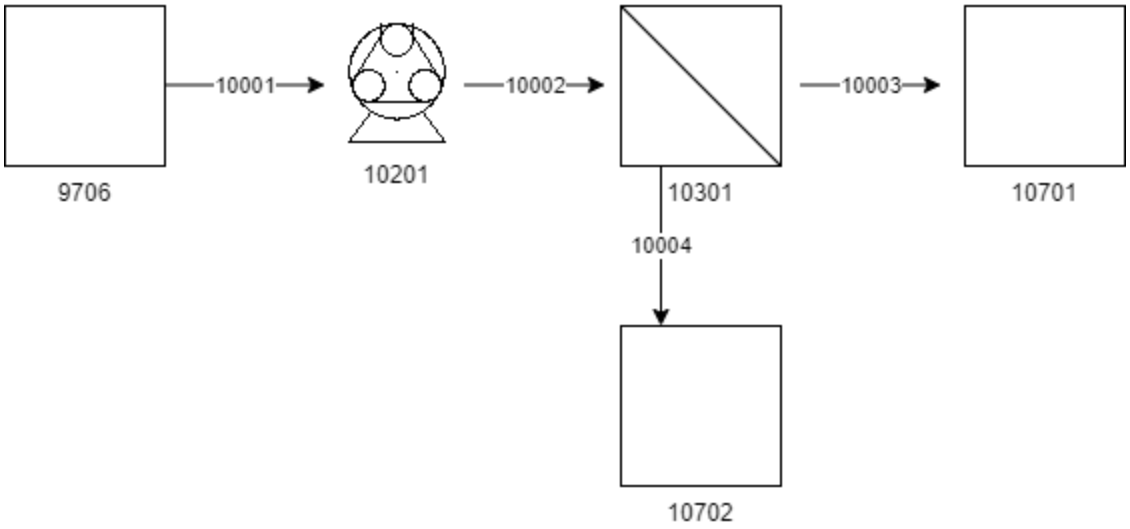

Figure 6.4.8: Sterile Filtration Processing Diagram

Table 6.4.8: Sterile Filtration PFD Label Descriptions

Equipment or Stream Label	Equipment or Stream Description
9706	Feed tank
10001, 1002	Feed stream
10201	Feed pump
10301	0.2 um filter
10004	Waste stream
10702	Waste holding tank
10003	Output filter
10701	Output holding tank

The output from size exclusion chromatography held in tank 9706 is pumped through filter 10301 by pump 10201 at 15.14 L/min. The permeate goes to the output holding tank 10701 for formulation. The filtration process takes 13.2 min.

6.4.9 Formulation

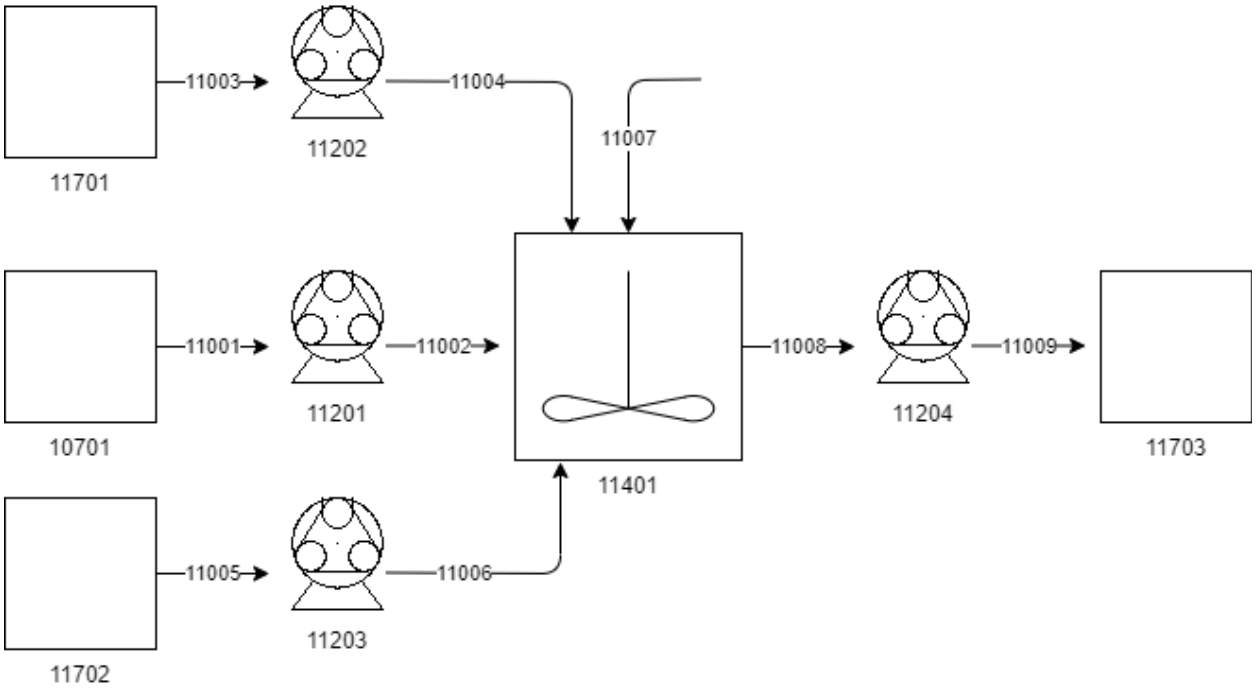

Figure 6.4.9: Formulation Processing Diagram

Table 6.4.9: Formulation PFD Label Descriptions

Equipment or Stream Label	Equipment or Stream Description
10701	Feed tank
11001, 11002	Feed stream
11201	Feed pump
11701	PBS holding tank
11003, 11004	PBS stream
11202	PBS pump
11702	AlOH holding tank
11005, 11006	AlOH stream
11203	AlOH pump
11007	TLR 7/8 and TM 2-phenoxyethanol dry powders
11401	Formulation mixing tank
11008, 11009	Output stream
11204	Output pump
11703	Output holding tank

After sterile filtration, PBS, and AlOH will be pumped from tank 11701 and tank 11702 into the 11401 formulation mixing tank with pump 11202 and pump 11203, respectively. TLR 7/8 and 2-phenoxyethanol will then be measured manually and be added to mixing tank 11401 via stream 11007. The mixing tank 11401 will operate at 750 RPM for 2 hours to ensure homogeneity before it is pumped into the holding tank 11703 via pump 11204.

VI. Material and Energy Balances

According to the schedules compiled in section 6.2, processing the contents of two 1000 L bioreactors occurs 83 % of the time during the first year of operation. Accordingly, the following material and energy balances showcase the materials and utilities required to generate and process that volume. The annual cost of raw materials and utilities for Year 1 are summarized in Table 15.5 in the appendix and Table 8.3.2 in Section 8.3.

7.1 Material Balances

UPSTREAM PROCESSING FOR TWO WEEKS IN Q1									
Unit Operation	**Inputs**			**Outputs**			**Waste**		
	Material	***Amount***	***Units***	***Material***	***Amount***	***Units***	***Material***	***Amount***	***Units***
Vero Cell Factory	Vero cells	2.00×10^8	cells	Vero cells	5.04×10^{11}	cells	Vero cells	1.24×10^{11}	cells
	VP-SFM	363. 70	L	VP-SFM	400	L			
	0.25% Tryp. EDTA	5.10	L						
	DPBS	13.60	L						
	L-Glutamine	203.60	g	L-Glutamine	187.27	g			
Bioreactor	Vero cells	5.04×10^{11}	cells	Whole Vero Cells	1.53×10^{11}	cells			
	VP-SFM	1611.65	L	VP-SFM	2000.00	L	VP-SFM	11.65	L
	PBS	37.86	L				PBS	33.37	L
	Virus	5.04×10^7	g	Virus	106.35	g			
	L-Glutamine	1028.73	g	HCP	183.74	g			
	Dry Cytodex-1 MC	291.26	g	Wet Cytodex-1 MC	6,000.00	g			
	Air	105.89	L/hr	Air (O_2 depleted)	105.89	L/hr			

DOWNSTREAM PROCESSING FOR TWO WEEKS IN Q1									
Unit Operation	**Inputs**			**Outputs**			**Waste**		
	Material	***Amount***	***Units***	***Material***	***Amount***	***Units***	***Material***	***Amount***	***Units***
Micro-carrier Seperation	Whole Vero cells	1.53×10^{11}	cells	Whole Vero cells	1.30×10^{11}	cells	Whole Vero cells	2.30×10^{10}	cells
	Cytodex-1 MC	6000.00	g				Cytodex-1 MC	6000.00	g
	Virus	106.35	g	Virus	106.35	g			
	HCP	183.74	g	HCP	183.74	g			
	VP-SFM	2000.00	L	VP-SFM	2000.00	L			
Micro-filtration with TFF	Whole Vero cells	1.30×10^{11}	cells	Whole Vero cells	4.43×10^{4}	cells	Whole Vero cells	1.29×10^{11}	cells
	Virus	106.35	g	Virus	101.37	g	Virus	4.98	g
	VP-SFM	2000.00	L	VP-SFM	1933.33	L	VP-SFM	66.67	L
	HCP	183.74	g	HCP	177.09	g	HCP	6.65	g
Benzonase Treatment	Whole Vero cells	4.43×10^{4}	cells	Whole Vero cells	4.43×10^{4}	cells			
	Vero Cell DNA	1.94×10^{-3}	g	Vero Cell DNA	1.94×10^{-3}	g			
	Virus	101.37	g	Virus	101.37	g			
	Benzonase Treat.	6.99×10^{-4}	L	Tris HCl Buffer	2000.00	L			
	Tris HCl	15,760.00	g						
	MgCl2	190.42	g						
	BSA	200.00	g						
	HCP	177.09	g	HCP	177.09	g			
	VP-SFM	1933.33	L						
	WFI	66.67	L						

UF/DF	Whole Vero cells	4.43×10^4	cells				Whole Vero cells	4.43×10^4	cells
	HCP	177.09	g	HCP	49.58	g	HCP	127.50	g
	Virus	101.37	g	Virus	101.37	g			
	$NaSO_4$ Buffer	482.83	L	$NaSO_4$ Buffer	144	L	$NaSO_4$ Buffer	338.83	L
	Tris HCl Buffer	2000	L	Tris HCl Buffer	6	L	Tris HCl Buffer	1994	L
Inactivation	BPL	3.75×10^{-2}	L	BPL	3.75×10^{-2}	L			
	$NaSO_4$ Buffer	150	L	$NaSO_4$ Buffer	150	L			
	HCP	49.58	g	HCP	49.58	g			
	Virus	101.37	g	Virus	101.37	g			
Affinity Chroma-tography	HCP	49.58	g	HCP	0.36	g	HCP	49.23	g
	Virus	101.37	g	Virus	93.23	g	Virus	8.14	g
	CHT Type 2 Resin	5,043.01	g				CHT Type 2 Resin	5,043.01	g
	Sodium Phosphate	16,713.98	g	Sodium Phosphate	3,515.70	g	Sodium Phosphate	13,198.28	g
	WFI	704.42	L	WFI	96.06	L	WFI	608.36	L
SEC	HCP	0.36	g	HCP	0.02	g			
	Virus	93.23	g	Virus	79.24	g			
	Tris + NaCl Buffer	314.00	L	Tris + NaCl Buffer	157.00	L	Tris + NaCl Buffer	157.00	L
	WFI	96.06	L				WFI	96.06	L
Sterile Filtration	Virus	79.24	g	Virus	79.24	g			
	HCP	0.02	g	HCP	0.02	g			
	Tris + NaCl Buffer	157.00	L	Tris + NaCl Buffer	157.00	L			
Formulation	$Al(OH)_3$ Gel	3,301.80	g	$Al(OH)_3$ Gel	3301.80	g			

	TLR 7/8	198.11	g	TLR 7/8	198.11	g			
	TM 2-phen.	33,018.01	g	TM 2-phen.	33,018.01	g			
	PBS	6,446.60	L	PBS	6,446.60	L			
	Virus	79.24	g	Virus	79.24	g			
	HCP	0.02	g	HCP	0.02	g			
	Tris + NaCl Buffer	157.00	L	Tris + NaCl Buffer	157.00	L			
Filling	Virus	79.24	g	Virus	71.32	g	Virus	7.92	g
	$Al(OH)_3$ Gel	3,301.80	g	$Al(OH)_3$ Gel	2,971.62	g	$Al(OH)_3$ Gel	330.18	g
	TLR 7/8	198.11	g	TLR 7/8	178.29	g	TLR 7/8	19.81	g
	TM 2-phen.	33,018.01	g	TM 2-phen.	29,716.21	g	TM 2-phen.	3,301.80	g
	PBS	6,446.60	L	PBS	5,801.94	L	PBS	644.66	L
	HCP	0.02	g	HCP	0.02	g	HCP	0.002	g
	Tris + NaCl Buffer	157.00	L	Tris + NaCl Buffer	141.30	L	Tris + NaCl Buffer	15.70	L

7.2 Energy Balances

Table 7.2a: Bioreactor Heating Jacket Startup Energy Balance

Component	Initial T (℃)	Final T (℃)	Mass (kg)	Mass Flow Rate (kg/s)
VP-SFM	5	37	800	N/A
PE Bag	23	37	60	N/A
Steel	23	37	1000	N/A
Heating Water	50	37.5		0.97
Power Consumption (kWh)				35.78
Duration (h)				0.88

Table 7.2b: Bioreactor Heating Jacket Operating Energy Balance

Heat Replenished by Jacket (kJ/s)	40℃ Heating Water Mass Flow Rate (kg/s)	Heat Gained by Atmosphere (kJ/s)
30.4	2.51	1.03
Power Consumption (kWh)		2.04
Duration (h)		144

Table 7.2c: Benzonase Heating Jacket Startup Energy Balance

Component	Initial T (℃)	Final T (℃)	Mass (kg)	Mass Flow Rate (kg/s)
VP-SFM	34	37	800	N/A
PE Bag	23	37	60	N/A
Steel	23	37	1000	N/A
Heating Water	40	37		0.03
Power Consumption (kWh)				8.95
Duration (h)				0.34

Table 7.2d: Benzonase Treatment Heating Jacket Operating Energy Balance

Heat Replenished by Jacket (kJ/s)	40℃ Heating Water Mass Flow Rate (kg/s)	Heat Gained by Atmosphere (kJ/s)
30.4	2.51	1.03
Power Consumption (kWh)		2.04
Duration (h)		24

Table 7.2e: Viral Inactivation Cooling Jacket Startup Energy Balance

Component	Initial T (℃)	Final T (℃)	Mass (kg)	Mass Flow Rate (kg/s)
UF/DF Retenante	20	4	200	N/A
Steel	23	4	327	N/A
Ethylene Glycol	0	8	90	0.275
Power Consumption (kWh)				6.912
Duration (h)				0.64

Table 7.2f: Viral Inactivation Operating Energy Balance

	Mass Flow Rate (kg/s)	Heat Lost by Atmosphere (kJ/s)
	0.056	1417
Power Consumption (kWh)		88529
Duration (h)		16

Table 7.2g: BPL Elimination Heating Jacket Startup Energy Balance

Component	Initial T (℃)	Final T (℃)	Mass (kg)	Mass Flow Rate (kg/s)
UF/DF Retenante	4	37	150	N/A
PE Bag	23	37	20	N/A
Steel	23	37	200	N/A
Water	40	37	90	0.55
Power Consumption (kWh)				6.84
Duration (h)				1

Table 7.2h: BPL Elimination Operating Energy Balance

Heat Absorbed by Jacket (kJ/s)	Mass Flow Rate (kg/s)	Heat Gained by Atmosphere (kJ/s)
10.6	0.87	0.35
Power Consumption (kWh)		0.39
Duration (h)		2

Table 7.2i: Formulation Startup Energy Balance in Q1

Component	Initial T (℃)	Final T (℃)	Mass (kg)	Mass Flow Rate (kg/s)
Elimination Output	37	6	150	N/A
Steel	23	6	10,000	N/A
Ethylene Glycol	0	6	90	0.275
Power Consumption (kWh)				6.912
Duration (h)*				0.64

*the amount of PBS needed changes as the amount of antigen fed to the stage changes, therefore, the time needed to cool it also changes

Table 7.2j: Formulation and Filling Operating Energy Balance in Q1

Heat Absorbed by Jacket (kJ/s)	Mass Flow Rate (kg/s)	Heat Lost by Atmosphere (kJ/s)
139.6	0.056	1417
Power Consumption (kWh)		88530
Duration (h)		29.72

VII. Process Economics

8.1 Purchased Equipment

Costs associated with purchased equipment are based on vendor quotes, if available, or an excel calculator based on the text Plant Design and Economics for Chemical Engineers (Peters, Timmerhaus, & West, 2003). Since this program provides equipment costs from 2003, the prices were adjusted using the CECPI from November 2020 of 606. This calculator stipulated minimum thresholds for volumes and flow rates for their prices, so prices were extrapolated to fit the size of our chemical plant. Main process and ancillary equipment costs are listed in Table 15.3. The breakdown of all purchased equipment is shown below in Table 8.1, details about pricing for process and single-use equipment are shown in Tables 15.3 and 15.6 in the appendix.

Table 8.1: Summary of Purchased Equipment

	Type of Expense	**Cost**
Process Equipment	Fixed	$33,273,221
Single-Use Equipment	Annual	$62,889,038

8.2 Capital Investment

8.2.1 Fixed Capital Investment

Fixed Capital Investment (FCI) is a portion of the total capital investment that generally covers physical and construction assets such as factories, vehicles, and machinery that are almost permanent (Hayes, 2020). The rules for different direct and indirect costs in Table 8.2.1a are based on estimations from Plant Design and Economic for Chemical Engineers (Peters, 2003). Peters indicates that the rules are pre design cost estimates for a typical chemical processing plant and can have errors of ± 20% or higher depending on many factors. The average of each rule was assumed as a basis for preliminary economic analysis. The percentage of FCI for each cost was normalized and shown in Table 8.2.1a. The values for each cost are relative to Purchased Equipment cost which is a known value. Table 8.2.1a indicates the FCI is $157,493,246.

Table 8.2.1a: Fixed Capital Investment Breakdown

	Rule	% of FCI (N)	Value
Direct Costs	**65-85% of FCI**	**65.15%**	**$118,119,935**
Purchased Equipment	15-40% of FCI	18.35%	$33,273,221
Installation, Insulation, etc.	25-55% of Purchased Equipment	7.34%	$13,309,288
Instrumentation and Controls	8-50% of Purchased Equipment	5.32%	$9,649,234
Piping	10-80% of Purchased Equipment	8.26%	$14,972,949
Electrical	10-40% of Purchased Equipment	4.59%	$8,318,305
Building, Process, Auxiliary	10-70% of Purchased Equipment	7.34%	$13,309,288
Service Facilities	40-100% of Purchased Equipment	12.85%	$23,291,255
Land	4-8% of Purchased Equipment	1.10%	$1,996,393
Indirect costs	**15-35% of FCI**	**21.72%**	**$39,373,312**
Engineering and Supervision	5-30% of Direct Costs	11.40%	$20,670,989
Legal Expenses	1-3% of FCI	1.74%	$3,149,865
Construction	10-20% of FCI	13.03%	$23,623,987
Contingency	5-15% of FCI	8.69%	$15,749,325
FCI	**Direct + Indirect Costs**		**$157,493,246**

8.2.2 Working Capital

Working Capital is estimated in Plant Design and Economic for Chemical Engineers as 10-20% of Total Capital Investment (Peters, 2003). Assuming an average of 15%, working capital is estimated to be $27,796,926.

8.3 Operating Costs

The cost of manufacturing (COM) for the chemical plant was estimated using equation 8.3a (Turton, 2018). Where C_{OL} is the cost of operating labor, C_{UT} is the cost of utilities, C_{WT} is the cost of waste treatment, and C_{RM} is the cost of raw materials. This equation accounts for depreciation. The total cost of manufacturing for Year 1 is $285,243,501. Subsequent years of manufacturing involve a 20% increase in product, using that as a rough basis for an increase in COM, the COM after the first year of manufacturing is $342,292,201. Waste from the process will be stored in biohazard containers and will be processed by a separate entity because of the enormous autoclaving expenses associated with sterilizing it. The annual cost of biohazardous waste from the manufacturing process is $416,541, which is included in the C_{UT} instead of C_{WT} as seen in Table 8.3.2. According to Eqn. 8.3a the category waste expenses is assigned does not impact calculations for COM.

$$COM = 0.280FCI + 2.73C_{OL} + 1.23(C_{UT} + C_{WT} + C_{RM}) \quad \text{(Eqn. 8.3a)}$$

8.3.1 Raw Materials

The annual cost of raw materials is $150,601,349, Tables 15.5 and 15.6 summarize each component. Figures 8.3.1a and 8.3.1b showcase the bioreactor and formulation are the majority of the expenses for upstream and downstream processing. The membranes and resins will be replaced with each batch fed to downstream processing. Single-use equipment is included in calculations for raw materials.

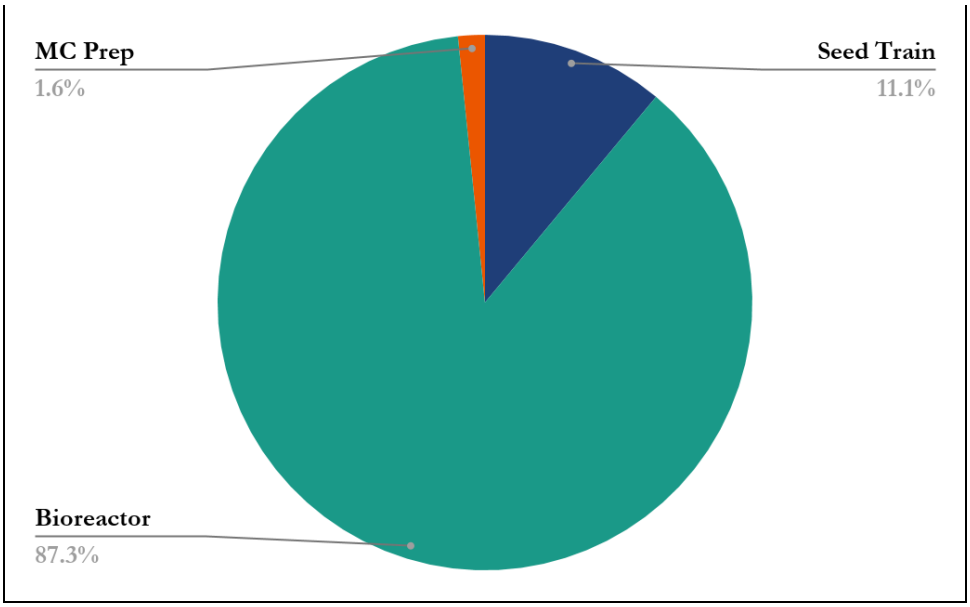

Figure 8.3.1a: Breakdown of Upstream Raw Materials Costs

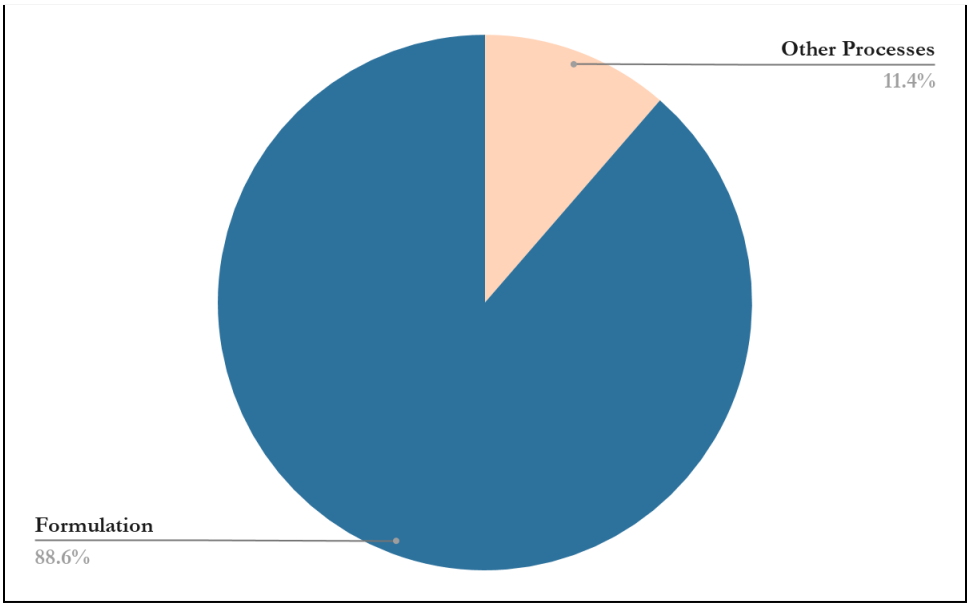

Figure 8.3.1b: Breakdown of Downstream Raw Materials Cost

8.3.2 Utilities

The annual cost of utilities is $504,472 and is illustrated in detail below in Table 8.3.2.

Table 8.3.2: Summary of Utility Costs

Equipment	Utility	Requirement	Annual Cost
Incubator	Power (kWh)	2580	$282
Autoclave	Power (kWh)	14919	$1,628
Autoclave	Water (kg)	20866	$4
1000 L Bioreactors	Power (kWh)	116,813	$12,744
200 L Bioreactor	Power (kWh)	6653	$726
Marine Impellers for Bioreactors	Power (kWh)	14651	$1,598
50 C Water	Water (kg)	5000	$776
Heat Jackets	Power (kWh)	4340	$474
Immersion Heater	Power (kWh)	431680	$47,096
Cooling Jackets	Power (kWh)	3046	$332
Cooling Jackets	Ethylene Glycol (kg)	396	$399
Cooler	Power (kWh)	177059	$19,317
Formulation Impeller	Power (kWh)	697	$76
Filling	Power (kWh)	17405	$1,899
Air Supply	Power (kWh)	17187	$149
Pumps	Power (kWh)	69	$8
Ruston Impellers for Ancillary Mixers	Power (kWh)	1050	$115
Labeller	Power (kWh)	2830	$309
Waste	Treatment (t)	207	$416,541
Total			**$504,472**

8.3.3 Labor

Labor costs were estimated using Eqn 8.3.3a from Turton et al.

$$N_{OL} = (6.29 + 31.7P^2 + 0.23N_{np})^{0.5} \quad \text{(Eqn 8.3.3a)}$$

N_{OL} indicates the number of operators needed per shift. P indicates the number of processes involving handling particulate solids. N_{np} indicates the number of non-particulate processes. The factory will include ten particulate processes and twenty non-particulate processes. The number of operators needed under these conditions per shift was found to be 56.4. Turton et al. estimates that the total operators needed to run a facility is 4.5 times the operators needed per shift so rounded up a total of 254 operators are needed (Turton, 2018). The median annual wage in 2020 for a single manufacturing operator is estimated at $69,329, including a 30% fringe rate (https://www.bls.gov/oes/current/oes_nat.htm; Tanski-Phillips, 2020). Peters also estimates that direct supervisory and clerical labor costs should be 10-20% of operator labor costs (Peter, 2003). Assuming supervision is 15% of operator labor costs, total labor cost is estimated to be $20,251,001 a year.

8.3.4 Miscellaneous

The COM includes direct manufacturing costs like laboratory charges for quality control and general manufacturing expenses like research and development and distribution and selling. Additional operators for quality control measures were included in the calculations for labor costs.

8.4 Financial Analysis

To determine if the implementation of a vaccine manufacturing plant following this report's design and expected costs, an Internal Rate of Return (IRR) is calculated using discounted cash flow analysis. IRR is calculated under the following assumptions:

1. Construction and validation takes one year and production can begin at the start of year two.
2. Production of the vaccine is constant for five years after which production ends.
3. The combined federal and state corporate tax rate is 45%.
4. Purchased equipment in FCI depreciates using the 3 year MACRS depreciation.
5. The cost per dose sold is $4.

Following these assumptions, an IRR of 629% was calculated.

Due to multiple potential indications that the original IRR is too high, a IRR was calculated according to Turton et al. estimation of a worst case scenario which has the following assumptions:

1. Revenue is 20% lower than expected
2. Cost of Manufacturing is 10% higher than expected
3. FCI is 30% higher than expected

Under these worst case scenario assumptions, the IRR is calculated to be 379% which is still extremely high indicating the project is economically feasible.

Increasing the price per dose significantly increased the IRR, if each dose were $15, the IRR in the generic and worst case scenario would be 2495% and 583%. A figure of cumulative cash flow can be found in the appendix (Figure 15.1).

Table 8.4 summarizes the cash flow for the life of the plant, the cumulative cash flow (CFF) after Year 5 is $4,891,160,054 under the worst case scenario conditions listed above.

Table 8.4 Production Plan Cash Flow for Worst Case Scenario

Year	Doses (millions)	Revenue	COM	Cash Flow	CCF
0				-$240,872,023	-$240,872,023
1	571	$1,825,623,973	$313,767,851	$867,648,058	$626,776,034
2	713	$2,282,029,966	$376,521,421	$1,096,210,126	$1,722,986,161
3	713	$2,282,029,966	$376,521,421	$1,064,082,616	$2,787,068,777
4	713	$2,282,029,966	$376,521,421	$1,056,061,578	$3,843,130,354
5	713	$2,282,029,966	$376,521,421	$1,048,029,700	$4,891,160,054

According to Table 8.4, revenue increases in Year 2 because the doses generated by the plant increases to 713 million, the total number of doses for a full year at full-scale manufacturing. The cost of manufacturing (COM) increases as well because of the additional raw materials needed. Using 3 year MACRS depreciation results in the FCI discount diminishing after Year 4.

The incredibly high IRR can be attributed to multiple factors. The R&D aspect of the COM could be inadequate because of viral mutations. The distribution calculations could also be inadequate because the vaccine needs to be able to reach virtually everyone in the world. These calculations also do not include advertising and fees that would be associated with running trails and seeking regulatory approval.

IX. Environmental, Health, and Safety Concerns

The US. Occupational Safety and Health Administration (OSHA) provides extensive regulations and guidelines for the safe operation of industrial facilities. These regulations for personal and process safety will be followed in every aspect of this process design. These precautions help ensure that all employees, contractors, and community members feel safe in and around this workplace. At the most basic level, personal protective equipment (PPE) will be required wherever needed throughout the manufacturing areas. PPE includes eye protection, head protection, hearing protection, and foot protection. Signs will be posted on doorways communicating the necessity of PPE leading to areas where they are required. It should also be noted that the construction of this plant is complicated by the ongoing global pandemic. The CDC has outlined guidelines for safe personal conduct during this time. Due to the pharmaceutical nature of this plant, additional environmental and safety precautions must be taken.

Live Sars-CoV-2 virions are present until the viral inactivation unit operation. Due to the high pathogenicity of the coronavirus, the CDC has specified that all Sars-CoV-2 specimens need to be processed in a Biosafety Level 3 (BSL-3) space (CDC, 2021). The safety guidelines specific to SARS are outlined by the National Institute of Health (NIH) in detail and will be integrated into all of the processing areas (NIH, 2020). The precautions to be observed are as follows.

There are many additional PPE requirements in a BSL-3 facility. Respiratory protection should be used by all personnel. Workers should wear solid front protective clothing, such as wrap-around gowns, scrub suits, or coveralls. This protective clothing should never leave the facility and must be decontaminated after every use. Face shields should be worn at any point in

the process where splashing may occur, such as during manual start-up procedures. Two pairs of gloves should be worn when appropriate, and shoe covers should be worn while inside the facility and thrown away before exiting. Personnel working in the facility must also be trained regarding the symptoms of COVID-19 infection and counseled to report any symptoms to their supervisor immediately. When possible, employees of the facility should be immunized against the virus.

In addition to PPE, the facility must be constructed to follow BSL-3 requirements. The doors to manufacturing areas must be lockable, allowing access only to authorized personnel. A clothing change room with self-closing doors should exist between manufacturing areas and unrestricted traffic flow areas, where undressings and decontamination will occur. Eyewash stations and handwashing stations should be placed near exits. Walls, ceilings, and floors should be coated in a sealed, smooth finish that can easily be cleaned and decontaminated. Chairs and benchtops should comprise non-porous materials. A ducted mechanical air ventilation system is required. This system should provide one-directional airflow, drawing air from "clean" areas toward "contaminated" areas. The facility should be designed such that under failure conditions, the airflow will never be reversed. The exhaust air will be HEPA filtered. (NIH, 2020)

Additionally, intense quality control measures will be adopted at this facility to ensure that the process is working as expected. Many tests will be performed throughout the process to ensure that chemical inactivation was complete and that live virions are no longer present. Apart from the biohazards, other chemicals that possess certain risks will also exist within the plant. All relevant chemicals used in this process and their respective risks are enumerated below in Table 9a.

Table 9a: Chemical Safety Risks Present in the Covaxin Industrial Process

Chemical Name	Risks	MSDS Sheet Link
VP-SFM	N/A	*MSDS_VPSFM*
Glutamine	Irritating to eyes, respiratory system and skin	*MSDS_glutamine*
Benzonase	Possibility of hazardous reactions with halides, strong oxidizing agents, and flammable gasses. Special consideration should be given to prevent spillage or contamination of this chemical	*MSDS_benzonase*
Tris HCl	Incompatible with bases and strong oxidizing agents. Irritating to eyes, respiratory system and skin	*MSDS_tris*
$MgCl_2$	May cause irritation and illness from ingestion or inhalation	*MSDS_MgCl2*
BSA	May cause allergic reaction for some individuals	*MSDS_BSA*
$NaSO_4$ Buffer	Irritating to eyes, respiratory system and skin	*MSDS_NaSO4*
Beta-propiolactone	Flammable and combustible. Causes skin irritation, serious eye irritation, fatal if inhaled. Moisture sensitive. Incompatible with acids, bases, and halogens. Carcinogenic to humans	*MSDS_BPL*
Trypsin-EDTA	N/A	*MSDS_trypsin/edta*

As shown in the table above, the only significantly dangerous chemical present in the process is beta-propiolactone, which is used in the chemical inactivation step. Well-trained professionals will be staffed on this unit operation and extreme caution will be designated to the transportation, handling, and usage of this chemical. The MSDS sheets pertaining to each chemical will be posted, visible and readily available to all employees in processing areas where such chemical exists.

This process yields biohazardous waste. In order to prevent environmental damage, all waste, such as bags, single use objects, filtration membranes, and spent resins will be autoclaved prior to disposal. The autoclave waste will be kept in locked biohazard waste containers. Hazardous waste disposal companies that specialize in pharmaceutical waste treatment will be

hired to retrieve, transport, and treat waste. This ensures the utmost care for the community and the planet by ensuring that waste is not neglected. It may also be noted that Vero cells will release CO_2 during their metabolic processes. This carbon dioxide will leave the bioreactor through an air output valve, then it will be filtered and released into the atmosphere at negligible levels.

X. Social Implications of the Project

Social implications of this project must be addressed for both the physical location of manufacturing as well as the greater population/target market of the vaccine. The plant will be located in Durham, NC. This location was chosen because of its familiarity with the pharma industry. We anticipate that experienced employees will be available for hire and that the community will be accepting of the construction of our plant. It has been documented that new industries often cause a population boom in areas due to the new jobs available. Without proper urban planning, this can lead to issues regarding transportation, housing, highway congestion, school facility requirements, etc. (Planning Advisory Service, 1951). To prevent any discomfort in the community, we will be sure to begin advertising the construction of the plant as early as possible, giving the town time to adapt.

The widespread availability of a COVID-19 vaccine will have powerful social implications across the world. Vaccines have been shown to improve equity of healthcare. A study based on the measles vaccine in Bangladesh in 1982 demonstrated improved health outcome equity (Bishai et al., 2003). Further, a study done on the rotavirus vaccine in India suggested that the vaccine would provide the poor with both health and financial benefits (Verguet et al., 2013). We make the assumption that widespread availability of the COVID-19 vaccine will also improve the equity of healthcare. We hope to mitigate the effects of COVID-19 on underprivileged groups in society- who have been disproportionately negatively affected by the pandemic- through vaccination.

This vaccine will also have beneficial impacts on healthcare infrastructure. The invention of this vaccine necessitates more national programs and government funding to implement vaccination efforts. More professionals will receive jobs to administer vaccines and provide the

required aftercare. The global logistics required to achieve vaccination of 70% of the world's population will facilitate partnerships between countries, companies, and public health programs that can be long lasting and beneficial through other health and social endeavors (Shearly, 1999; Rodrigues & Plotkin, 2020).

Finally, vaccinating the world's population against COVID-19 will have far-reaching positive effects on mental health. The pandemic and resulting economic recession have put many in excruciating financial positions, negatively affecting people's mental health. Additionally, the death toll of the virus thus far has placed inexplicable hardships on millions of families worldwide. Necessary public health measures, such as working from home and quarantine has resulted in isolation, loneliness, and poor mental health outcomes. In a study done regarding pandemic-era mental health, it was found that 41.1% of adults reported symptoms of anxiety disorder and/or depressive disorder in January 2021, as compared to only 11.0% of adults reporting these symptoms in January 2019 (Panchal et al., 2021). With vaccination against COVID-19, it is expected that the world will return to some sort of "normalcy". Families will be able to reunite with grandparents, businesses can reopen, and many will be able to return to in-person work. Bringing back face-to-face interactions will restore the social communities in which human beings are meant to exist; this vaccine will aid in this long-anticipated transition.

XI. Conclusions and Recommendations

The data used in this paper is based on small lab scale experiments and extrapolation of available data. Our team recommends conducting these experiments in-house and updating the design accordingly to ensure the utmost quality and safety of our product. Additionally, finding companies with more economical prices for raw materials, such as the CHT resin, VP-SFM, and PBS, would help decrease the cost of operation. Another area that we did not explore was to create our own master seed bank for Vero cells to eliminate the additional steps and costs associated with it. At the start of the process, we can obtain the necessary amount of Vero cells from our own cell bank without propagation, which can decrease our total production time.

Our team recommends implementing this production line to meet the increasing demand around the globe and to help end the pandemic. Most of the unit operations are currently being implemented in the industry to produce other similar products and the work in this project demonstrated that the overall process can be executed. Additionally, the economics analysis demonstrated the economic feasibility of the project, with the IRR of 379%, under the worst conditions. The plant will produce 570 million doses the first year and 713 million doses annually the years after.

XII. Acknowledgements

We offer our gratitude to the faculty of the chemical engineering department for their support and guidance in developing this capstone project. First, we would like to recognize our capstone advisor, Eric Anderson, for his continued assistance throughout this endeavor. We extend an expression of gratitude to Dr. Michael King for taking the time to guide us in the vaccine and vaccine manufacturing field. We want to thank Dr. Giorgio Carta and his graduate student Preston Fuks for their instruction and expertise in chromatography. For his help with bioreactor design and microbe growth kinetics, we want to thank Dr. George Prpich.

XIII. Nomenclature

Symbol	Units	Definition
A	m^2	Area
B	Unitless	Weight of solid particle per weight of liquid
C*	$\frac{g}{L}$	Saturation oxygen concentration
C_0	$\frac{g}{L}$	Initial concentration
C_p	J/kg-K	Specific heat capacity
$C_{O2,Critical}$	$\frac{g}{L}$	Critical oxygen concentration
DBC	$\frac{g}{L}$	Dynamic binding capacity
D_i	m	Impeller diameter
D_p	m	Average particle size
D_t	m	Tank diameter
g	$\frac{m}{s^2}$	Gravitational acceleration constant
GUR	$\frac{mmol\ Glucose}{g*h*X}$	L-Glutamine uptake rate
HCP_i	Unitless	Host cell protein percentage of size i
H_t	m	Tank height
kLa	hr^{-1}	Oxygen transfer coefficient
Ks	g	Monod constant
k_t	W/m-K	Thermal conductivity
L	m	Length
L_{SU}	m	Height of single use bag
$\dot{m}$	kg/s	Mass flow rate
M	kg	Mass
MOI	Unitless	Multiplicity of infection
N	RPM	Impeller rotations per minute
N_a	Unitless	Aeration number
n_c	RPM	Critical rotation speed
N_i	Unitless	Number of impellers
Np	Unitless	Power number
OUR	$\frac{mmol\ O_2}{g*h*X}$	Oxygen uptake rate
OUR_{max}	$\frac{mmol\ O_2}{g*h*X}$	Maximum oxygen uptake rate

P	psi	Pressure
ΔP	psid	Pressure difference
P_{atm}	atm	Atmospheric pressure
P_g	W	Power requirement of a gassed system
P_{O2}	atm	Partial pressure of component i
P_r	W	Ungassed power
P_w	W	Power
Q	$\frac{L}{min}$	Permeate flow rate
Q_{steel}	J/s	Heat loss through steel
Q_g	$\frac{m^3}{min}$	Volumetric air inflow rate
q	J	Heat duty
q_{O2}	$\frac{mmol\ O_2}{g*h*X}$	Specific oxygen consumption rate
Re	Unitless	Reynolds number
r_{SU}	m	Radius of single use bag
r_{steel}	m	Steel thickness
s	$\frac{m}{s}$	Impeller tip speed
S	Unitless	Shape factor
t	s or min	Time
T	^{0}C	Temperature
T_c	^{0}C	Coolant temperature
T_{HW}	^{0}C	Temperature of heating water
T_i	^{0}C	Initial temperature
T_{in}	^{0}C	Inner temperature
T_f	^{0}C	Final temperature
T_{out}	^{0}C	Outer temperature of steel
ΔT	^{0}C	Temperature difference
TOI	hours	Time of infection
u	$\frac{cm}{hr}$	Linear velocity
U	W/m^2-K	Overall heat transfer coefficient
v	$\frac{L}{min}$	Volumetric flow rate
V	L	Volume
V_0	L	Initial volume
v_s	$\frac{m}{hr}$	Superficial gas velocity

V_w	L	Washing volume
X	$\frac{g}{L}$	Cell concentration
$Y_{x/s}$	$\frac{g\ of\ biomass}{g\ of\ substrate}$	Substrate yield coefficient
X	$\frac{g}{L}$	Cell concentration
α	$\frac{L}{m^2}$	Filter capacity
ΔA_{260}	Optical density units	Magnitude of absorbance at the wavelength 260 nm
μ	Pa*s	Viscosity
μ_{max}	hr^{-1}	Maximum specific growth rate
ϱ	$\frac{kg}{m^3}$	Density
σ	Unitless	Rejection coefficient
Φ	$\frac{m}{min}$	Flux
ν	$\frac{m^2}{s}$	Kinematic viscosity

XIV. References

Ankur. (2016, April 8). Solid-liquid mixing in agitated vessels (Just Suspended Speed) [Blog post]. Retrieved from https://www.cheresources.com/invision/blog/4/entry-511-solid-liquid-mixing-in-agitated-vessels-just-suspended-speed/

Bar-On, Y. M., Flamholz, A., Phillips, R., & Milo, R. (2020). SARS-CoV-2 (COVID-19) by the numbers. *eLife*, *9*, e57309. https://doi.org/10.7554/eLife.57309

Bharat Biotech. (n.d.). *Fact Sheet for Vaccine Recipients & Caregivers*. https://www.bharatbiotech.com/images/covaxin/covaxin-fact-sheet.pdf

Bio-Rad. (n.d.). *CHT Ceramic Hydroxyapatite Type II Media.* https://www.bio-rad.com/en-us/product/cht-ceramic-hydroxyapatite-type-ii-media?ID=5ded4ec5-ff5a-47b7-bf10-07253005c83f

Bio-Rad. (2020). *Process Resin Selection Guide* https://www.bio-rad.com/webroot/web/pdf/lsr/literature/Bulletin_6713.pdf

Bishai D, Koenig M, Ali Khan M. (2003). Measles vaccination improves the equity of health outcomes: evidence from Bangladesh. *Health Econ. 12*(5). 415-9. doi: 10.1002/hec.732.

Blades, J. E. (1980). *Injectable rabies vaccine composition and method*. https://patents.google.com/patent/EP0049296A1/en

Bovine serum albumin. (2021). In *wikipedia*. Retrieved March, 16, 2021, from https://en.wikipedia.org/wiki/Bovine_serum_albumin

Carpenter, K.J. (2011) Agitated Vessel Heat Transfer. *Thermopedia.* doi: 10.1615/AtoZ.a.agitated_vessel_heat_transfer

Carta, G. (2020). Membrane Based Separations [Powerpoint slides]. Retrieved from https://collab.its.virginia.edu/access/content/group/0cfe6c95-bbbc-4e58-93d0-20309c169879/Lecture%20slides/4_Membrane_Based_Separations_2020.pdf

Cekinski, E., Giulietti, M., & Seckler, M. M. (2012). A new approach to characterize suspensions in stirred vessels based on computational fluid dynamics. *Brazilian Journal of Chemical Engineering, 27*(2), 265-273. Retrieved from http://www.scielo.br/pdf/bjce/v27n2/v27n2a05.pdf

Center for Disease Control and Prevention. (2019, Aug 5). *What's in Vaccines?* Retrieved Mar. 10, 2021, from https://www.cdc.gov/vaccines/vac-gen/additives.htm

Center for Disease Control and Prevention. (2020a, October). *Forecasts of COVID-19 Deaths*.

Retrieved from https://www.cdc.gov/coronavirus/2019-ncov/covid-data/forecasting-us.html#ensembleforecast

Center for Disease Control and Prevention. (2020b, November). *Case Forecasts*. Retrieved from https://www.cdc.gov/coronavirus/2019-ncov/cases-updates/forecasts-cases.html

Center for Disease Control and Prevention. (Jan. 6, 2021). Biosafety for Specimen Handling. Retrieved from https://www.cdc.gov/coronavirus/2019-ncov/lab/lab-biosafety-guidelines.html

Center for Disease Control and Prevention. (n.d.). *Injection Safety For Healthcare*. https://www.cdc.gov/injectionsafety/PDF/Injection-Safety-For-Healthcare-P.pdf

Chang, S., & Bestul, A. (1973). Heat capacities of polyethylene from 2 to 360 K. Standard samples of linear and branched polyethylene whole polymer. *Journal of Research of the National Bureau of Standards Section A: Physics and Chemistry, 77A*(4), 395.

Chu, H., Chan, J. F.W., Yuen, T. T. T., Shuai, H., Yuan, S., Wang, Y., … Yuen, K. Y. (2020). Comparative tropism, replication kinetics, and cell damage profiling of SARS-CoV-2 and SARS-CoV with implications for clinical manifestations, transmissibility, and laboratory studies of COVID-19: an observational study. Lancet Microbe, 1(1), e14-e23. doi: 10.1016/ S2666-5247(20)30004-5

Cook, Robert (2010, October 27). *Codes, Tags and Labels—Interpreting Piping and Instrumentation Diagrams.* AICHE https://www.aiche.org/chenected/2010/10/codes-tags-and-labels-interpreting-piping-and-instrumentation-diagrams

Corum, J., Wee, S., & Zimmer, C. (2020, October 19). Coronavirus Vaccine Tracker. *The New York Times*. Retrieved from https://www.nytimes.com

Cytiva (2021). Hollow fiber cartridges and systems for membrane separations- Selection handbook. *Global Life Sciences Solutions USA LLC.* Retrieved from https://cdn.cytivalifesciences.com/dmm3bwsv3/AssetStream.aspx?mediaformatid=10061&destinationid=10016&assetid=12861

Cytiva. (September 2015). *Capto Core 700 in Vaccine Processing*. http://www.processdevelopmentforum.com/articles/capto-core-700-in-vaccine-processing/

Dolgin, E. (2021, January 12). How COVID unlocked the power of RNA vaccines. Retrieved March 31, 2021, from https://www.nature.com/articles/d41586-021-00019-w

Doran, P. (2013). *Bioprocess Engineering Principles* (2nd ed.). Elsevier Ltd. https://doi.org/10.1016/C2009-0-22348-8

Engineers Edge. (2015, January 11). Specific heat capacity of metals table chart. Retrieved April 16, 2021, from https://www.engineersedge.com/materials/specific_heat_capacity_of_metals_13259.htm

Erickson, K. (2018, April 23). *Chromatography scale-up: Don't get tied down by bed height.* https://www.cytivalifesciences.com/en/us/news-center/chromatography-scale-up-using-column-volume-instead-of-bed-height-10001

FDA. (2004, September). *Sterile Drug Products Produced by Aseptic Processing - Current Good Manufacturing Practice.* https://www.fda.gov/media/71026/download

FDA. (2018, Feb. 1). *Thimerosal and Vaccines*. Retrieved Mar. 10, 2021, from https://www.fda.gov/vaccines-blood-biologics/safety-availability-biologics/thimerosal-and-vaccines#othr

Fluid heat transfer coefficients - heat exchanger surface combinations. (n.d.). The Engineering Toolbox. Retrieved April 15, 2021, from https://www.engineeringtoolbox.com/overall-heat-transfer-coefficients-d_284.html

Ganneru, B., Jogdand, H., Dharam, V. K., Molugu, N. R., Prasad, S. D., Vellimudu, S., Vadrevu, K. M. (2020). Evaluation of safety and IMMUNOGENICITY of an Adjuvanted, TH-1 Skewed, Whole virion inactivated sars-cov-2 vaccine - BBV152. *BioRxIv*. doi:10.1101/2020.09.09.285445

GE Healthcare Life Sciences. (2005a, April). Microcarrier cell culture: Principles and methods. Retrieved from https://www.gelifesciences.co.kr/wp-content/uploads/2016/07/023.8_Microcarrier-Cell-Culture.pdf

GE Healthcare. (2005b). Operating Handbook- Hollow fiber cartridges for membrane separations. *General Electric Company*. Retrieved from https://www.gelifesciences.co.kr/wp-content/uploads/2020/04/Operating-handbook-Hollow-fiber-cartridges.pdf

GE Healthcare. (2009, August). *Cytodex surface microcarriers.* https://www.cytivalifesciences.co.jp/catalog/pdf/18106061_cytodex.pdf

GE Healthcare. (2014). Cross Flow Filtration Method Handbook. *General Electric Company*. Retrieved from http://www.processdevelopmentforum.com/files/articles/Cross-Flow_Filtration_Handbook.pdf

Ghosh, P. (2021, January 13). *Explained: How much will one dose of Covishield and Covaxin cost?* Hindustan Times. https://www.hindustantimes.com/india-news/explained-what-is-the-cost-of-covishield-and-covaxin-101610526317829.html

Hayes, A. (2020). *Fixed capital.* https://www.investopedia.com/terms/f/fixed-capital.asp#:~:text=Fixed%20capital%20is%20the%20portion,more%20than%20one%20accounting%20period.

Hooker, L., & Palumbo, D. (2020, December 18). *Covid vaccines: Will drug companies make bumper profits?* BBC News. https://www.bbc.com/news/business-55170756

InvivoGen. (n.d.). *Alhydrogel® adjuvant 2%*. https://www.invivogen.com/alhydrogel

Jaimes, J. A., André, N. M., Chappie, J. S., Millet, J. K., & Whittaker, G. R. (2020). Phylogenetic Analysis and Structural Modeling of SARS-CoV-2 Spike Protein Reveals an Evolutionary Distinct and Proteolytically Sensitive Activation Loop. *Journal of Molecular Biology*, *432*(10), 3309-3325. doi: 10.1016/j.jmb.2020.04.009

Jiang, Y., van der Welle, J. E., Rubingh, O., van Eikenhorst, G. Bakker, W. A. M., & Thomassen, Y. E. (2019). Kinetic model for adherent Vero cell growth and poliovirus production in batch bioreactors. *Process Biochemistry, 81*(1), 156-164, doi: 10.1016/j.procbio.2019.03.010

Kish, S. (2021, March 23). *COVID-19 Vaccination Hesitancy Remains Unchanged*. Carnegie Mellon University. https://www.cmu.edu/dietrich/news/news-stories/2021/march/covidcast-vaccine.html

Kornecki, M., Mestmäcker, F., Zobel-Roos, S., Heikaus de Figueiredo, L., Schlüter, H., & Strube, J. (2017). Host Cell Proteins in Biologics Manufacturing: The Good, the Bad, and the Ugly. *Antibodies (Basel, Switzerland)*, *6*(3), 13. https://doi.org/10.3390/antib6030013

Kurosawa, Y., Saito, M., Yoshikawa, D., & Snyder, M. (2014). *Mammalian virus purification using ceramic hydroxyapatite.* http://www.bio-rad.com/webroot/web/pdf/lsr/literature/Bulletin_6549.pdf

Kwok, K. O., Lai, F., Wei, W. I., Wong, S., & Tang, J. (2020). Herd immunity – estimating the level required to halt the COVID-19 epidemic in affected countries. *Journal of Infection*. *80*(6), e32-e33. doi: 10.1016/j.jinf.2020.03.027

Mayo Clinic. (2020, June). *Herd Immunity and COVID-19 (coronavirus): What you need to know.* Retrieved from https://www.mayoclinic.org/diseases-conditions/coronavirus/in-depth/herd-immunity-and-coronavirus/art-20486808

Mayvan, A., Ghobadian, B., Najafi, G. (2014). Analytical and FEM Design of Mixing System in STR Biodiesel Production. *Advances in Environmental Biology. 8*(1), 325-334.

Meissner. (2020, April 07). *STyLUX filter.* https://www.meissner.com/products/filter-media-cartridges/stylux-pes-membrane-hydrophilic

Meyer, B. K., Ni, A., Hu, B., & Shi, L. (2007). Antimicrobial preservative use in parenteral products: past and present. *Journal of Pharmaceutical Science*, *96*(12), 3155-55. NIH. 10.1002/jps.20976.

MilliporeSigma. (2018, March). *Determining agitation requirements for microcarrier processes: Method development using the Mobius® 50 L single-use bioreactor.* Retrieved from https://www.google.com/url?sa=t&rct=j&q=&esrc=s&source=web&cd=&cad=rja&uact=8&ved=2ahUKEwict5vXy9nvAhUxGVkFHXpRCl0QFjAAegQIBBAD&url=https%3A%2F%2Fwww.merckmillipore.com%2FINTERSHOP%2Fweb%2FWFS%2FMerck-JP-Site%2Fja_JP%2F-%2FJPY%2FShowDocument-Pronet%3Fid%3D201501.279&usg=AOvVaw17BzLbr9TP7jasuv0ZOkkv

MilliporeSigma. (2020, November). Benzonase endonuclease. Retrieved from https://www.google.com/url?sa=t&rct=j&q=&esrc=s&source=web&cd=&ved=2ahUKEwiN0_jB89bvAhV4GFkFHciaB5MQFjABegQIBRAD&url=https%3A%2F%2Fwww.emdmillipore.com%2FWeb-US-Site%2Fen_CA%2F-%2FUSD%2FShowDocument-Pronet%3Fid%3D201312.078&usg=AOvVaw0dA0fFNuO40vYwvQYBFIr2

Mirro, R., & Voll, K. (2009). Which Impeller is Right for Your Cell Line?. *BioProcess International. 7*(1). Retrieved from http://portal.unimap.edu.my/portal/page/portal30/Lecture%20Notes/KEJURUTERAAN_BIOPROSES/Semester%202%20Sidang%20Akademik%2020142015/BIOPROCESS%20ENGINEERING%20PROGRAMME/YEAR%203/ERT314%20Bioreactor%20System/Impellers_for_Stirred_Tank_Bioreactors.pdf

Mundle, S., & Anderson, S. (2013). *WO2013106337A1.* World Intellectual Property Organization. https://patents.google.com/patent/WO2013106337A1/en

Ng, M. L., Tan, S. H., See, E. E., Ooi, E. E., & Ling, A. E. (2003). Proliferative growth of SARS coronavirus in Vero E6 cells. *Journal of General Virology, 84*(12), 3291-3303. Doi: 10.1099/vir.0.19505-0

NIH. (2020). *Biosafety in Microbiological and Biomedical Laboratories* (6th ed.). Department of Health and Human Services. https://www.cdc.gov/labs/pdf/CDC-BiosafetyMicrobiologicalBiomedicalLaboratories-2020-P.pdf

Oller, A., Buser, C., Tyo, M., Thilly, W. (1989). Growth of mammalian cells at high oxygen concentrations. *Journal of Cell Science, 94*(1), 43-49.

Our World in Data. (2021). *Coronavirus (COVID-19) Vaccinations*. Our World in Data. https://ourworldindata.org/covid-vaccinations

Panchal, N., Kamal, R., Cox, C., Garfield, R. (2021). The Implications of COVID-19 for Mental Health and Substance Use. *Kaiser Family Foundation.* Retrieved from: https://www.kff.org/coronavirus-covid-19/issue-brief/the-implications-of-covid-19-for-mental-health-and-substance-use/

Peters, M. S., Timmerhaus, K. D., & West, Ronald E. (Ronald Emmett) (2003). *Plant Design and Economics for Chemical Engineers* (5th ed. / Max S. Peters, Klaus Timmerhaus, Ronald E. West.). Boston: McGraw Hill.

Petiot, E., Guedon, E., Blanchard, F., Geny, C., Pinton, H., & Marc, A. (2010). Kinetic characterization of Vero cell metabolism in a serum-free batch culture process. *Biotechnology and Engineering, 107*(1), 143-153. doi: 10.1002/bit.22783

Pietranski, J. F. (n.d.). Heating and Cooling of Agitated LiquidBatches: Isothermal Medium. Retrieved April 16, 2021, from https://pdhonline.com/courses/k101/Isothermal%20Medium.pdf

Planning Advisory Service. (1951, October). Impact of Large Industries on Small Communities. *American Society of Planning Officials*, 1-40.

Porex Filtration. (2021). *Understanding Cross Flow Filtration.* http://www.porexfiltration.com/learning-center/technology/what-is-cross-flow-filtration/

Roghanian, A., & Newman, R. (2021, March). B cells, British Society for Immunology. https://www.immunology.org/public-information/bitesized-immunology/cells/b-cells

Rodrigues, C., & Plotkin, S. (2020). Impact of Vaccines; Health, Economic and Social Perspectives. *Frontiers in Microbiology*, *11*, 1526. 10.3389/fmicb.2020.01526

S. Ranil Wickramasinghe, Shane E. Bower, Zhen Chen, Abhik Mukherjee, Scott M. Husson. (2009). Relating the pore size distribution of ultrafiltration membranes to dextran rejection. *Journal of Membrane Science*. *340*(1-2), 1-8. https://doi.org/10.1016/j.memsci.2009.04.056.

Scheller, C., Krebs, F., Minkner, R., Astner, I., Gil‐Moles, M., & Wätzig, H. (2020). Physicochemical properties Of SARS‐CoV‐2 for drug targeting, VIRUS inactivation and Attenuation, vaccine formulation and quality control. *ELECTROPHORESIS, 41*(13-14), 1137-1151. doi:10.1002/elps.202000121

Shearley, A. E. (1999). The societal value of vaccination in developing countries. *Vaccine* 17, (Suppl. 3), S109–S112

Specific heat of some common substances. (n.d.). The Engineering Toolbox. Retrieved April 16, 2021, from https://www.engineeringtoolbox.com/specific-heat-capacity-d_391.html

Status of COVID-19 Vaccines within WHO EUL/PQ evaluation ... (2021, March 23). Retrieved https://extranet.who.int/pqweb/key-resources/documents/status-covid-19-vaccines-within-who-eulpq-evaluation-process

Synthecon Inc. (n.d.) The Rotary Cell Culture System Operation Manual. Retrieved from: https://synthecon.com/files/132_user_manual-stem_cell_culture_system.pdf

Szmigiera, M. (2021, March 30). *World population by age and region 2020*. statista. https://www.statista.com/statistics/265759/world-population-by-age-and-region/

Tagawa, A., Dohi, N., Kawase, Y. (2006). Dispersion of Floating Solid Particles in Aerated Stirred Tank Reactors: Minimum Impeller Speeds for Off-Surface and Ultimately Homogeneous Solid Suspension and Solids Concentration Profiles. *Ind. Eng. Chem. Res. 45*(2). 818-829. https://doi.org/10.1021/ie050634k

Tanksi-Phillips, M. (2020, November). What in the World is a Fringe Benefit Rate? Retrieved from https://www.patriotsoftware.com/blog/payroll/fringe-benefit-rate/

ThermoFisher. (2017). *25 L and 50 L Harvestainer BioProcess Container*. https://www.thermofisher.com/document-connect/document-connect.html?url=https%3A%2F%2Fassets.thermofisher.com%2FTFS-Assets%2FLSG%2Fbrochures%2F25-50-harvestainer-data-sheet.pdf&title=RGF0YSBTaGVldDogMjUgTCBhbmQgNTAgTCBIYXJ2ZXN0YWluZXIgQmlvUHJvY2VzcyBDb250YWluZXI

ThermoFisher. (2020). *Nunc Cell Factory equipment.* https://www.thermofisher.com/document-connect/document-connect.html?url=https%3A%2F%2Fassets.thermofisher.com%2FTFS-Assets%2FBPD%2Fbrochures%2Fnunc-cell-factory-equipment-brochure.pdf&title=TWF4aW1pemUgcHJvZHVjdGl2aXR5IHdpdGggYXV0b21hdGlvbiBzb2x1dGlvbnMgZm9yIHNjYWxlLXVwIG9mIHlvdXIgQ2VsbCBGYWN0b3J5IHN5c3RlbXMgW0VOXQ==

ThermoFisher. (2018). *Microcarrier bead separation and cell harvesting using the Harvestainer large-scale system.* https://assets.thermofisher.com/TFS-Assets/BPD/Application-Notes/large-scale-harvestainer-app-note.pdf

ThermoFisher Scientific. (n.d.a). VP-SFM(1X). In *Additional Selective and Differential Culture Media*. Retrieved from https://www.thermofisher.com/order/catalog/product/11681020#/11681020

ThermoFisher (n.d.b). Macromolecular Components of E. coli and HeLa Cells. Retrieved from https://www.thermofisher.com/us/en/home/references/ambion-tech-support/rna-tools-and-calculators/macromolecular-components-of-e.html

ThermoFisher (n.d.c). DNA and RNA Molecular Weights and Conversions. Retrieved from https://www.thermofisher.com/us/en/home/references/ambion-tech-support/rna-tools-and-calculators/dna-and-rna-molecular-weights-and-conversions.html

Toinon, A., Fontaine, C., Thion, L., Gajewska, B., Carpick, B., Nougarede, N., & Uhlrich, S. (2018). Host cell protein testing strategy for hepatitis B antigen in Hexavalent vaccine – Towards a general testing strategy for recombinant vaccines. *Biologicals*, *54*, 1-7. https://doi.org/10.1016/j.biologicals.2018.05.006

Tomai, M. A., & Vasilakos, J. P. (2017). *Immunopotentiators in Modern Vaccines* (2nd ed.). Academic Press. 10.1016/B978-0-12-804019-5.00008-6

Turton, R., & O'Reilly Online Learning: Academic/Public Library Edition (2018). Analysis, Synthesis and Design of Chemical Processes (Fifth ed.). Boston, Massachusetts: Prentice Hall.

Verguet, S., Murphy, S., Anderson, B., Johansson, K. A., Glass, R., and Rheingans, R. (2013). Public finance of rotavirus vaccination in India and Ethiopia: an extended cost-effectiveness analysis. *Vaccine* 31, 4902–4910.

Wolf, M. W., & Reichl, U. (2011). Downstream processing of cell culture-derived virus particles. *Expert review of vaccines*, *10*(10), 1451–1475. https://doi.org/10.1586/erv.11.111

Zimmer, C. (2020, October 15). First, a Vaccine Approval. Then 'Chaos and Confusion.' *The New York Times*. Retrieved from https://www.nytimes.com

Zimmer, C., Corum, J., & Wee, S. (2021). *Coronavirus Vaccine Tracker*. The New York Times. https://www.nytimes.com/interactive/2020/science/coronavirus-vaccine-tracker.html

200 L power mix sst CARRIER w/ temp sensor, load CELLS, asme mxrj200tla. (n.d.). Sigma Aldrich. Retrieved April 16, 2021, from https://www.sigmaaldrich.com/catalog/product/mm/mxrj200tla?lang=en®ion=US

XV. Appendix

Table 15.1: Description of Raw Materials for Upstream Processes of Covaxin Production

Product	Purpose
Seed SARS-CoV-2 cells	Stock virus cells used to infect the cell line
Vero cells	The substrate used to grow viral pathogens
VP-SFM	Media for Vero cell and virus propagation
L-glutamine	Amino acid supplement, an energy source for the cell culture
Fetal Bovine Serum (FBS)	Supplemental growth media for Vero cell cultures
Water for Injection (WFI)	Supplies water necessary for the process
Microcarriers Cytodex 1	Surface for cell adhesion
Minimum Essential Medium (MEM)	Media for Vero cell revitalization

Table 15.2: Description of Raw Materials for Downstream Processes of Covaxin Production

Product	Purpose
50 L microfiltration bag	Separates microcarriers from bioreactor cell culture
Depth filtration filters	Removes cell debris and other particles in the supernatant larger than ~1 µg
β-propiolactone (BPL)	An agent used for inactivation of the virus
Ultrafiltration/Diafiltration filters	Retains virus in solution, allows other particles to pass through
Phosphate buffer solution (PBS)	Bioreactor wash solution and chromatography buffer
Benzonase	Cleaves DNA into smaller pieces
Sepharose 4 Fast Flow	Size exclusion chromatography resin
Fractogel® EMD DWAE(M)	Weak anion exchanger

Table 15.3: Fixed Capital Investment

Unit Operation	Equipment	Quantity	Price	Cost
Seed Train	Incubator	1	$11,035	$11,035
Bioreactor	Autoclave*	1	$56,929	$88,368
	10 L Glass Bottles	3	$162	$486
	1000 L Sartorius Bioreactor	3	$4,050,000	$12,150,000
	1000 L Holding Tank*	6	$9,457	$88,078
	10 L Holding Tank*	3	$2,773	$12,913
Microfiltration	3000 L Holding Tank*	1	$17,271	$26,809
Benzonase Treatment	50 L Mixer*	1	$3,075	$4,772
	1000 L Sartorius Bioreactor	3	$4,050,000	$12,150,000
UF/DF	250 L Mixer*	1	$4,583	$7,114
	3000 L Holding Tank*	1	$17,271	$26,809
	200 L Holding Tank*	1	$4,206	$6,528
Inactivation	200 L Sartorius Bioreactor	1	$810,000	$810,000
Affinity Chromatography	500 L Mixer*	2	$6,468	$20,080
	1000 L Holding Tank*	1	$9,457	$14,680
	100 L Holding Tank*	1	$3,452	$5,358
	Column	1	$11,510	$11,510
SEC	250 L Mixer	2	$4,206	$13,057
	500 L Holding Tank	1	$6,486	$10,068
	200 L Holding Tank	2	$4,206	$13,058
	1000 L Waste Tank	1	$9,457	$14,680
	Column	1	$15,908	$15,908
Sterile Filtration	200 L Holding Tank*	1	$4,206	$6,528
	50 L Holding Tank*	1	$3,075	$4,772
Formulation	10000 L Stirred Tank*	1	$66,300	$66,300
	10000 L Holding Tank*	2	$33,417	$103,743
	5 L Holding Tank*	1	$2,735	$4,246
Ancillary	Labeller	1	$250,000	$250,000
	Filling Line	1	$7,000,000	$7,000,000
	Pumps*	33	$6,519	$333,932
	Immersion Heater	1	$1,539	$2,389

	5000 L Holding Tank	2	$22,853	$70,947
Spare Equipment	Pumps*	16	$6,519	$161,906
	10 L Glass Bottles	2	$162	$324
	200 L Holding Tank*	1	$4,206	$6,528
	1000 L Holding Tank*	3	$9,457	$44,039
	10000 L Holding Tank*	1	$33,417	$51,872
Total				**$33,273,221**

*Prices were calculated using the CECPI from Nov 2020

Table 15.5: Raw Materials Yearly Cost for Year 1

Material	Annual Quantity	Unit Quantity	Unit Price	Annual Cost
Vero cells	144,000,000	1,000,000	$784	$112,896
VPSFM (L)	85,904	1	$107	$9,191,694
L-Glutamine (g)	54,275	5	$33	$358,215
DPBS (L)	326	20	$658	$10,739
Trypsin EDTA (L)	122	0.5	$45	$11,016
Cytodex-1 MCs (g)	13,980	5000	$25,000	$69,902
PBS (L)	318,766	3.785	$59	$4,968,874
WFI (L)	75,262	200	$1,183	$445,122
Benzonase (units)	8,382,000	25000	$237	$79,461
Tris HCl (g)	803,987	500	$67	$107,364
MgCl2 (g)	9,140	5000	$178	$325
BSA (g)	9,600	100	$201	$19,296
Sodium Phosphate (L)	232	10	$215	$4,982
BPL (L)	1	1	$62	$41
Sodium Phosphate (g)	16,714	1	$2	$36,904
CHT Type 2 Resin (g)	5,043	1	$66	$333,141
NaCl (g)	17,616	10000	$209	$368
Capto Core 700 Resin (L)	754	0.025	$256	$7,721,779
Al (OH)3 gel (L)	65	0.25	$270	$70,724
TLR 7/8 (g)	9,508	0.05	$337	$64,087,008
2-phenoxyethanol (L)	1,432	2.5	$144	$82,458
Total				**$87,712,311**

Table 15.6: Single-Use Equipment Yearly Cost for Year 1

	Annual Quantity	Unit Quantity	Price	Cost
T175	48	30	$233	$373
T225	576	30	$280	$5,376
Bioreactor Bag	96	1	$126,000	$12,096,000
Bioreactor Air Filter	96	1	$150	$14,400
Harvestainer	42	1	$12,000	$504,000
M w/ TFF Filters	96	1	$2,044	$196,224
BT Bag	96	1	$126,000	$12,096,000
UF Filter	247	1	$7,315	$1,806,921
DF Filter	96	1	$7,315	$702,285
Inactivation Bag	48	1	$25,560	$1,226,880
SF Filter	48	1	$211	$10,128
10 mL Vials	28,525,375	1	$1	$34,230,450
Total				**$62,889,038**

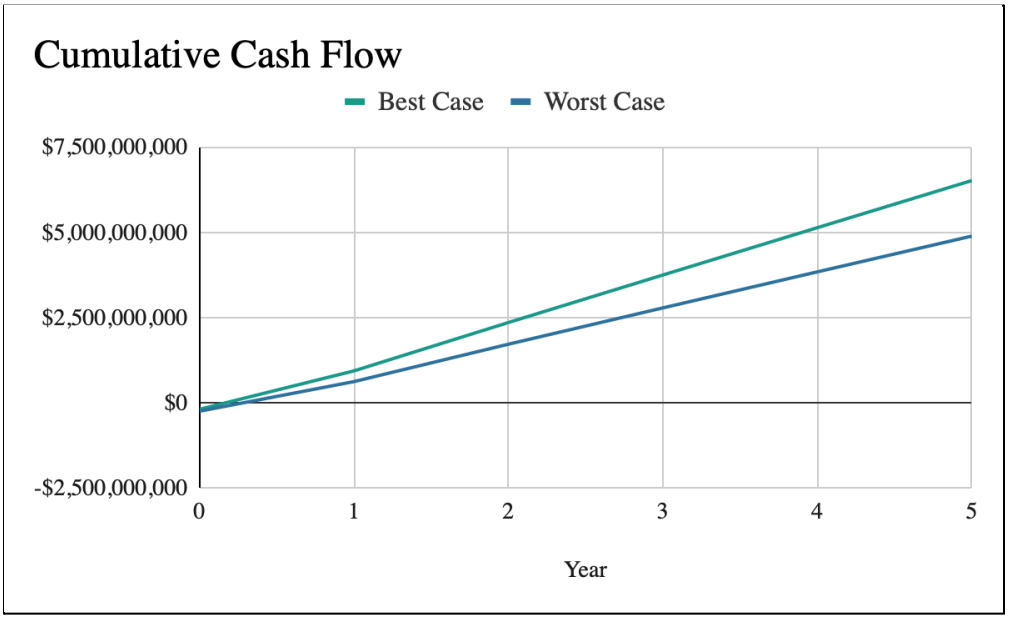

Figure 15.1 Cumulative Cash Flow for $4 a Dose